SOME INVESTIGATIONS ON THE SCATTERING AND ABSORPTION OF HETEROGENEOUS BEAMS OF X-RADIATION.

Kurt Kellner.

THESIS

submitted for the degree of Ph.D.

TABLE OF CONTENTS.

INTRODUCTION.

The experiments performed in this Laboratory in connection with the researches done on the scattering of X-rays are of two different types, namely the scattering experiment and the filtering experiment. Both these experiments have been developed by Prof. Barkla and his collaborators in the course of many years. Their interpretation is exceedingly complicated and difficult owing to the fact that a number of factors (e.g. heterogeneity of radiation, polarization etc.) influence the result. The results obtained must therefore be a superposition of various effects. It is however possible by means of theory (using a number of approximations) to get some idea of what kind of result can be expected from such experiments. The results obtained by various research workers in this laboratory are stated to be not in agreement with accepted theory and all attempts have hitherto failed to reconcile experimental results with theory.

In the course of the development of these experiments a number of "irregularities" began to appear. It had been found that there are several alternative results possible for one type of experiment and that by varying one or other of the experimental conditions on one apparatus, one possible result could be made to change over into another. And yet, under what appear to be identical experimental conditions for another

apparatus, or even for the same apparatus at different periods, no such change-over from one result to another appears, although the variations of experimental conditions are the same as before.

In order to get a better understanding of these results, a short description of the scattering and filtering experiments will be given. The arrangement of the apparatus is the same in both experiments (Fig.1). The radiation from an X-ray tube, (the tube is fixed horizontally with the cathode ray stream parallel to the scattered beam) after passing through an aperture system J' and J falls on to the scatterer. In all experiments here described the entire heterogeneous radiation is employed. The scatterer consists of some material of small atomic number or a combination of these, (paraffin wax, filter paper, carbon, aluminium) as such substances do not emit characteristic radiations which are appreciable under the conditions of the experiments. The greater part of the radiation is transmitted through the scatterer (primary radiation) but a fraction is scattered in all directions (secondary radiation). By choosing suitable apertures S_1 and S_2 it is possible to define a beam of scattered radiation making an angle of approximately 90° with the primary. The primary beam is further limited by a small aperture P. Both primary and secondary radiations are received in ionization chambers and the ionization (which for radiations of given quality is a measure of

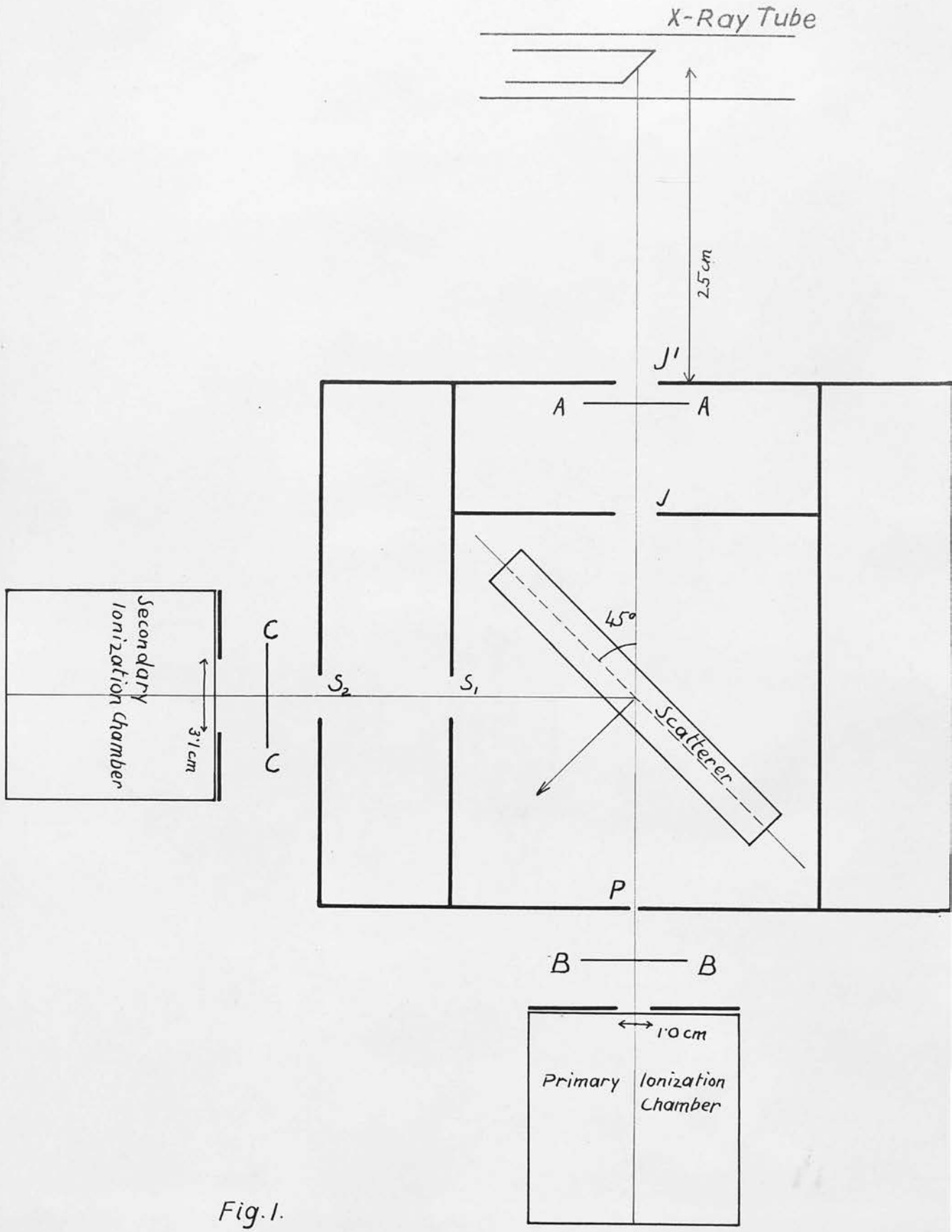
X-Ray Tube
2.5 cm
J'
A
A
J
45°
Scatterer
Secondary
Ionization Chamber
3.1 cm
C
C
S2
S1
P
B
B
1.0 cm
Primary
Ionization
Chamber

Fig. 1.

their intensities) produced by them is measured in electroscopes. As it would not be practicable to measure the absolute values of the intensities, we confine ourselves to expressing the ionization produced by the secondary radiation (S) relative to that produced by the primary (P). By measuring the ratio S/P a means is provided of studying the quality of the scattered radiation as compared with the primary.

(a) The Scattering Experiment.

In this experiment the scattered radiation is compared with the transmitted primary radiation when the quality of that radiation is varied. This variation in hardness of the heterogeneous primary beam can be brought about by two entirely different methods,

(1) by a variation of the voltage on the tube. In the experiments performed by the writer this was done between 30 KV and 90 KV (which was the maximum obtainable voltage). When using this method the maximum frequency is increased with increasing voltage and the maximum intensity of the spectrum is shifted towards higher frequencies. The total intensity of the radiation also increases with increasing voltage, when the supply of electrons is kept constant.

(2) by maintaining constant voltage and by progressive elimination of the softer components by filtering the primary radiation. This can be achieved by inserting aluminium filters of various

thicknesses in the path of the main beam (at AA Fig.1). Although as before the average frequency increases, in this case the maximum frequency remains constant. The total intensity of the radiation of course decreases with increasing thickness of filtering aluminium.

It is therefore not surprising that the result of the scattering experiment should show two distinct characteristics corresponding to the two methods of hardening the radiation. In a graphical representation of these results the ratio S/P has to be plotted against some measure of the hardness of the radiation i.e. against voltage for the one part of the result and against thickness of filtering aluminium for the other part. In order to bring these two different parts to the same continuous scale, an average mass absorption coefficient $\overline{\mu/\rho}$ (see Page 44.) has been defined and the quality of the radiation described in terms of this quantity. An increase in voltage and increase in thickness of filtering aluminium correspond to a decrease in $\overline{\mu/\rho}$ i.e. a small value of $\overline{\mu/\rho}$ corresponds to a hard radiation and a large value of $\overline{\mu/\rho}$ corresponds to a soft radiation. It has to be pointed out, however, that $\overline{\mu/\rho}$ (which is always measured in aluminium for the primary beam after transmission through the scattering substance) has not a unique meaning. One value of $\overline{\mu/\rho}$ can represent various beams of entirely different

constitution. This is however of no importance in the present work.

The general type of the result of the scattering experiment is shown in Fig. 2). Its main features are:

(1) With increasing voltage on the X-ray tube (i.e. decreasing $\overline{\mu/\rho}$) the ratio S/p shows a gradual increase. The slope of the graph increases as the thickness of the scatterer increases.

(2) From a certain voltage (critical voltage) upwards, the ratio S/p remains constant. The slope of the graph changes abruptly at this critical point, although the experimental conditions are subject only to a gradual change. The position of this point depends on the thickness of the scatterer; it moves towards higher voltages as the thickness of the scatterer is increased.

S/p remains constant up to the highest voltage which may safely be applied. This voltage limit depends on the X-ray tube and high tension supply and in this work it was 90 KV. At this point then, the radiation is of the highest average frequency which can be obtained by a variation of the voltage only.

(3) If the radiation is further hardened by filtering, a decrease of S/p with increasing thickness of aluminium filter results. Here again the

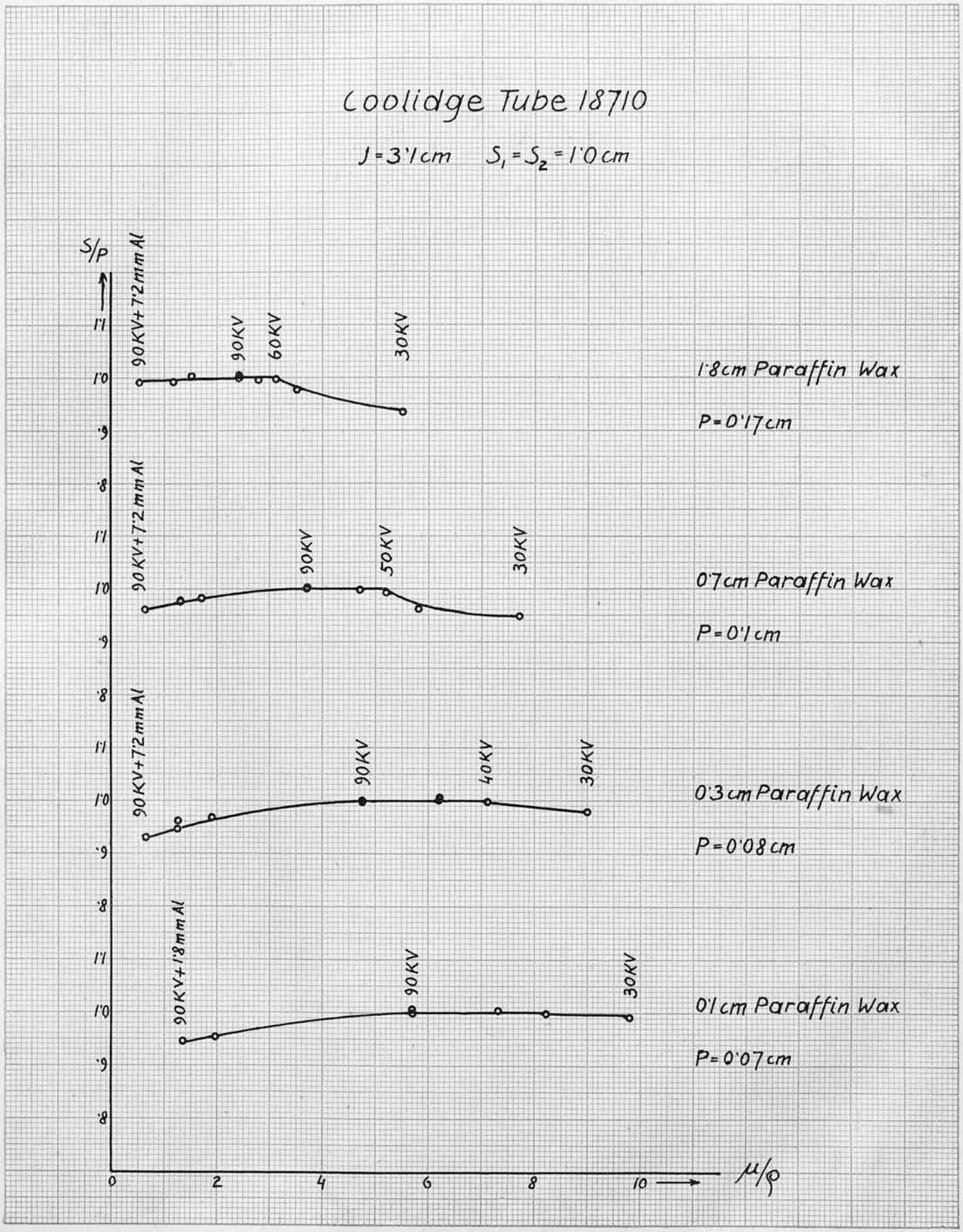
Coolidge Tube 18710
J = 3·1 cm S1 = S2 = 1·0 cm
S/P
90 KV + 7·2 mm Al
90 KV
60 KV
30 KV
1·8 cm Paraffin Wax
P = 0·17 cm
90 KV + 7·2 mm Al
90 KV
50 KV
30 KV
0·7 cm Paraffin Wax
P = 0·1 cm
90 KV + 7·2 mm Al
90 KV
40 KV
30 KV
0·3 cm Paraffin Wax
P = 0·08 cm
90 KV + 1·8 mm Al
90 KV
30 KV
0·1 cm Paraffin Wax
P = 0·07 cm
1·1
1·0
·9
·8
0
2
4
6
8
10
μ/ρ

Fig. 2.

slope of the graph depends on the thickness of the scatterer, being very small or zero for thick scatterers (i.e. the graph is horizontal) and increasing as the thickness of the scatterer is decreased.

Although the general features of the results, obtained from four different sets of apparatus (in use at the same time in this laboratory) were similar, it became apparent that they could be divided into two distinct groups[1]. While two sets in one room (A and B) showed a decrease in the ratio S/P even for the thinnest sheet of aluminium filter placed in the path of the radiation before being scattered (no matter what the thickness of the scatterer), the other two sets (C and D) in another room showed a marked equality of S/P for thick scatterers whatever the thickness of the filtering aluminium. For thinner scatterers, however, S/P slowly decreases with increasing thickness of aluminium filter. Hitherto, no explanation for this difference in the results had been found[1]. However, the two sets (C and D) which showed this marked equality of S/P, gave also another striking result. For thin scatterers, when using tubes with a Lindemann window (in which case a larger proportion of the soft radiation appears), the ratio S/P remains remarkably constant for a very extensive range of voltage and even with thick sheets of filtering aluminium. This constancy of S/P appears also with other tubes when very

small primary apertures are used. The horizontality of the graph (S/P against $\overline{\mu/\rho}$) is so pronounced that it was and still is regarded as being of fundamental importance. An extensive horizontal line cannot be obtained on sets A and B. In one case [1], for apparatus A, it has been found that a change of primary aperture from 0·06 cms. to 0·1 cms. in diameter, changed the result completely. For the latter aperture no horizontal portion could be observed at all.

All attempts to ascribe the difference in the results to certain parts of the apparatus have failed so far. The persistency of the occurrence of the results characteristic for A and B and those characteristic for C and D (although many parts of C and D have been replaced by parts from A and B, e.g. apertures, ionization chambers, scatterers, etc., the result remained unchanged) have led to the suggestion of a room effect[1], i.e. if one apparatus could be completely transferred from one room into another, the result of the scattering experiment would change from one type into another. Facts bearing on this point of view will be discussed later on.

(b) <u>The Filtering Experiment</u>.

This experiment is designed to study the quality of the scattered radiation as compared with the primary. The voltage on the tube is kept constant throughout the whole of the experiment. The emitted, and therefore

primary and secondary radiations are unchanged during the experiment. If the primary and secondary radiations are of equal constitution (i.e. in the case of heterogeneous radiation, if they have the same intensity-wavelength distribution) then, by placing simultaneously an equal amount of absorbing material (usually aluminium) into the path of primary and secondary radiation (at BB and CC of Fig.1), no changes in the ratio $^{S}/_{P}$ should occur. If $^{S}/_{P}$ is plotted against the thickness of the filtering aluminium in both beams, then the resulting graph should be a horizontal line. This is what would be expected from the simplest classical theory according to which all constituents have the same scattering coefficient . If however the scattered radiation is softer than the primary, then equal thicknesses of aluminium will absorb the scattered radiation more than the primary. The graph therefore should show a decreasing $^{S}/_{P}$ with increasing thickness of aluminium filter. Such a result would be expected to follow the observed increase in wavelength on the scattering (Compton-effect) as explained by Quantum theory.

Barkla showed that the secondary radiation from heavy atoms possessed an absorbability characteristic of the scattering atom and greater than that for the primary radiation. In addition the secondary radiation was comparatively homogeneous, even when excited by a markedly heterogeneous radiation. This led to the discovery of the fluorescent radiations

characteristic of the radiating elements.(2) When examining the radiation scattered by light elements it was found that the secondary radiation was slightly softer than the primary, although no known characteristic radiation should have appeared. By analogy with the softening caused by the process of emission of the K, L, M... characteristic radiations, it was only natural to look for evidence of a new characteristic radiation of shorter wavelength than the K, the J-radiation.(3) And indeed, it seemed for some time that the absorption discontinuity corresponding to the characteristic J-radiation had been discovered.(4) These discontinuities, however, apart from differences in magnitude (they were of a magnitude only about 1% of that of the K-discontinuity) differed from the corresponding K- and L-discontinuities by the fact that they were not under control; they seemed to be dependent upon some unknown factor, in consequence of which they disappeared or reappeared again without any apparent reason. Despite great efforts all attempts to discover this governing factor were in vain. But whereas Barkla's results regarding the K- and L-radiation were completely verified by spectroscopic examination, this failed to reveal any indication regarding the J-radiation.(5) It thus became impossible to explain the softening due to scattering by a characteristic radiation. From the theoretical point of view a shorter characteristic radiation than the K-radiation

cannot be accounted for unless it be a nuclear radiation. Barkla therefore gave another description by assuming a J-transformation (instead of J-radiation). According to this new interpretation,(6) the scattered radiation from a primary heterogeneous beam undergoes certain changes in its properties when passing through an absorbing medium.

As in the case of the scattering experiment, the filtering experiment showed various groups of results. When the J-phenomenon did occur, the graph (S/P against the thickness of the filtering aluminium) was horizontal until a certain thickness of filtering aluminium was reached, or more correctly when a certain value of $\overline{\mu/\rho}$ was reached, as the discontinuity seemed to depend more on the value of $\overline{\mu/\rho}$ than on the thickness of filtering aluminium.

At this point the ratio S/P dropped suddenly (sometimes by as much as 7%) and on further increasing the thickness of aluminium, the graph continued to remain horizontal, but at a lower level than before the discontinuity. As many as five such discontinuities could be observed when using aluminium as absorber (e.g. Barkla loc. cit.). When the J-phenomenon did not occur, then the graph was a smooth curve with a concave slope upwards. In certain cases intermediate results were obtained when the J-phenomenon occurred.

There was, however, another type of filtering curve which appeared very frequently.(7) This result

was very similar to the result of the scattering experiment and in fact a very close relationship between them could be established. The ratio S/P was constant up to a certain thickness of filtering aluminium at which point the slope of the graph suddenly changed and S/P decreased (as in other experiments) for increasing thickness of aluminium. This horizontal portion of the filtering curve existed only if the voltage (at which the filtering curve was taken) lay on the horizontal part of the corresponding scattering curve. (Both experiments were carried out under the same experimental conditions.) The nearer the voltage to the voltage producing the discontinuity in the scattering experiment, the shorter was the horizontal part in the filtering experiment. For voltages lower than the critical voltage, below which the scattering curve was not horizontal, the filtering curve showed no horizontality.

From this short summary it can be seen that a great variety of results is possible, and all attempts so far have failed to find the fundamental factor which determines the nature of the result. A peculiarity of most of these results (of both experiments) is the equality of S/P over an appreciable range of voltage and thickness of filtering aluminium. The horizontality of the graphs is so marked, and appears even under a great variety of experimental conditions, that a suggestion has been put forward that it represents

some fundamental property of the radiation, apart from change in wavelength, polarization, etc. (e.g. J.Reekie Ph.D. Thesis 1937). In fact, Reekie states "that present theories while affording a fairly accurate description of the results obtained with homogeneous radiation, are not adequate to account for the behaviour of heterogeneous beams of radiation". The results obtained in a long series of experiments made by the writer do not support this statement.

THE THEORIES OF X-RAY SCATTERING.

(a) Classical Theory (Undulatory Theory).

The hypothesis that the sudden stopping of fast moving electrons causes a disturbance of the electromagnetic field, which spreads with the velocity of light in the form of X-rays, was first put forward by Wiechart, Stokes and J.J. Thomson and later on developed by Lorentz and Sommerfeld.[8] According to the laws of classical electrodynamics, the field-strength of the radiation emitted by an electron of charge e and acceleration a is given, at a certain point P, by the expressions:

(1)

$$|E| = \frac{e \cdot a \cdot \sin\theta}{r \cdot c^2} \quad \text{and} \quad |H| = \frac{e \cdot a \cdot \sin\theta}{r \cdot c^2}$$

where E is the electric and
H the magnetic vector,
θ the angle between the direction of the electron acceleration and the direction of the propagation of the radiation, and
r the distance between the electron and the point of consideration (P).

(E is expressed in electrostatic and H in electromagnetic units.)

The vectors E and H lie in a plane perpendicular to the direction of propagation of the radiation

and orientated so that E should be parallel to the projection of the acceleration vector of the electron on to the plane formed by E and H .

The intensity of the radiation emitted in the direction θ is given by Poynting's radiation vector

$$(2) \qquad I_\theta = \frac{c}{4\pi} [E \cdot H]$$

where $[E \cdot H] = |E| \cdot |H| \cdot \sin 90°$.

Since $|E| = |H|$

$$(3) \qquad I_\theta = \frac{c}{4\pi} \cdot |E|^2 \qquad \text{or}$$

$$I_\theta = \frac{e^2 a^2}{4\pi c^3 r^2} \cdot \sin^2\theta$$

The total intensity of the emitted radiation is obtained by integrating equation 3. over the whole sphere and is given by:

$$(4.) \qquad S = \frac{2}{3} \cdot \frac{e^2 a^2}{c^3}$$

From these considerations it can be seen that the emitted white radiation (Bremsstrahlung) should be completely polarized in the plane containing the direction of the electron-acceleration and the axis of the emitted radiation. Experiment, however, only shows partial polarization in this plane, owing to the fact that the impinging electron is being deviated from its original path in the anticathode before coming to rest. Experiments with very thin anticathodes using fast moving electrons, show almost complete

polarization, thus verifying the prediction of classical theory.

For electron-velocities comparable with that of light, a relativity correction has to be applied which gives for equation 1.

$$(5.) \qquad |E| = |H| = \frac{e\alpha}{c^2 r} \cdot \frac{\sin\theta}{(1-\beta\cos\theta)^3}$$

where $\beta = \frac{v}{c}$.

(9)

According to the classical theory of scattering, a wave, traversing a free electron, will set the latter into forced oscillation with a frequency equal to the frequency of the exciting wave. The electron in turn, in virtue of its accelerating motion, will radiate energy in the form of a wave, which then forms the scattered radiation.

For an unpolarized primary radiation the electric vector E can be resolved into two components E_p and E_N , each of which is plane polarized and are normal to each other. An electron of charge e and mass m, traversed by a radiation which is plane polarized in the plane containing E_p , will have an acceleration given by

$$(6.) \qquad \ddot{p} = \frac{e\,|E_p|}{m}$$

This electron, according to classical laws, will radiate a wave whose electric vector at a point $P(\theta, r)$ will be given by equation 1.,

$$(7.)\quad |E_{S(P)}| = \frac{e\cdot|E_P|}{m}\cdot\frac{e\cdot\sin\theta}{r\cdot c^2} = \frac{e^2\cdot\sin\theta}{r\,m\,c^2}\cdot|E_P|\,.$$

Since the intensity of the scattered radiation is proportional to the square of the electric vector, the ratio of the intensities of the primary and scattered ray is

$$(8.)\quad \frac{I_{S(P)}}{I_{(P)}} = \frac{|E_{S(P)}|^2}{|E_P|^2} = \frac{e^4\cdot\sin^2\theta}{r^2\,m^2\,c^4}$$

From this equation it follows that the scattered radiation, from a polarized primary radiation, has to have a maximum intensity in a direction normal to the electric vector ($\theta = 90^\circ$, $\sin\theta = 1$) and zero intensity in a direction parallel to the electric vector ($\theta = 0^\circ$, $\sin\theta = 0$).

For an unpolarized primary radiation we have

$$E = E_P + E_N$$

$$\therefore\ E^2 = E_P^2 + E_N^2$$

Since in the average, owing to symmetry $|E_P| = |E_N|$, it follows that

$$I_P = I_N = \frac{1}{2} I$$

where I is the total intensity of the primary unpolarized radiation.

The total scattered intensity from an unpolarized primary radiation at a point P (r, ϕ) is given by

$$(9.) \quad I_e = I_{S(P)} + I_{S(N)} = I_P \cdot \frac{e^4}{r^2 m^2 c^4} + I_N \cdot \frac{e^4 \cdot \cos^2\phi}{r^2 m^2 c^4}$$

$$(10.) \quad I_e = \frac{1}{2} \cdot I \cdot \frac{e^4}{r^2 m^2 c^4} (1 + \cos^2\phi)$$

where $I_{S(P)}$ and $I_{S(N)}$ are the scattered intensities due to the components of the primary beam I_P and I_N, and ϕ is the angle between primary and scattered radiation.

From equation 10 it follows that for $\phi = 90°$ i.e. when the direction of the scattered radiation coincides with the direction of one of the components of the primary beam, the secondary radiation must be completely polarized. This has been completely verified by Barkla[10] in his well known polarization experiments.

If n electrons scatter independently of each other, the intensity of the scattered beam becomes:

$$(11.) \quad I_s = \frac{1}{2} \cdot I \cdot \frac{n e^4}{r^2 m^2 c^4} (1 + \cos^2\phi)$$

By integrating equation 11 over the surface of the sphere of radius r, we obtain the total power of the scattered radiation:

$$P_s = \int_0^{\pi} I_s \cdot 2\pi r \sin\phi \; r \, d\phi$$

$$(12.) \quad P_s = \frac{8\pi}{3} \cdot I \cdot \frac{n e^4}{m^2 c^4}$$

The fraction of the primary radiation scattered per cm^3 of the irradiated material is called the scattering coefficient and is given by

$$(13.) \qquad \sigma = \frac{P_s}{I} = \frac{8\pi n e^4}{3 m^2 c^4}$$

where I is the energy of the primary beam per cm^2 per second, and

n the number of electrons per cm^3 of the irradiated material.

It has to be noted that all the results are independent of the wave length of the radiation employed.

The measurements of the scattering coefficient however show wide departures from the theoretically calculated value. For scattering from very light substances the scattering coefficient is nearly independent of the wave length (for a wide range of frequencies) and increases with atomic number. The agreement of theory and experiment in this case is good.

For very short waves, however, the scattering coefficient diminishes rapidly with decreasing wave length.

For medium and long waves it was found that the scattering coefficient rises slightly with increasing wave length for light elements and more rapidly as the atomic number of the scatterer increases. This, together with the excess scattering for small scattering angles can easily be explained qualitatively by taking

into account the interference of the scattered rays coming from different electrons in the same atom.

According to equation 10 the intensity of the scattered radiation should follow a $(1+\cos^2\phi)$ - law which implies that the intensity scattered in the forward direction should be equal to the intensity scattered backwards. Experiment has shown however, that this is not the case, the scattering at small angles (i.e. in the forward direction) being much bigger than theory predicts. A theoretical treatment of these interferences of scattered X-rays has been given by Debye and J.J. Thomson.[11] In this case, the independence-condition of the electrons no longer holds.

For the simple case of two electrons a distance s apart, the scattered intensity in a direction ϕ (using unpolarized primary radiation) is

$$(14.) \qquad I_\phi^{(2)} = 2I_e\left(1+\frac{\sin x}{x}\right)$$

where $x = \frac{4\pi s}{\lambda}\cdot\sin\frac{\phi}{2}$ and

I_e the intensity of the radiation scattered by a single independent electron given by equation 10.

It can be seen that for large values of x i.e.

$$s \gg \frac{\lambda}{\sin\frac{\phi}{2}}, \qquad \frac{\sin x}{x} \ll 1,$$

$$I_\phi^{(2)} = 2I_e$$

i.e. for large scattering angles the electrons scatter independently of each other, whereas if x becomes

small, for large distances between the electrons, long wavelengths and small scattering angles, $\frac{\sin x}{x} = 1$

and $I_\phi^{(2)} = 4\, I_e$ i.e. the scattered intensity is 4 times that for a single independent electron.

For Z electrons at fixed distances from each other the intensity becomes:

(15.) $$I_\phi^{(Z)} = I_e \sum_{m=1}^{Z} \sum_{n=1}^{Z} \frac{\sin x_{m,n}}{x_{m,n}}$$

where $$x_{m,n} = \frac{4\pi s_{m,n}}{\lambda} \sin\frac{\phi}{2}$$ and

$s_{m,n}$ is the distance between the m th and n th electron.

By evaluating the summation in equation 15 it can be found, that the intensity of the scattered radiation in a direction ϕ $(I_\phi^{(Z)})$, is proportional to Z for large values of x , and proportional to Z^2 for small values of x . For constant $s_{m,n}$, large values of x correspond to short waves and large scattering angles, whereas small values of x correspond to long waves and small scattering angles. On the other hand, since with increasing atomic number (Z) the distance between the electrons becomes smaller, the scattered intensity for large values of $s_{m,n}$ should be proportional Z (for light elements) and for small values of $s_{m,n}$ (heavy elements) proportional to Z^2 .

The next step is the calculation of the intensity of the radiation scattered by a group of electrons which move independently of each other about an atomic

nucleus.[12] It can be shown that the scattered radiation consists of two parts, the coherent and incoherent radiation. The intensity at a point $P(r,\phi)$ is:

$$(16.) \quad I_\phi = I_e\left[Z + \sum_{\substack{m=1 \\ m\neq n}}^{Z} \sum_{n=1}^{Z} \cos(\delta_m - \delta_n) \right]$$

where $\delta_1, \delta_2, \ldots \delta_Z$ are the phases of the waves scattered by the Z electrons to the point P, and

I_e the intensity due to one electron given by equation 10.

Since the electrons are moving independently and do not remain at fixed distances from each other, the phase differences between the rays scattered will change accordingly, and therefore we have to take the statistical average for

$\cos(\delta_m - \delta_n)$ which gives:

$$(17.) \quad \left[\int_0^\infty u(a) \frac{\sin ka}{a} \, da \right]^2 = f^2$$

where $u(a)\,da$ is the probability that any particular electron will lie between a and $a + da$,

a is the distance of the electron from the centre of the atom and

$k = \frac{4\pi}{\lambda} \sin\frac{\phi}{2}$

f is called the "electronic structure factor". Equation 16 becomes then

$$(18.) \qquad I_\phi = I_e\left[Z+(Z^2-Z)f^2\right]$$

The coherent scattered radiation can be calculated to be $I_c = I_e Z^2 f^2$; therefore the incoherent part is given by

$$I_i = I_\phi - I_c = I_e Z\left(1-f^2\right),$$

and the intensity scattered by such an atom becomes:

$$(19.) \qquad I_\phi = \underbrace{I_e Z^2 f^2}_{\text{coherent}} + \underbrace{I_e Z\left(1-f^2\right)}_{\text{incoherent}}$$

A generalisation of these considerations was given by Woo and Jauncey[13] by assuming each electron in the atom to have its own probability $u_n(a)\,da$ of lying between distances a and $a+da$ from the centre of the atom. (Equation 19 was derived on the assumption, that the probabilities for the different electrons are the same, thus making no distinctions between K, L, M... electron groups). The intensity is then found to be

$$(20.) \qquad I_\phi = I_e\left(F^2+Z-\sum_{n=1}^{Z} f_n^2\right) \qquad \text{where}$$

$$(21.) \qquad F = \sum_1^Z f_n = \sum_1^Z \int_0^\infty u_n(a)\,\frac{\sin ka}{ka}\,da\,,$$

is the "atomic structure factor". Values of F for a number of atoms were determined by James and Brindley.[14]

The application of equation 20 is, however, restricted to atoms with electron distributions having a spherical symmetry. This should only be true for atoms with completed electron shells, e.g. the inert gases. Experiments[15] have shown that equation 20 does not give a true representation of the electron distribution within the atom, but it has shown the way that by comparing observed scattering intensities with those calculated for the electron distributions of the various atomic theories, a means is provided of studying the extranuclear structure of atoms.

Many properties of scattered X-rays can be accounted for, qualitatively and quantitatively, on the classical theory of scattering, but it failed completely to account for the decrease in scattered intensity when very short waves are being scattered at large angles. Although many attempts,[16] based on classical electrodynamics, have been made to account for this diminution of scattered intensity, all of them have been equally unsuccessful, since none of them could account for the change of wave length of scattered radiation (Compton effect).[17]

(b) Quantum Theory (Corpuscular Theory).

According to the classical theory of scattering, the frequency of the scattered radiation should be the same as that of the primary radiation. Spectroscopic

investigation of the scattering from light elements shows, however, that the scattered radiation consists of two distinct lines, one being of the same wave length as the primary radiation (unmodified line), the other one being of slightly longer wave length (modified line). The scattered radiation of changed wave length corresponds to the incoherent radiation of the classical theory (although the latter cannot account for the change in wave length). To explain this change in wave length, Compton[18] made a daring but very successful application of the quantum theory. He assumed the primary radiation to consist of photons, which, according to Einstein, are definitely directed quanta of radiant energy, which can be scattered by individual electrons. Each photon possesses energy $h\nu$ and momentum $\frac{h\nu}{c}$. Treating the scattering process as a collision of two perfectly elastic particles (photon and electron), Compton arrives at the following result:

$$(22.) \qquad \delta\lambda = \frac{h}{mc}(1-\cos\phi)$$

where $\frac{h}{mc} = 0{\cdot}0243$ Å.U.

h being Planck's constant

$\delta\lambda = \lambda' - \lambda$ the change in wavelength between modified (λ') and unmodified (λ) radiation, and

ϕ = angle of scattering.

It has been found that equation 22 is in complete

agreement with experiment.[19] The theory predicts a change in wave length independent of the wave length of the primary radiation, that it should be the same for all substances, and that the change of wave length should increase for large scattering angles. Moreover, from the derivation of equation 22, it follows that, associated with the scattering process, there should be a type of β-radiation (recoil electrons) of a certain energy and ejected in a definite direction. Energy and direction of a β-ray, stand in exact mathematical relationship with the energy and direction of the corresponding scattered photon. This is in sharp contrast to the classical theory. From the excellent agreement between theory and experiment it can be concluded that the modified line is being brought about by a scattering from electrons which are free or loosely bound (their binding energy being very small compared with the energy of the primary radiation). On the other hand, if an electron is firmly bound within an atom, it has to be assumed that the scattering atom as a whole receives the impulse of the photon and in this case the wave length change $\delta\lambda$ will be smaller by a factor $\frac{\text{mass of electron}}{\text{mass of atom}}$. $\delta\lambda$ will then be so small that it is impossible at present to detect it. This corresponds to the unmodified line.

In further agreement with this theory of photon scattering is the fact that for ordinary light all the

energy of the scattered radiation should be in the unmodified line,[20] whereas for γ -rays nearly all scattered radiation should be modified.[21]

A defect of the corpuscular theory of X-ray scattering is its inability to account for the polarization of primary and scattered radiation.

(c) Wave Mechanical Theory.

We are faced with the facts that the undulatory theory fails to explain the Compton change of wave length and the corpuscular theory fails to explain polarization, though there is experimental proof of the dualistic nature of radiation. It is however possible, with the help of de Broglie's wave mechanics to bring these two conceptions of the nature of radiation into a unified whole, thus providing the basis for a new theory of scattering of X-rays, which, as far as it has been tested, shows remarkably good agreement with experiment.

Schrödinger [22] succeeded in showing that a simple application of wave mechanics leads to exactly the same results regarding the relation between frequency and direction of scattering of the Compton effect, as were obtained from the photon theory (equation 22). The scattering can be regarded as a diffraction of X-ray waves on a Bragg-grating. This grating is formed by two superposing ψ -waves (representing the electron) which move in opposite

directions to each other.

The calculation of the intensity of the radiation scattered by a free electron in a direction ϕ , leads according to this theory to the following formula, which was first derived by Breit[23] for the incoherent radiation.

$$(23.) \qquad I_\phi = I_e \cdot (1+\alpha \operatorname{vers} \phi)^{-3} = I_e \cdot \left(\frac{\nu'}{\nu}\right)^3$$

where I_e represents the value calculated on the classical theory (equation 10),

$$\alpha \equiv \frac{h\nu}{mc^2}$$ and

$$\operatorname{vers} \phi \equiv 1 - \cos\phi \, .$$

Integrating equation 23 in respect of ϕ , we obtain the fraction of the energy of the primary beam which is scattered (the scattering coefficient):

$$(24.) \qquad \sigma = \sigma_0 \frac{3}{4} \cdot \frac{1+\alpha}{\alpha^3} \left\{ \frac{2\alpha(1+\alpha)}{1+2\alpha} - \log(1+2\alpha) \right\}$$

where σ_0 is the classical scattering coefficient by a single electron as given by equation 13.

A further improvement of this theory was given by Klein and Nishina[24] on the basis of the relativistic quantum-mechanics, developed by Dirac.[25] Dirac's quantum-mechanics is invariant with Lorentz transformations, and, should accordingly hold for all velocities. According to this theory, the incoherent scattered intensity by a free electron is

$$(25.) \qquad I_\phi = I_e (1+\alpha \operatorname{vers} \phi)^{-3} \left[1 + \frac{\alpha^2 \operatorname{vers}^2 \phi}{(1+\cos^2\phi)(1+\alpha \operatorname{vers} \phi)} \right]$$

and

$$(26.)\quad \sigma = \frac{3}{4}\sigma_0 \left\{ \frac{1+\alpha}{\alpha^3}\left[\frac{2\alpha(1+\alpha)}{1+2\alpha} - \log(1+2\alpha)\right] + \right.$$

$$\left. + \frac{1}{2\alpha}\log(1+2\alpha) - \frac{1+2\alpha}{(1+3\alpha)^2} \right\}$$

Equation 25 differs from equation 23 only by a term proportional to α^2 which, according to Klein and Nishina,[26] represents an almost completely unpolarized ray.

An experimental test of equation 24 and 26 was carried out in the hard X-ray region by Read and Lauritsen[27] and in the γ-ray region by Chao.[28] There is, as already mentioned, absolutely no agreement between experiment and classical theory (according to classical theory $\frac{\sigma}{\sigma_0} = 1{\cdot}00$). As regards Breit's formula 24, the agreement with experiment is not very good which, of course, is only to be expected since for the radiations used (very short wave lengths), the relativity correction is very marked and equation 24 does not take account of this. The Klein-Nishina formula (equation 26) is however completely verified for the wave length range investigated.

It was shown by Sommerfeld and Wentzel[29] and later more accurately by Dirac[30] that, according to wave mechanics, the resulting scattered radiation, apart from the additional term in Klein-Nishina's relativistic formula 25) should be polarized just as on the classical theory, which is in excellent agreement

(31)

with experiment. Experiments with very short waves, have completely confirmed Nishina's prediction of an unpolarized component of the scattered radiation proportional to α^2 (i.e. ν^2), although for medium and longer waves, the scattered radiation shows complete polarization.

Sommerfeld and Wentzel[29] developed the wave-mechanical theory for the case of scattering from bound electrons, in which case, interference effects between the rays scattered from different electrons in the atom become very marked. Wentzel[32] calculated the intensity for an atom with many electrons, which then would allow a comparison with experiment. He found this expression for the intensity of the unmodified radiation

(27.)

$$I_{unm.} = I_e \left[\sum_k \iiint (\psi_k \psi_k^*) \cos(k_1 a \cos\alpha) \, d\tau \right]^2$$

where I_e is the intensity due to the classical scattering for one electron

ψ_k the wave function of order k ,

ψ_k^* the conjugate complexe of ψ_k

$\psi_k \cdot \psi_k^*$ a function of order k proportional to the electric charge density at any point,

$k_1 \equiv \frac{4\pi}{\lambda} \sin\frac{\phi}{2}$ and

$k_1 a \cos\alpha$ the phase difference between a wave scattered from the centre of the atom,

and from the volume element $d\tau$ at a distance a from the centre.

In analogy to the classically calculated value of the unmodified intensity in equation 19 we can write:

$$(28.) \qquad \iiint (\psi_k \psi_k^*) \cos(k, a\cos\alpha)\, d\tau \equiv f_{kk}$$

where f_{kk} is identical with the "electronic structure factor" (equation 17).

This definition of the "electronic structure factor" is more general than that leading to the classical value of equation 17, since no assumption has been made regarding the spherical symmetry of the electron distribution of the atom.

Equation 27 can no be written:

$$(29.) \qquad I_{unm.} = I_e \left[\sum_k f_{kk}\right]^2$$

and using the "atomic structure factor" of equation 21

$$I_{unm.} = I_e F^2$$

The intensity of the modified radiation was found to be:

$$(30.) \qquad I_{mod.} = I_e \left(Z - \sum_k f_{kk}^2\right)$$

which however, is only an approximation since a factor $\left(\frac{\nu'}{\nu}\right)^3$ has been omitted in the derivation of this formula.

According to Wentzel the total scattering inten-

sity in a direction ϕ is therefore:

$$(31.) \qquad I_\phi = I_e \left\{ \left(\sum_k f_{kk} \right)^2 + Z - \sum_k f_{kk}^2 \right\}$$

which is a generalized form of equation 20 derived from classical theory.

An exact derivation of the intensity of the modified ray was given by Waller and Hartree[33] by taking account of the electron spin. Equation 30 becomes then:

$$(32.) \qquad I_{mod.} = I_e R \left\{ Z - \sum_k f_{kk}^2 - \sum_{k \neq l} \sum f_{kl}^2 + Z I_M \right\}$$

where $R = \left(\frac{\nu'}{\nu} \right)^3$ and

$$I_M = \frac{\alpha^2 \, vers \, \phi}{(1 + \cos^2 \phi)(1 + \alpha \, vers \, \phi)}$$

which is the second term in Klein-Nishina's expression (equation 25).

In the light of the latest development in theory, the complete expression for the intensity of the scattered radiation becomes therefore:

$$(33.) \qquad I_\phi = I_{unm.} + I_{mod.} =$$

$$= I_e \cdot \left\{ \left(\sum_k f_{kk} \right)^2 + R \left(Z - \sum_k f_{kk}^2 - \sum_{k \neq l} \sum f_{kl}^2 + Z I_M \right) \right\}$$

Waller and Hartree's correction is very small and can generally be neglected, but in extreme cases it may

amount to as much as 10% of the incoherent scattering intensity. If on the other hand the wave length of the radiation is not too short, then the term ZI_M (Klein-Nishina's relativity correction) can be neglected also.

This theory as far as it has been tested shows very good agreement with experiment. One example already mentioned is the diminishing polarization for very short waves, due to Klein-Nishina's relativity correction term ZI_M . Using Hartree's approximation of the wave mechanical electron distribution in the atom[34] the study of the scattering of X-rays from monatomic[35] and diatomic gases,[36] has confirmed the predictions of wave mechanics. Experiments on the diffuse scattering of X-rays by a single crystal of NaF ,[37] have supplied a very good test for the incoherent scattering. The angular distribution of scattered β -rays[38] and X-rays of very short wave length,[39] show very good agreement with theory.

We can use equation 33 to calculate the intensity of the radiation scattered at 90° (making use of the fact that Waller and Hartree's electron spin correction and Klein and Nishina's relativity correction can be neglected), and compare this theoretically found value with the experiments performed in this work. A calculation of this kind was first carried out by Miss M.A.S. Ross[40] based on the values of $\sum f_{kk} = F$ and $\sum f_{kk}^2$ as determined by James and Brindley[14]

and tabulated in Compton and Allison (loc. cit.) on page 781 and 782. The values calculated on table 1 from equation 33 give:

$$\left(\Sigma f_{kk}\right)^2 + R\left(Z - \Sigma f_{kk}^2\right) = \frac{I_{90}}{I_e} \quad \text{i.e.}$$

the intensity of the radiation scattered at 90° relative to Thomson's classical value for a single electron.

It has to be pointed out, however, that the intensities could only be calculated up to values of $\frac{1}{\lambda}\cdot\sin\frac{\phi}{2} = 1{\cdot}1$. Values of Σf_{kk} and Σf_{kk}^2 have not been determined for $\frac{1}{\lambda}\cdot\sin\frac{\phi}{2} > 1{\cdot}1$. This corresponds to a shortest wave length of 0.64 Å.U. and an excitation peak voltage of approx. 19 KV. Since in the present work, the voltage on the tube was varied from 30 KV to 90 KV, i.e. well above the calculated region, it is evident that these calculations cannot furnish the exact interpretation of the experimental result. They are nevertheless very useful, because, being the only theoretical approach to this extremely complicated problem of X-ray scattering, they supply ample information as regards the kind of result that is to be expected and how it is to be interpreted.

The intensities are calculated for hydrogen, carbon, oxygen and aluminium. Values for paraffin wax (approx. $C_n H_{2n}$) and filter paper (cellulose $C_6 H_{10} O_5$) are calculated from the chemical formulae. Fig. 3 is a graphical representation of the

TABLE 1. CALCULATED INTENSITIES OF SCATTERED X-RAYS AT VARIOUS WAVELENGTHS.
(radiation scattered at 90° to primary)

$1/\lambda . \sin \phi/2$ ($\phi = 90^\circ$)	0·0	0·1	0·2	0·3	0·4	0·5	0·6	0·7	0·8	0·9	1·0	1·1
Wavelength in Å.U.	∞	7·07	3·53	2·36	1·77	1·41	1·18	1·01	0·88	0·79	0·71	0·64
Hydrogen Z = 1; F^2	1·00	0·66	0·23	0·06	0·02	0·00	0·00	0·00	0·00	0·00	0·00	0·00
$Z - \Sigma f_{kk}^2$	0·00	0·34	0·77	0·94	0·98	1·00	1·00	1·00	1·00	1·00	1·00	1·00
$R(Z - \Sigma f_{kk}^2)$	0·00	0·34	0·76	0·92	0·95	0·96	0·95	0·94	0·92	0·92	0·90	0·90
$F^2 + R(Z - \Sigma f_{kk}^2)$	1·00	1·00	0·99	0·98	0·97	0·96	0·95	0·94	0·92	0·92	0·90	0·90
I_{90}/I_e	1·00	1·00	0·99	0·98	0·97	0·96	0·95	0·94	0·92	0·92	0·90	0·90
Carbon Z = 6; F^2	36·00	21·16	9·00	4·84	3·61	2·89	2·56	1·96	1·69	1·44	1·00	0·81
$Z - \Sigma f_{kk}^2$	0·00	2·00	3·30	4·20	4·50	4·70	5·00	5·20	5·30	5·40	5·50	5·60
$R(Z - \Sigma f_{kk}^2)$	0·00	1·98	3·24	4·10	4·35	4·51	4·75	4·91	4·88	4·94	4·97	5·02
$F^2 + R(Z - \Sigma f_{kk}^2)$	36·00	23·14	12·24	8·94	7·96	7·40	7·31	6·87	6·57	6·38	5·97	5·83
I_{90}/I_e	6·00	3·86	2·04	1·49	1·33	1·23	1·22	1·15	1·10	1·06	1·00	0·97

TABLE 1 (contd.)

$1/\lambda . \sin \phi/2$ ($\phi = 90^\circ$)	0.0	0.1	0.2	0.3	0.4	0.5	0.6	0.7	0.8	0.9	1.0	1.1
Oxygen $Z = 8$; F^2	64.00	50.41	28.09	15.21	8.41	4.84	3.24	2.56	2.25	1.96	1.82	1.56
$Z - \Sigma f_{kk}^2$	0.00	1.60	4.10	5.60	6.00	6.40	6.50	6.70	6.80	6.90	7.10	7.20
$R(Z - \Sigma f_{kk}^2)$	0.00	1.59	4.03	5.47	5.80	6.14	6.18	6.32	6.26	6.31	6.42	6.45
$F^2 + R(Z - \Sigma f_{kk}^2)$	64.00	52.00	32.12	20.68	14.21	10.98	9.42	8.88	8.51	8.27	8.24	8.01
I_{90}/I_e	8.00	6.50	4.02	2.59	1.78	1.37	1.18	1.11	1.06	1.03	1.03	1.00
Aluminium $Z = 13$; F^2	169.00	121.00	80.10	60.06	43.56	30.25	20.25	13.69	9.61	7.02	5.29	4.00
$Z - \Sigma f_{kk}^2$	0.00	2.80	5.20	7.00	8.50	9.60	10.40	10.80	11.10	11.30	11.50	11.60
$R(Z - \Sigma f_{kk}^2)$	0.00	2.77	5.11	6.83	8.22	9.22	9.88	10.20	10.22	10.34	10.40	10.40
$F^2 + R(Z - \Sigma f_{kk}^2)$	169.00	123.77	85.21	66.89	51.78	39.47	30.13	23.89	19.83	17.36	15.69	14.40
I_{90}/I_e	13.00	9.52	6.55	5.14	3.98	3.04	2.32	1.83	1.52	1.34	1.21	1.11
Filter paper (cellulose $C_6H_{10}O_5$) I_{90}/I_e	6.35	4.74	2.84	1.94	1.49	1.27	1.17	1.10	1.06	1.03	1.00	0.98
Paraffin wax (approx. $C_n H_{2n}$) I_{90}/I_e	4.75	3.14	1.78	1.36	1.24	1.17	1.15	1.09	1.08	1.03	0.97	0.95

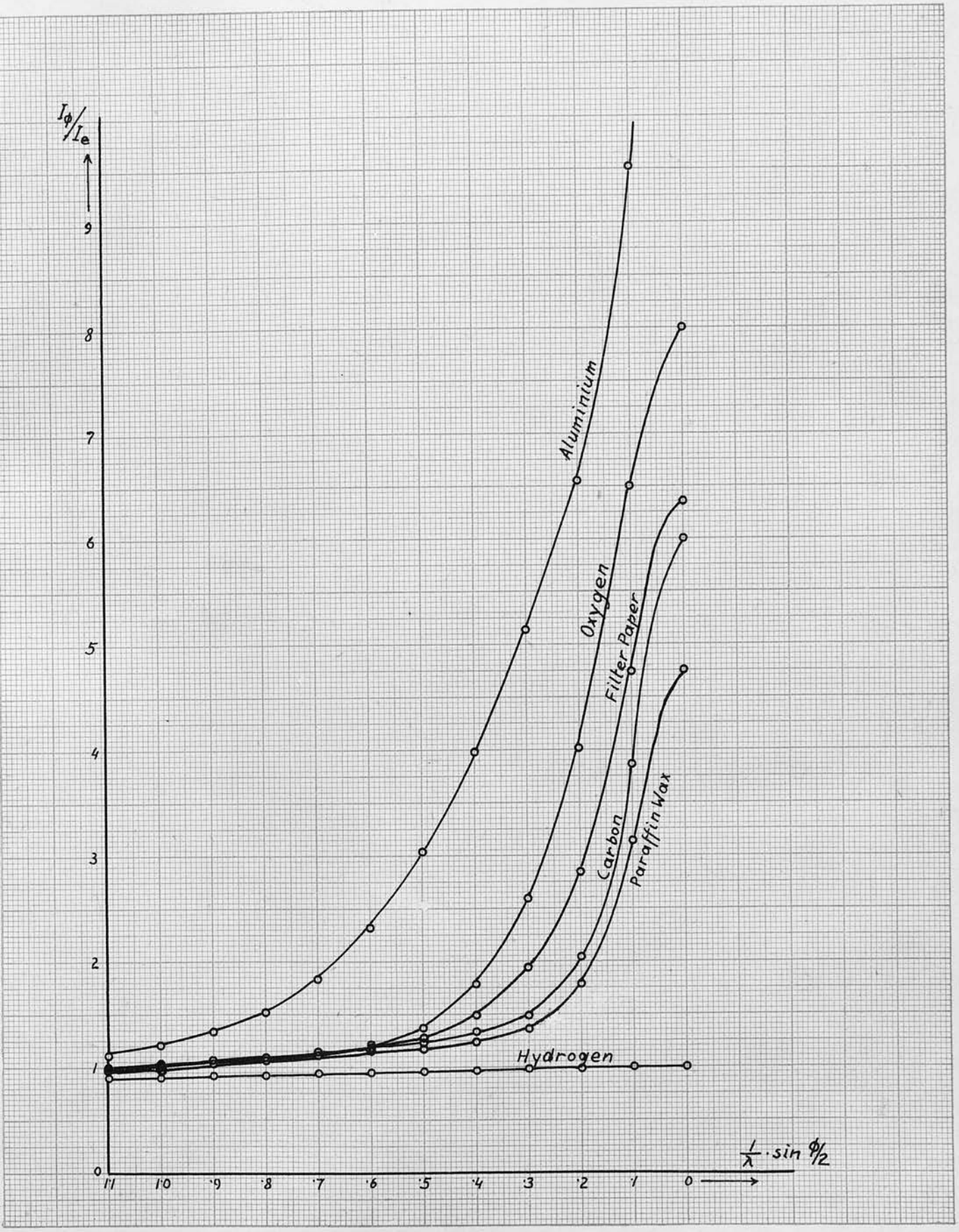
I_ϕ/I_e
9
8
7
6
5
4
3
2
1
0
Aluminium
Oxygen
Filter Paper
Carbon
Paraffin Wax
Hydrogen
$\frac{1}{\lambda}\cdot\sin\phi/2$
·11
·10
·9
·8
·7
·6
·5
·4
·3
·2
·1
0

Fig. 3.

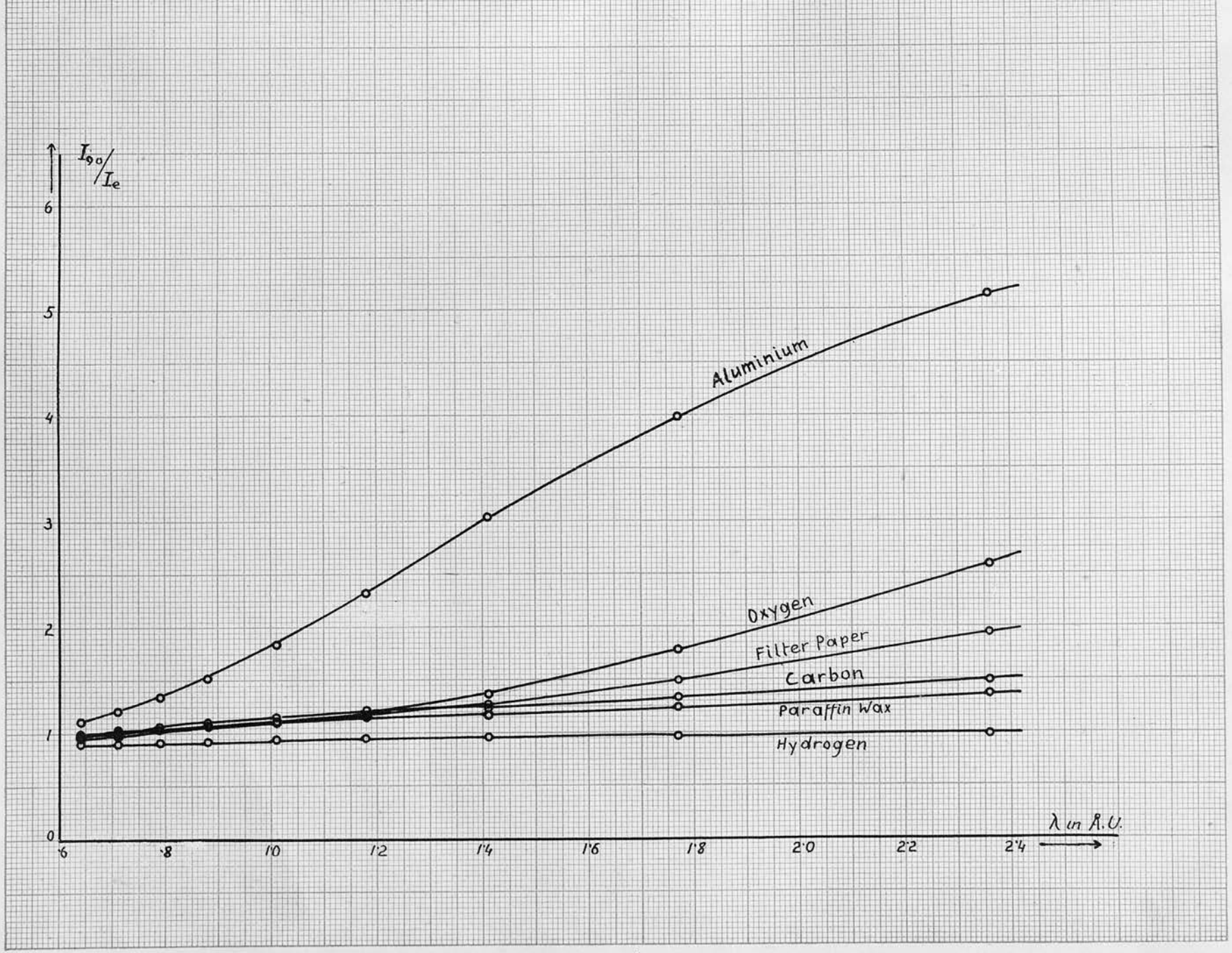
I_{90}/I_e
6
5
4
3
2
1
0
Aluminium
Oxygen
Filter Paper
Carbon
Paraffin Wax
Hydrogen
·6
·8
1·0
1·2
1·4
1·6
1·8
2·0
2·2
2·4
λ in Å.U.

Fig. 4.

results of table 1, the scattered intensity being plotted against $\frac{1}{\lambda} \cdot \sin \frac{\phi}{2}$. Fig. 4 is identical with Fig. 3, the intensity plotted against the wave length.

Since in the present work only heterogeneous X-ray beams have been used, equation 33 would have to be integrated over all possible wave lengths. This is however impossible, since the intensity-wave length distribution is unknown. An integration would in general lower the slope of the graph. The calculated results apply however only to wave lengths above 0·64 Å.U. For wavelengths between 0·64 Å.U. and 0·136 Å.U. (at 90 KV) the factor $R = \left(\frac{\nu'}{\nu}\right)^3$ becomes very marked and $\frac{I_{90}}{I_e}$ would decrease with decreasing wave length. Taking into consideration heterogeneous radiation (for wave lengths above 0·136 Å.U.) we would therefore expect the following result:

For hydrogen, the intensity of the scattered radiation will be nearly independent of $\overline{\mu/\rho}$. (In fact there will be a slight decrease of the intensity for decreasing wave length).

For carbon, oxygen, paraffin wax and filter paper, the intensity of the scattered radiation increases slowly with increasing $\overline{\mu/\rho}$.

For aluminium, the intensity of the scattered radiation increases markedly with increasing $\overline{\mu/\rho}$.

The increase of the intensity of the scattered radiation with increasing $\overline{\mu/\rho}$ is proportional to the atomic number of the scatterer.

There is however another important correction which has to be applied when interpreting experimental results, namely, the wave length sensitivity of the ionization chambers. The energy required to produce a pair of ions in a gas is independent of the wave length of the radiation. If the whole of the radiation is absorbed in the gas before it reaches the walls of the ionization chamber, then the ionization-current will be proportional to the intensity of the radiation, no matter what the wave length. The ionization chamber would in this case be the ideal instrument to measure X-ray intensities. As it is not very practical to build the chambers large enough to absorb all of the radiation (especially when they are filled with some heavy gas,) Allison and Andrews,[41] using a number of approximations, have shown that a correction has to be applied for the energy escaping from the chamber in the form of X-rays. Based on this calculation, Miss Ross [40] worked out a correction for the ionization chambers used by her. The ionization chambers used in this work were almost identical in dimensions to those used by Miss Ross in her work. She has shown that, to a first approximation, classical and modified scattered radiations produce equal ionizations in the particular ionization chambers used. To a high degree of accuracy this correction compensates the factor $R = \left(\frac{\nu'}{\nu}\right)^3$ of equation 33. Thus, the scattered radiation may then be treated as a pure classical scattered radiation except when the

absorption between scatterer and ionization chamber is sufficient to introduce measurably different reductions in the intensities of modified and unmodified radiations, which is hardly the case in the scattering experiments to be described later. Owing to the fact that the ionization chamber is more sensitive to soft than to hard radiation, a relatively larger correction will have to be applied at the hard end of the spectrum. When this correction is applied to the theoretically obtained values (Figs. 3 and 4) for the intensity of the scattered radiation, the following result is obtained:

The relative ionization (produced by the radiation scattered at 90° per unit intensity of the primary per scattering electron) will increase with increasing wave length. The amount of increase of relative ionization is least for hydrogen and increases in the following order of scatterers: paraffin wax, carbon, filter paper, oxygen, aluminium.

THEORY OF X-RAY ABSORPTION.

When a homogeneous X-ray beam traverses a thickness x of a material, some of its energy will be absorbed. The diminution of intensity follows an exponential law and can be represented by

(34.) $$I = I_0 e^{-\mu x}$$ where

I_0 is the intensity of the beam before traversing the material,

I the intensity after having traversed the thickness x of the material.

μ is a factor which depends on the wave length and on the absorbing material. It is called the "total linear absorption coefficient" and is defined as the fraction of energy, absorbed per cm^3 of traversed material.

The most commonly used form of the absorption formula is obtained, by defining the total mass absorption coefficient μ/ρ (ρ density of absorber) which is the fraction of the energy absorbed per unit mass of the substance per unit cross sectional area. The advantage of using the total mass absorption coefficient (or mass absorption coefficient) is, that it is independent of the physical state of the absorber (to a certain approximation). The absorption law then becomes

$$(35.) \qquad I = I_0 e^{-\mu/\rho \cdot \rho x} \qquad \text{or}$$

$$\mu/\rho = \frac{1}{\rho x} \log \frac{I_0}{I}$$

In order to carry out accurate measurements of μ/ρ the following precautions have to be taken:

(1) The radiation has to be homogeneous. This point is extremely important for, if a heterogeneous beam is used, the longer waves will be more absorbed in

the first layers of the absorber, thus changing the wave length-intensity distribution within the substance. The fraction of the absorbed energy decreases with increasing thickness x, whereas in the case of homogeneous radiation it should remain constant.

(2) The beam must be limited by small apertures and must have a small divergence if the radiation has to traverse equal thicknesses of the absorber.

(3) The rapid increase of absorption coefficient with atomic number makes it necessary that if the absorber is a substance of low atomic weight (carbon, or as commonly used, aluminium), it must be free from impurities of heavy elements. If on the other hand heavy elements are used as absorbers and therefore have to be rather thin, special care has to be taken to ensure uniform thickness.

It is important to distinguish between two types of absorption processes, namely the true (or photo electric) absorption (τ) and the scattering absorption (σ). Therefore, the total linear absorption coefficient can be written:

(36.) $$\mu = \tau + \sigma$$

and the mass absorption coefficient:

$$(37.)\quad \mu/\rho = \frac{\tau}{\rho} + \frac{\sigma}{\rho}$$

($\frac{\sigma}{\rho}$ mass scattering coefficient).

Many attempts have been made to establish a relation between the mass absorption coefficient on one side, and wave length and atomic number of the absorber on the other side.(42) Summing up the results of the researches on this subject, we can write as a general equation:

$$(38.)\quad \mu/\rho = \frac{N}{A} \cdot C \cdot Z^m \cdot \lambda^n + \frac{N}{A}\sigma(Z,\lambda)$$

where N is Avogadro's number

A the atomic weight, and

Z the atomic number.

By comparison with equation 37, the first term of the sum is identical with the true absorption and the second term with the scattering absorption (which includes both modified and unmodified radiation).

Much work has been done on the difficult problem, of finding the proper values for the exponents m and n of equation 38. Although this problem is still far from being solved (as research on this subject is extremely difficult to carry out, the various authors obtain different values), we are perfectly justified in putting $n = 3$, at least to a very close approximation and $m = n + 1 = 4$. The constant C

changes its value abruptly whenever a critical absorption limit is reached. The change of C is given by the absorption jump ratio $r = \frac{C_1}{C_2}$ where C_1 is the value of C on the short wave length side, and C_2 the value of C on the long wave length side of the critical absorption limit.

For heavier elements and longer waves, $\sigma(Z,\lambda)$ is very small compared with $C \cdot Z^m \cdot \lambda^n$, and can be neglected. For light elements and short waves, its value becomes quite appreciable. Using the classical value for σ from equation 13 we obtain:

$$\frac{N}{A}\sigma(Z,\lambda) = \frac{\sigma}{\rho} = \frac{8\pi}{3} \cdot \frac{L.Z}{\rho} \cdot \frac{e^4}{m^2c^4} \doteq 0{\cdot}20$$

(L, number of atoms per cm^3)

This is only an approximation, and a discussion on t his point has been given in the previous section.

It has to be pointed out that a theoretical treatment of this question is extremely difficult and complicated. It is, however, quite sufficient for our purpose here to neglect this term without introducing too large an error. Equation 38 can now be written as:

$$(39.) \qquad \mu/\rho = \frac{N}{A} \cdot C \cdot Z^4 \cdot \lambda^3 = C' \cdot \lambda^3$$

where C' is a constant for a given substance.

Let us consider a primary beam of intensity P_o and wavelength λ . This primary beam produces an unmodified scattered beam of intensity $S_o^{(u)}$ and

wavelength λ , and a modified scattered beam of intensity $S_o^{(M)}$ and wave length $\lambda+\delta\lambda$, where $S_o^{(U)} + S_o^{(M)} = S_o$ the total scattered intensity and $\delta\lambda$ the Compton change in wave length. If both, primary and secondary beams, pass through equal thicknesses x of absorbing material, the intensities, as measured in the ionization chambers, will be given by

$$P = P_o e^{-\mu_p \rho x}$$

$$S^{(U)} = S_o^{(U)} e^{-\mu_p \rho x}, \quad S^{(M)} = S_o^{(M)} e^{-\mu_M \rho x}$$

where μ_p and μ_M are the mass absorption coefficients for the primary (and unmodified) and modified beam respectively, and $\mu_M > \mu_p$.

$$S = S^{(U)} + S^{(M)} = S_o^{(U)} e^{-\mu_p \rho x} + S_o^{(M)} e^{-\mu_M \rho x}$$

Therefore the relative intensity S/P will be:

(40.)
$$\frac{S}{P} = \frac{S_o^{(U)}}{P_o} + \frac{S_o^{(M)}}{P_o} \cdot e^{-(\mu_M - \mu_p)\rho x}$$

From equation 39 we have:

$$\mu_p = C \cdot \lambda^3 \qquad \text{and} \qquad \mu_M = C(\lambda+\delta\lambda)^3$$

$$\mu_M - \mu_p = C\left[(\lambda+\delta\lambda)^3 - \lambda^3\right]$$

Equation 40 now becomes:

(41.)
$$\frac{S}{P} = \frac{S_o^{(U)}}{P_o} + \frac{S_o^{(M)}}{P_o} \cdot e^{-C\left[(\lambda+\delta\lambda)^3 - \lambda^3\right]\rho x}$$

From this relation, we can draw certain conclusions. If $\lambda \gg \delta\lambda$ i.e. in the case of long waves, we can write $\lambda + \delta\lambda \doteq \lambda$ or $\delta\lambda \doteq 0$. This is the region where the Compton change of wave length can be neglected. We get

$$\frac{S}{P} = \frac{S_o^{(U)}}{P_o} + \frac{S_o^{(M)}}{P_o} \cdot / = \frac{S_o}{P_o}$$

The ratio $\frac{S}{P}$ remains constant whatever the thickness of the absorber; both primary and secondary beams are of the same wave length. In regions where the Compton effect cannot be neglected i.e. where $\delta\lambda$ is comparable with λ , the ratio decreases exponentially with increasing thickness of absorber and approaches, for very great values of x , the constant ratio $\frac{S_o^{(U)}}{P_o}$ for the unmodified radiation.

The theory discussed so far applies only to strictly homogeneous radiation. Since all the experiments in this work were carried out using the entire radiation emitted by the X-ray tube, i.e. heterogeneous radiation, it is therefore necessary to correct the theory for heterogeneous beams. An exact solution of this problem is extremely difficult since as mentioned already, a theoretical intensity wave length function is unknown as yet.

Since the heterogeneous radiation is composed of homogeneous constituents, the intensities of which depend on the particular wave length, the correct procedure would be to work out the solution for a

homogeneous radiation and integrate this result over all possible wave lengths. The wave lengths can assume any value from a certain shortest wave length (which depends on the excitation voltage on the tube) to infinity. This, of course, implies the use of the principle of superposition which states that the intensity of the entire heterogeneous radiation is equal to the sum of the intensities of the individual homogeneous components, i.e. if $I(V)$ is the intensity of the heterogeneous beam and

$$I_1(\lambda_1,V),\ I_2(\lambda_2,V)\ldots\ I_i(\lambda_i,V)\ldots$$ the intensities of the homogeneous constituents, we have:

$$I(V) = I_1(\lambda_1,V) + I_2(\lambda_2,V) + \cdots + I_i(\lambda_i,V) + \cdots$$

or

(42.) $$I(V) = \int_{\lambda=\lambda_V}^{\infty} I(\lambda,V)\,d\lambda$$

where $I(\lambda,V)$ is the intensity wave length distribution and

λ_V (the lower limit of λ) is a function of the voltage.

For a certain excitation voltage we can write:

(43.) $$I = \int_{\lambda=\lambda_V}^{\infty} I(\lambda)\,d\lambda$$

This problem can unfortunately not be solved since $I(\lambda)$ is not yet known. But even so, by making use of some approximations it is possible to draw certain

conclusions as regards the result.

If a homogeneous beam of intensity I_o passes through an absorber of thickness x , the intensity of the emergent beam will be given by:

$$I = I_o e^{-\mu/\rho \, \rho x} \qquad \text{or} \qquad \mu/\rho = \frac{1}{\rho x} \log \frac{I_o}{I}$$

For a heterogeneous beam we have:

$$I_1(\lambda_1) = I_{o,1}(\lambda_1)\, e^{-\mu/\rho(\lambda_1)\rho x}$$

$$I_2(\lambda_2) = I_{o,2}(\lambda_2)\, e^{-\mu/\rho(\lambda_2)\rho x}$$

$$\cdots\cdots\cdots$$

$$I_l(\lambda_l) = I_{o,l}(\lambda_l)\, e^{-\mu/\rho(\lambda_l)\rho x}$$

Therefore the total intensity of the beam will be:

$$\int_\lambda I(\lambda, x)\, d\lambda = \int_\lambda I_o(\lambda)\, e^{-\mu/\rho(\lambda)\rho x}\, d\lambda .$$

We can now define an "average mass absorption coefficient" $\overline{\mu/\rho}(x)$ so that

$$\int_\lambda I(\lambda, x)\, d\lambda = e^{-\overline{\mu/\rho}(x)\rho x} \int_\lambda I_o(\lambda)\, d\lambda$$

From equation 43 follows:

$$I(x) = I_o e^{-\overline{\mu/\rho}(x)\rho x}$$

or

(44.)
$$\overline{\mu/\rho}(x) = \frac{1}{\rho x} \log \frac{I_o}{I(x)}$$

Since $\overline{\mu/\rho}(x)$ varies for various thicknesses x of absorbing material ($\overline{\mu/\rho}(x)$ decreases as x increases), a method for determining $\overline{\mu/\rho}(x)$ must be

defined. The average mass absorption coefficient was always determined in aluminium for the primary beam only. The thickness of the absorbing aluminium was adjusted so as to give a 50% diminution of the ionization of the primary beam (i.e. $I(x) = \frac{1}{2} I_o$) where both intercepted and unintercepted beams were measured against a standard deflection in the secondary.

Applying equation 40 for heterogeneous radiation we get:

$$\frac{S}{P}(\lambda_1) = \frac{S_o^{(U)}}{P_o}(\lambda_1) + \frac{S_o^{(M)}}{P_o}(\lambda_1) \cdot e^{-[\mu_M(\lambda_1) - \mu_P(\lambda_1)]\rho x}$$

$$\frac{S}{P}(\lambda_2) = \frac{S_o^{(U)}}{P_o}(\lambda_2) + \frac{S_o^{(M)}}{P_o}(\lambda_2) \cdot e^{-[\mu_M(\lambda_2) - \mu_P(\lambda_2)]\rho x}$$

.....

$$\frac{S}{P}(\lambda_l) = \frac{S_o^{(U)}}{P_o}(\lambda_l) + \frac{S_o^{(M)}}{P_o}(\lambda_l) \cdot e^{-[\mu_M(\lambda_l) - \mu_P(\lambda_l)]\rho x}$$

and on integration we obtain:

$$\int_\lambda \frac{S}{P}(\lambda)\, d\lambda = \int_\lambda \frac{S_o^{(U)}}{P_o}(\lambda)\, d\lambda + \int_\lambda \frac{S_o^{(M)}}{P_o}(\lambda)\, e^{-[\mu_M(\lambda) - \mu_P(\lambda)]\rho x}\, d\lambda$$

$\int \frac{S}{P}(\lambda)\, d\lambda = \frac{S}{P}$ as measured in the ionization chambers

$$\int \frac{S_o^{(U)}}{P_o}(\lambda)\, d\lambda = \frac{S_o^{(U)}}{P_o}$$

$$\int \frac{S_o^{(M)}}{P_o}(\lambda)\, e^{-[\mu_M(\lambda) - \mu_P(\lambda)]\rho x}\, d\lambda =$$

$$= \int \frac{S_o^{(M)}}{P_o}(\lambda)\, e^{-(\overline{\mu_M} - \overline{\mu_P})\rho x}\, d\lambda = e^{-(\overline{\mu_M} - \overline{\mu_P})\rho x} \cdot \frac{S_o^{(M)}}{P_o}$$

where $\overline{\mu_M} = \overline{(\mu/\rho)}_M$ and $\overline{\mu_P} = \overline{(\mu/\rho)}_P$

$\overline{\mu_M} - \overline{\mu_P}$ decreases as x increases.

(45.) $$\frac{S}{P} = \frac{S_o^{(v)}}{P_o} + \frac{S_o^{(M)}}{P_o} \cdot e^{-(\overline{\mu_M} - \overline{\mu_P})\rho x}$$

The deductions which can be made from this equation are the same as for equation 41 for homogeneous radiation. There is, however, one difference. In the case of heterogeneous radiation $\overline{\mu_M} - \overline{\mu_P}$ is in the average smaller than $\mu_M - \mu_P$ for homogeneous radiation and therefore, S/P for heterogeneous radiation will decrease more slowly than S/P for homogeneous radiation. Apart from that, $\frac{S_o^{(v)}}{P_o}$ for heterogeneous radiation is bigger than $\frac{S_o^{(v)}}{P_o}$ for homogeneous radiation. Therefore, if heterogeneous radiation is employed, the function $S/P\,(x)$ should be a very flat curve decreasing with increasing x and the difference between $S/P\,(x)_{x=0}$ and $S/P\,(x)_{x=a}$ should be smaller than for the corresponding function for a homogeneous radiation. (See Fig. 5)

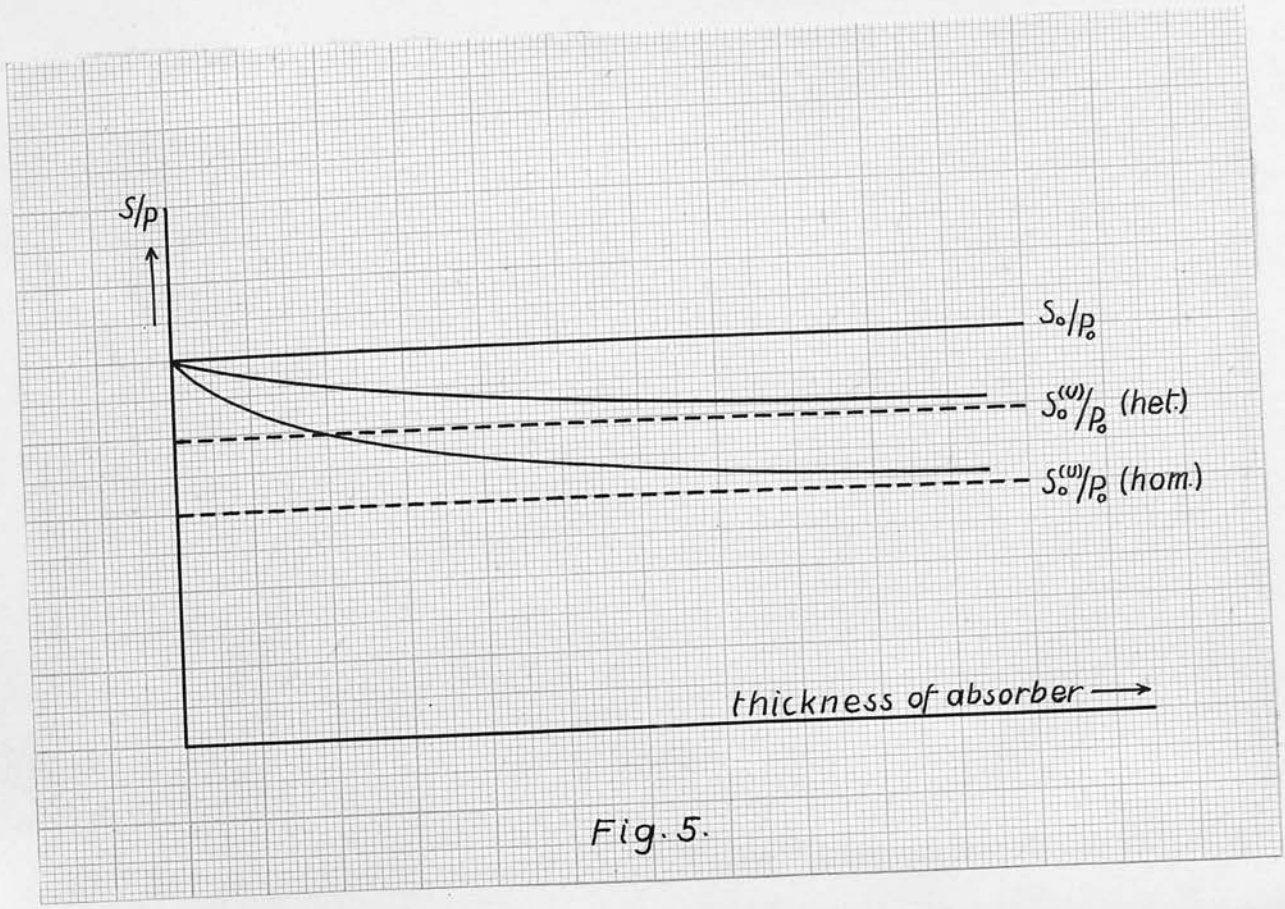

Fig. 5.

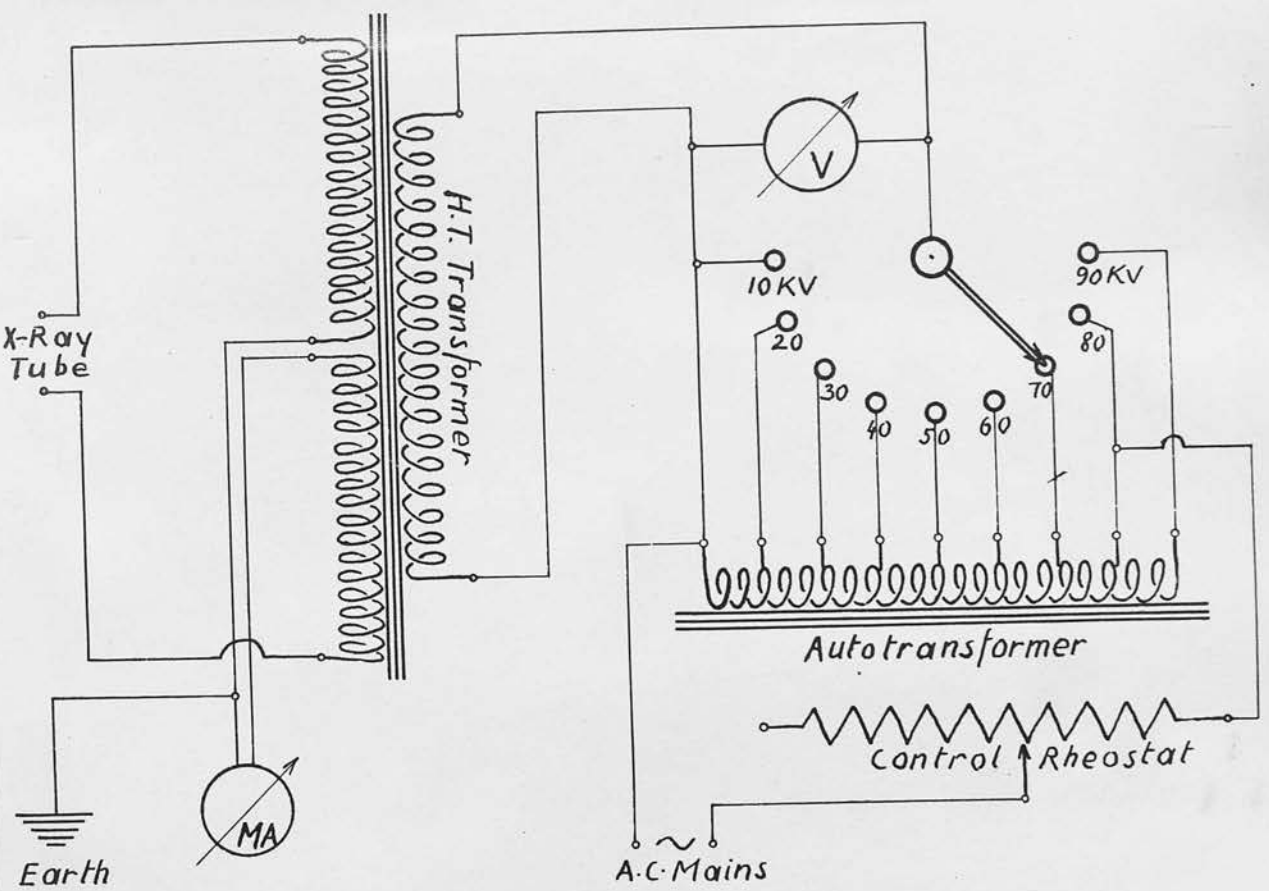

High Tension Supply

Fig. 6.

EXPERIMENTAL ARRANGEMENTS.

The X-ray Tubes.

The X-ray tubes used throughout this work were of the hot cathode type. A few experiments were carried out with an old gas tube excited by an induction coil but these were not satisfactory and are not mentioned here.

Coolidge Tube 18710

The filament of this tube is wound in the form of a spiral and surrounded by a small metal cup (for better focussing). The anode of the tube is made of tungsten, the exposed surface being inclined at 45° to the cathode ray stream. The focal spot is very broad, approx. 0·6 cms. in diameter. The maximum current is 1·5 MA at 90 KV. The anode, being cooled only by radiation, becomes red hot.

Coolidge Tube 31395.

This is the same type of tube as the one described above, with the same characteristics. The only difference is that, in this case, the radiation emitted is on the average much harder than that for the previous tube. This can be seen from the range of absorption coefficients measured in aluminium. The values are 2·27 at 90 KV and 5·18 at 30 KV, whereas those for the Coolidge Tube 18710 are 4·75 at 90 KV and 9·0 at 30 KV. The tube is now out of action, having been punctured.

Philips Metalix Heavy Anode Tube No I 1325, Type 20620.

This is a very powerful modern tube, with which most of the experiments discussed here, have been performed. The anode is made of tungsten and the exposed surface makes an angle of 71° with the axis of the cathode ray beam. The focal spot is rectangular, but, viewed in the direction normal to the cathode ray beam (i.e. the direction of the investigated X-radiation), it appears to be a square of about 2 mm. edge. The rating of the tube is 6 KW at 100 KV. As a precautionary measure, the current at high voltages was never increased beyond 2·8 MA, in order to prevent excessive heating of the anticathode. (It was necessary to run for 4 hours or more continuously during each experiment.) Special cooling fins are attached to the anode end of the tube.

Cuthbert Andrews Tube No. 33983.

With the exception of having a water cooled anode, this tube is very similar to the above-mentioned Philips tube. The rating of the tube is 6 KW. The emitted radiation as measured by the absorption coefficients is of approximately the same quality as that emitted by the Philips tube.

The High Tension Supply.

The potential on the X-ray tube was supplied by a H.T. transformer, the tube being self-rectifying. The transformer ratio is approx. 1:400. The centre point

of the secondary winding is earthed and at this point a milliameter could be inserted (Fig. 6) to enable the tube current to be measured. The power was taken from the 230 V, A.C. mains supply through an autotransformer (with a number of tappings) and an adjustable rheostat as shown in Fig. 6. By adjusting the autotransformer and the rheostat, the voltage on the primary of the H. T. transformer could be varied, thus controlling the voltage on the tube. A special calibration of the H.T. transformer had to be made. A typical example of this is shown in Fig. 7. The graph shows the voltage across the X-ray tube plotted against the voltage on the primary of the transformer for various tube currents. The voltage on the primary was measured with an ordinary voltmeter, while the voltage on the secondary was measured with a 10 cms. sphere spark gap. The calibration was performed for 3 or 4 different currents. Once the transformer was calibrated, it was only necessary to adjust the primary voltage for a certain tube current, to obtain any desired value for the secondary voltage. The value of the primary voltage for any intermediary values of tube currents was estimated from the graph. The filament current for the tube was supplied by a 12 volt accumulator battery.

The Apparatus.

A plan of the apparatus, used throughout all the experiments mentioned here is shown in Fig. 8.

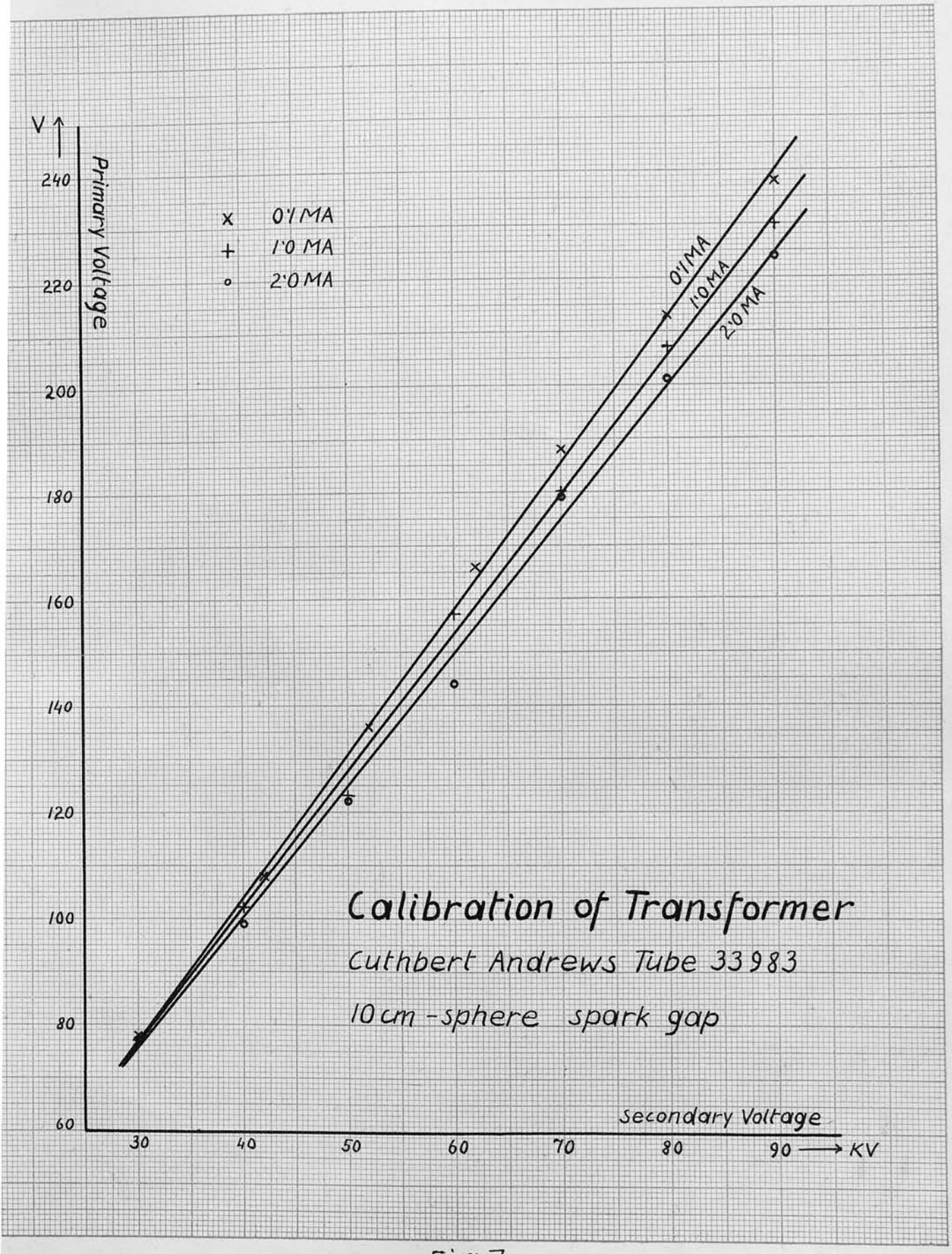
V
240
220
200
180
160
140
120
100
80
60
Primary Voltage
x 0·1 MA
+ 1·0 MA
∘ 2·0 MA
0·1 MA
1·0 MA
2·0 MA
Calibration of Transformer
Cuthbert Andrews Tube 33983
10 cm - sphere spark gap
Secondary Voltage
30
40
50
60
70
80
90 → KV

Fig. 7.

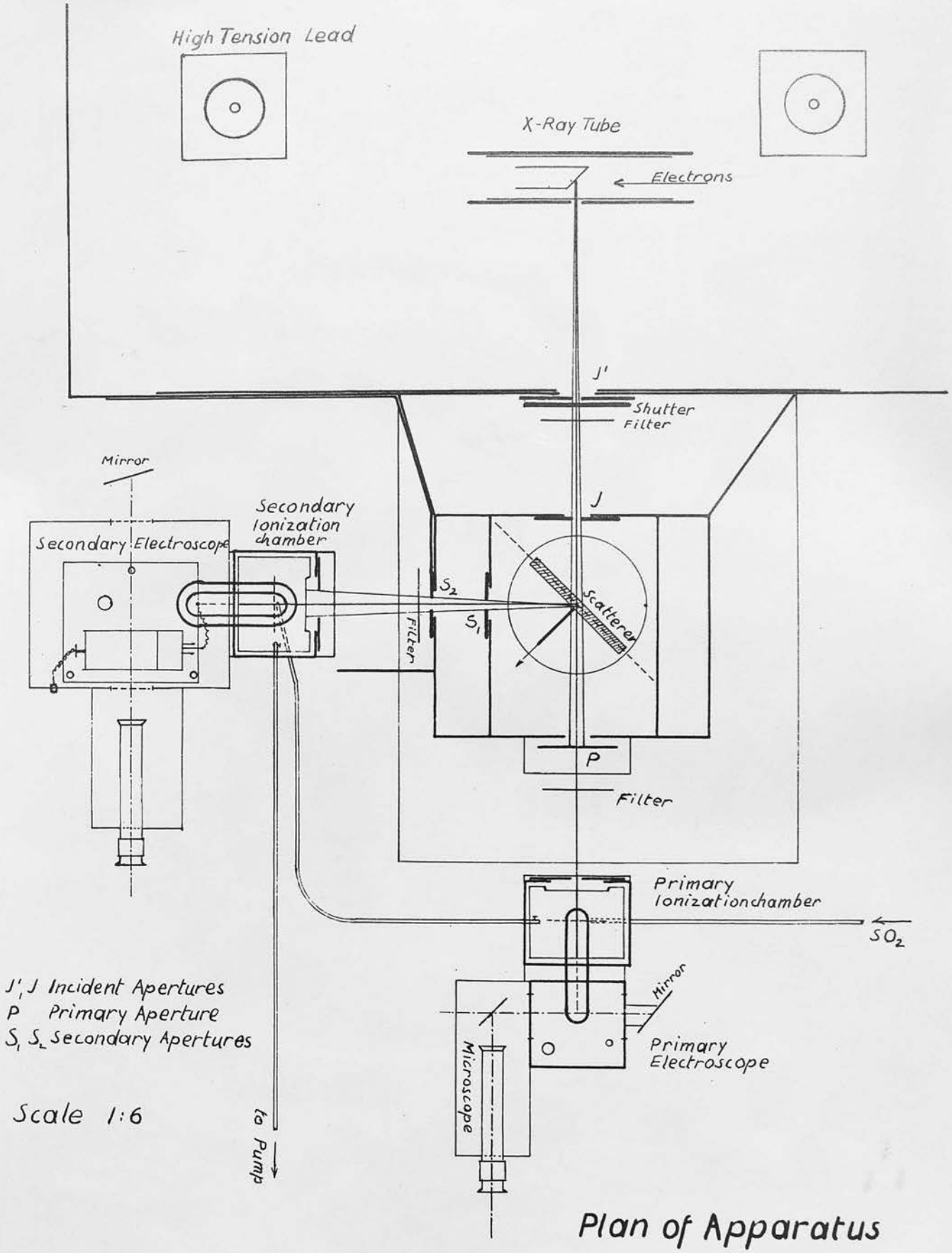

Plan of Apparatus

Fig. 8.

The tube, which is mounted on an insulated stand, is enclosed in a box (approx. 100 x 70 x 80 cms.) made of lead sheet 3 mms thick. The stand is built in such a way as to enable the tube to be rotated about the axis of the X-ray beam. This is important if polarization correction experiments are to be carried out. Originally, the whole aperture system was made of lead sheet 3 mms thick, which however proved to be insufficient when high voltages were being used. Therefore, all parts of the apparatus, which came in direct contact with the primary or secondary beams, e.g. all the apertures, were made of lead 4 to 6 mms thick.

The emitted radiation, after passing through the two apertures J' and J, which are approx. 13 cms apart, falls on the scatterer. The diameters of these two apertures could be adjusted as desired, but, with the exception of a few experiments, they were both circular holes of 1·6 cms. diameter. The X-ray tube itself was in most experiments arranged so that the distance between anticathode and first aperture (J') was approximately 25 cms. The importance of keeping this distance constant will be obvious when certain experiments are discussed later. It is evident from the diagram that, although the beam is limited by the two apertures J' and J, the diameter of the irradiated area of the scatterer depends on the distance between anticathode and the apertures. A shutter at J' allowed the radiation to be cut off as desired.

The scatterer was adjusted so as to make an angle of 45° with both primary and secondary beams, the position being indicated in the diagram. In this case both transmitted and scattered radiations have to pass through equal thicknesses of scattering material and suffer almost equal absorption in the scatterer.

The transmitted beam was further limited by the aperture P before it was received by the ionization chamber, whereas the apertures S_1 and S_2 were arranged so that the line connecting their centres was orientated at 90° with the primary. Thus S_1 and S_2 defined a beam which was scattered at 90°.

The ionization chambers, which served to measure the radiation are represented by Fig. 9. (The figure only shows the secondary chamber but the primary was the same in its main dimensions.) They were cylindrical, made of brass 10·3 cms. in diameter and 7·5 cms. deep. The radiation entered the chamber by an aluminium window 0·011 cms. thick. A lead aperture inside the aluminium window limited the diameter of the beam entering the chamber. The diameter of the aperture was bigger for the secondary chamber (6 cms.) than for the primary (4·9 cms) in order to receive as large a secondary beam as possible. The walls of the chambers were lined with aluminium and 3 sheets of filter paper, to absorb any radiation and electrons emitted by the walls. The electrode inside the chamber was made of cotton gauze and covered with colloidal graphite

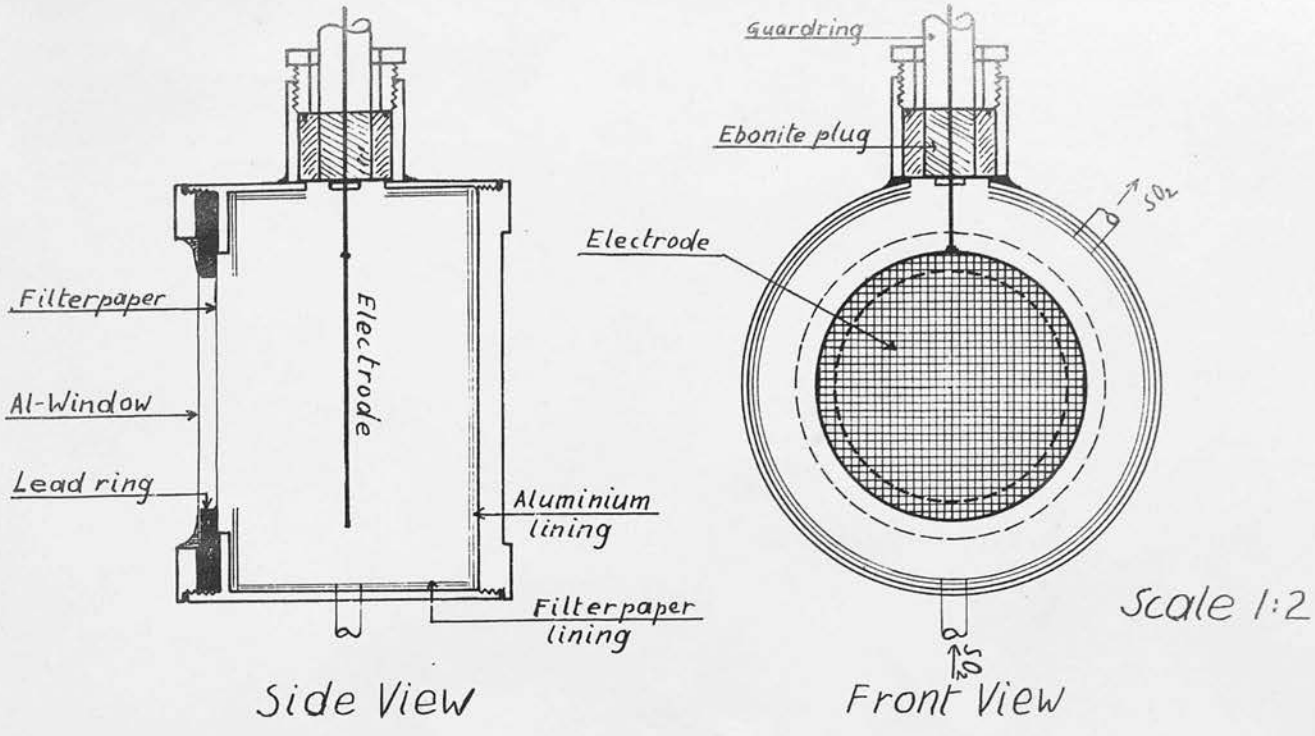

Secondary Ionization Chamber

Fig. 9.

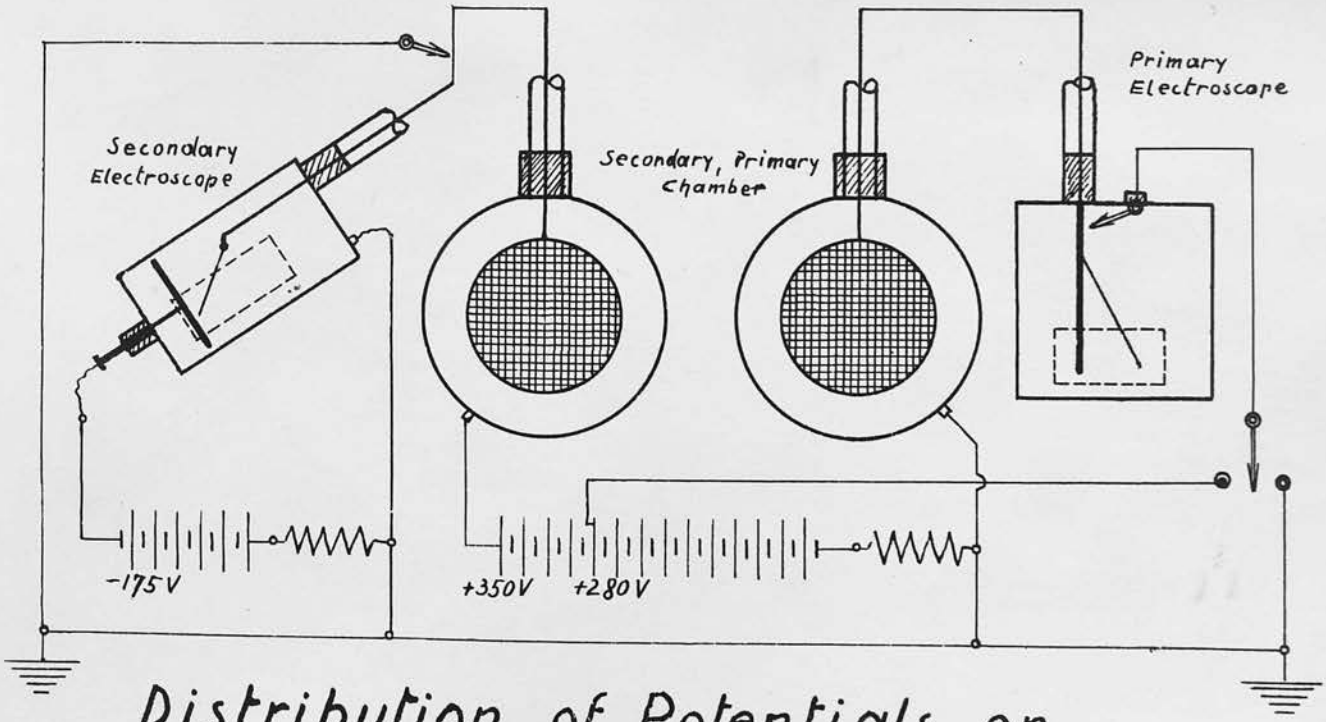

Distribution of Potentials on Chambers and Electroscopes

Fig. 10.

(Aquadag) to render it conducting. The gauze was mounted on a ring made of aluminium wire 7 cms. (primary) and 7.5 cms. (secondary) in diameter, its plane being parallel to the window. The distance between window and electrode was approx. 3.5 cms. The electrode was electrically insulated from the rest of the chamber, and held in position by an ebonite plug, which, at the same time, made an airtight fitting. A thick shielded copper wire connected the electrode to the gold leaf system of an electroscope. In order to minimise electrical leakage, the ebonite plug was made of two concentric parts with a guard ring at suitable potential between them. The chambers were filled with SO_2 at atmospheric pressure. Before being filled, they were sealed with wax and tested for gas leakage. An electrically insulated lead tube connected the chambers in order to maintain equal pressure. Both chambers were entirely covered with lead, the radiation being admitted by apertures in front of the windows (in most cases 1.0 cm. diameter for primary and 3.1 cms in diameter for secondary).

The electroscopes used for measuring the ionization produced in the chambers were of two different types. In virtue of the high intensity of the transmitted beam (even after passing through a small aperture P), the ordinary cubical box gold leaf electroscope was used. This is a very crude type of instrument of low sensitivity, but it was quite sufficient for this purpose. A gold leaf (2.5 - 5 cms long and approx. 0.2 cms.

broad, cut from a sheet of beaten gold) is mounted on a brass electrode, which in turn, is connected to the inner electrode of the primary ionization chamber. The electrode was enclosed in a brass box (approx. 8·5 cms × 8·5 cms. × 9·0 cms) which on the outside was covered with lead. The gold leaf system was electrically insulated from the box (which was kept at earth potential) by an ebonite plug. The system gold leaf-ionization chamber electrode was raised to a certain high potential (the ionization chamber being constantly kept at earth potential as well) and the position of the gold leaf could be observed with a long focus microscope. Readings were estimated to $^{1}/_{10}^{th}$ of a division on the engraved scale of 100 divisions (= 1 cm), fitted in the eyepiece. An exposure of the ionization chamber to the radiation produced a change in the position of the gold leaf. A special arrangement was provided to recharge the ionization chamber electrode-gold leaf system after each reading (Fig.10).

A much more sensitive type of instrument was required to measure the ionization produced in the secondary chamber owing to the smaller intensity of the scattered radiation. A suitable instrument was C T.R. Wilson's tilted electroscope. A gold leaf is attached to the end of a brass electrode, which is electrically insulated by ebonite from the case of the electroscope. A metal plate, well insulated from the case and raised to a high potential, can be brought to any desired distance from the gold leaf, the adjustment

being made by means of a screw. The sensitivity of the electroscope can be adjusted by a variation of the voltage on the plate, the distance between plate and gold leaf, and by adjusting the tilt of the whole instrument by the screw provided for this purpose. The gold leaf system is connected to the inner electrode of the secondary chamber, the connecting wires (as in the case of the primary electroscope) being surrounded by earthed brass tubes. A special key is provided to bring the electrode gold leaf system to earth potential after each reading. The electroscope is enclosed in an earthed metal box to shield the sensitive system from stray electric fields. The deflection of the gold leaf can be measured in the same way as the primary by means of a long focus microscope.

A precaution had to be taken against the disturbing influence of temperature changes. It was found, that as the temperature in the room varied (which was specially liable to occur in winter), the zero and sensitivity of the secondary electroscope changed.

Under these conditions, accurate working was impossible, since effects of the order of 10% were involved (all other experimental conditions being left unchanged). Another disturbing factor was draughts in the room, which caused a slow oscillating movement especially in the primary electroscope, although the

instrument itself was made as airtight as possible.*)

The covering of both electroscopes with cotton wool (actually the boxes surrounding the instruments) not only diminished the temperature effects to a very great extent, it also stopped the swinging motion of the gold leaves, provided it was not too windy outside. The error due to changes in sensitivity, after having covered the instrument, was at its worst approximately 1 - 2%, but generally much less.

The potentials, for ionization chambers and electroscopes, were provided by a number of H.T. batteries, which were enclosed in an earthed metal box and covered with sawdust and cotton wool to avoid changes of E.M.F. of the batteries, due to changing temperature. Special lead screened cables connected the measuring appliances to the batteries.

It was found suitable to keep the secondary chamber at a constant high potential (approx. + 350V) and the electrode-gold leaf system initially earthed. The plate of the secondary electroscope was kept at a potential of approx. 175 V below earth. The sensitivity of the secondary electroscope was adjusted to a

*) Draughts could not have influenced the gold leaf directly as it was enclosed in an air tight box, but it was impossible to find that particular part or parts of the apparatus, which were actually affected and in turn caused the swinging motion of the leaf. This disturbing movement of the gold leaves was especially marked on very windy days, being sometimes as much as ± 1 division and more. Naturally it was impossible to do any work under such conditions. This error increased with increasing sensitivity of the electroscope.

suitable value, usually between 4 and 9 divisions/volt although sensitivities as high as 30 div/volt have been used. The disadvantage of using high sensitivity (apart from effects mentioned before) is the big correction for leakage. It was better to use rather low sensitivity (and wider secondary apertures) than to introduce a large experimental error by increasing the sensitivity. The sensitivity was measured with a Weston standard cell.

The primary ionization chamber was kept at earth potential and so was the case of the primary electroscope. The electrode-gold leaf system was charged to approx.+280 v.

It is necessary to ensure that saturation conditions hold when using ionization chambers, for only under these conditions is the ionization current proportional to the intensity of the radiation. A test for this was made from time to time and a typical example is shown in Fig. 11.

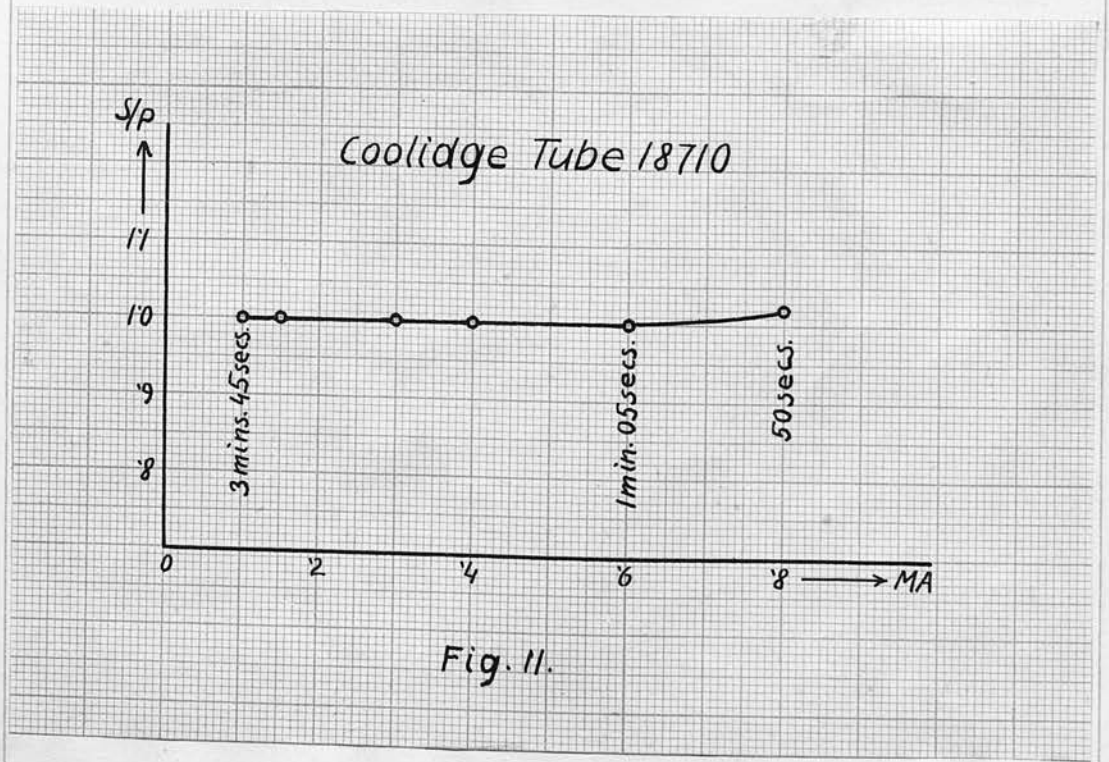

Fig. 11.

This graph was obtained by measuring the ratio S/P for various tube currents. It can be seen that saturation conditions exist (S/P independent of current) until the time taken for the reading becomes very short (the corresponding times are marked on the graphs). In the experiments discussed in this thesis the shortest readings did not take less than 80 seconds for a deflection of 10 scale divisions in the secondary.

The deflection of the secondary electroscope has always been taken as the standard, owing to the non-linear relationship between sensitivity and deflection of the gold leaf, when high sensitivities are being used.

The primary aperture was always adjusted so as to give the ratio S/P a value between $\frac{1}{1}$ and $\frac{1}{2}$, its size varying from 0·05 cms. to 0·17 cms. in diameter. It has been found, that a change of primary aperture (above a certain minimum size) and a change in the tube current, do not alter the result provided both are being kept constant in the course of one experiment. Owing to the small diameter of the primary aperture as compared with its depth (0·4 cms.), special care had to be taken to have it placed in its proper position, (that is, its plane perpendicular to the axis of the X-ray beam) if effects due to the edges of the aperture are to be avoided. Special holders made it possible to move the aperture in its

own plane i.e. vertical to the primary beam and to turn it about a vertical or horizontal axis. The position of the aperture was altered systematically until its position was such that the intensity of the radiation passing through became a maximum.

Corrections for Leaks.

The accuracy of every measurement was greatly affected by the correction, which had to be applied to compensate electrical leakage. This correction becomes very marked when very long readings are being taken (longer than 20 minutes, say). For shorter readings this error is never more than 1% which, perhaps with a few exceptions, has been found to be the experimental error. In the earlier experiments, in order to avoid too big a correction for long readings, the tube current had to be increased whenever the time taken for a reading became too long. Of course, a check had to be made to see whether the ratio S/P for a certain point changes with changing current. Very often it had been found that this was the case (i.e. the variation in S/P exceeded the limits of error) owing to the influence of the tube current on the spectral distribution of the radiation. It was therefore better to keep the current constant throughout the experiment, and to apply a larger correction for leakage. The correction for readings which took between 20 and 45 minutes was never more than 2%. The leaks were measured at the

initial and final points of the deflection of the gold leaves. The mean value of initial and final leak was taken to be the correction.

EXPERIMENTAL RESULTS.

PART I. THE SCATTERING EXPERIMENT.

(a) Scattering from Paraffin Wax.

i. General description of the results of the scattering experiment.

With the exception of a few early experiments (carried out with Coolidge tube No. 18710, the results of which are shown in Fig. 2*) and which are typical of the experiments performed by other workers in this laboratory, the results obtained by the writer were invariably of one kind. The constancy of the writer's results and the fact that they could be reproduced at will to within the experimental error, needs to be specially emphasised, as a variability in results has so frequently been reported by others. Although there is no doubt about the accuracy of the actual measurements of the writer's early experiments (Fig. 2), their value as a basis for argument is questionable. The reason for this is that large apertures J' and J were used; the X-ray beam was therefore poorly defined, the irradiated area of the scatterer was large and scattering did not take place at a well defined angle of 90°. The sensitivity of the secondary electroscope was made very high and this

---

* Here and in all other figures the ratio $S/_P$ has always been reduced so that $S/_P = 1{\cdot}00$ for 90 KV.

involved rather big corrections for leaks. The primary aperture had not been adjusted so as to allow the passage of radiation at maximum intensity. All this does not however explain the difference between the two sets of results, since it has been shown by other workers and by the writer that by using small apertures J' and J and low sensitivity of the secondary electroscope, the results may remain unchanged. Between the writer's early experiments and the later ones, a series of experiments was carried out (see Page **65**) which involved a systematic change of apertures, and of other parts of the apparatus. After this, it was not possible to go back to the original arrangement and probably for this reason all attempts made by the writer to reproduce the results of Fig. 2 have been unsuccessful.

Fig. 12 shows the results obtained for the radiation scattered from various thicknesses of paraffin wax (Philips' Metalix Tube No. 1325). These results are typical of all except the earliest scattering experiments performed by the writer. The difference between the results of Fig. 12 and Fig. 2 lies in the fact that the former do not exhibit any discontinuity in slope whatsoever, at least not outside the limits of experimental error. But apart from the discontinuity, the features of the graphs of Fig. 12 are similar to those of Fig. 2. S/P increases steadily with decreasing $\overline{\mu/\rho}$ until the highest voltage obtainable is reached. A further decrease of $\overline{\mu/\rho}$,

Philips Metalix Tube 1325
(horizontal)

$J' = J = 1{\cdot}6$ cm, $S_1 = S_2 = 1{\cdot}6$ cm

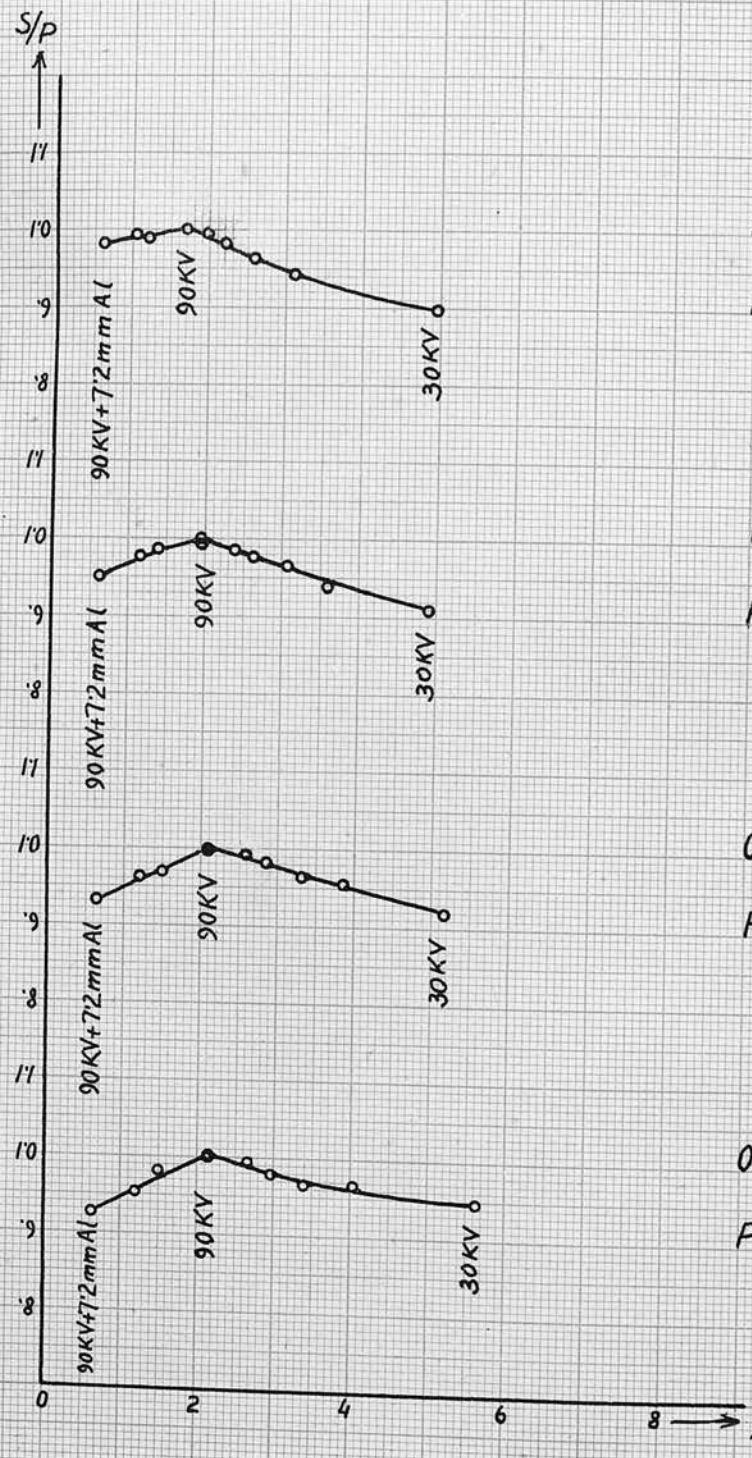

1·8 cm Paraffin Wax

P = 0·14 cm, 1·2 MA

0·7 cm Paraffin Wax

P = 0·09 cm, 1·8 MA

0·3 cm Paraffin Wax

P = 0·07 cm, 2·6 MA

0·1 cm Paraffin Wax

P = 0·05 cm, 2·8 MA

Fig. 12.

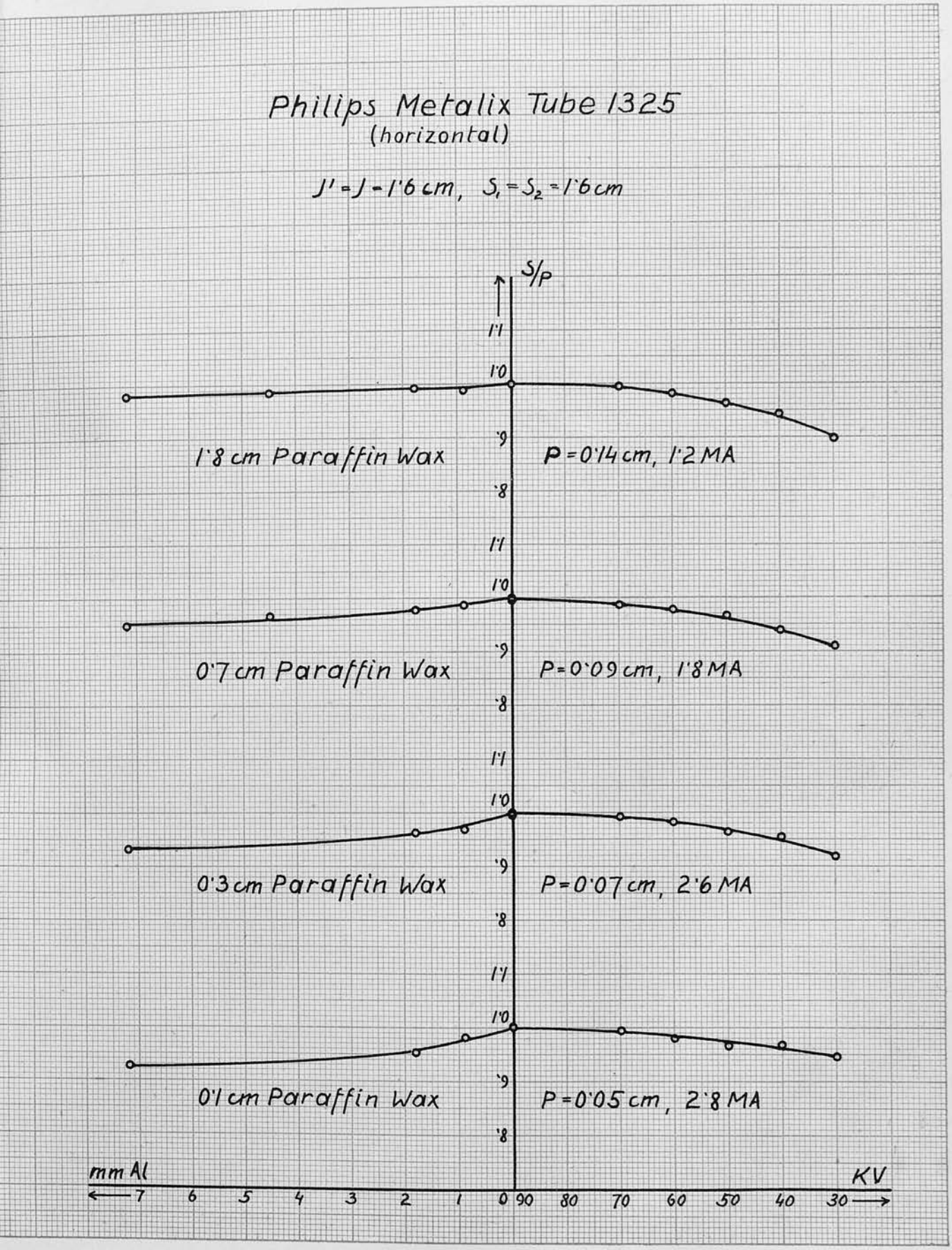
Philips Metalix Tube 1325
(horizontal)
J' = J - 1·6 cm, S1 = S2 = 1·6 cm
S/P
1·1
1·0
·9
·8
1·8 cm Paraffin Wax
P = 0·14 cm, 1·2 MA
0·7 cm Paraffin Wax
P = 0·09 cm, 1·8 MA
0·3 cm Paraffin Wax
P = 0·07 cm, 2·6 MA
0·1 cm Paraffin Wax
P = 0·05 cm, 2·8 MA
mm Al
7 6 5 4 3 2 1 0
90 80 70 60 50 40 30
KV

Fig. 13.

brought about by filtering the incident radiation, results in a decrease of S/P. As in Fig. 2, the slope of the graph depends on the thickness of the scatterer.

Owing to the ambiguity of $\overline{\mu/\rho}$, it is preferable to split up the graph into two parts and plot S/P against the voltage on the tube (KV) and the thickness of the filtering aluminium respectively. This is shown in Fig. 13 (for the results of Fig.12). The advantage of this will be obvious when carbon and aluminium scatterers are being used since, owing to the tremendous amount of absorption taking place within these scatterers, the range of absorption coefficients is very small. The graph S/P against KV is a perfectly smooth curve with the convex side upwards; it approaches horizontality for very thin scatterers. The graph S/P against the thickness of aluminium filter shows a decrease of S/P with increasing thickness of aluminium, which becomes more marked as the thickness of the scatterer is reduced.

ii. Effect of tube current and apertures.

The only variations in experimental conditions in the experiments described in Fig. 12, apart from changes in the thickness of the scatterer, were changes in the dimensions of the primary aperture and variations of the tube current. As the thickness of the scatterer is reduced, it becomes impossible to keep the primary aperture constant. These changes are

unavoidable because the ratio of the intensities in the primary and secondary beams is thereby altered. The reduction of scatterer thickness reduces the intensity of the scattered beam in proportion to the reduction of scattering material. This changed ratio may be compensated for either by an increase of the sensitivity of the secondary electroscope (which involves bigger corrections for leaks), or by a change in the relative sizes of primary and secondary apertures. It is both more convenient and more accurate to keep the sensitivity of the secondary electroscope unchanged and to decrease the dimensions of the primary aperture (P). This change in turn involves another. The time required to reach a standard deflection of the electroscopes is increased by reduction of primary aperture and secondary beam intensity, and reading times tend to become unduly long. It then improves the accuracy of the experiment to raise the current in the X-ray tube. It has been shown by other workers[7] and by the writer that a change of the tube current does not alter the shape of the graph, provided the current is being kept constant in the course of one experiment. On the other hand, a change of primary aperture has been found by some to influence the result. According to Miss Wilson, a change of the primary aperture from 0·1 cms. to 0·06 cms. in diameter changes the graph appreciably. No such effect could be observed with the apertures used in this work

(they varied in size from 0·05 cms. to 0·17 cms. in diameter).

In Fig. 14 is shown a selection of scattering curves for 0·3 cms. paraffin wax scatterer under a variety of experimental conditions. The primary aperture varied from 0·05 cms. to 0·1 cm. in diameter, the tube current was varied between 1·0 MA and 2·6 MA and the secondary apertures were 1·6 cms. and 3·0 cms. in diameter. While they do not represent a systematic test of all the variables one by one, the curves in this figure are typical of all the writer's experiments in that the shape of the graphs shows very slight changes.

In this connection it may be of interest to mention one of the results (Fig. 15 bottom curves) obtained with Cuthbert Andrews Tube No. 33983 for 0·3 cms. paraffin wax scatterer, using a primary aperture consisting of four holes, each of 0·034 cms. in diameter and situated on the corners of a square of of 0·5 cms. side length. (The drill of 0·034 cm. diameter was the smallest drill available). Apertures of this kind (pin holes), and of even bigger diameter, gave results[7] which, as reported by others, were quite different from those normally obtained from the scattering experiment (Fig.2). Pin hole apertures usually gave a horizontal line, i.e. constant S/P , no matter what the voltage on the tube. These results, however, could not be confirmed in the present work; the scattering curve obtained by the writer

Philips Metalix Tube 1325

0·3 cm paraffin wax scatterer

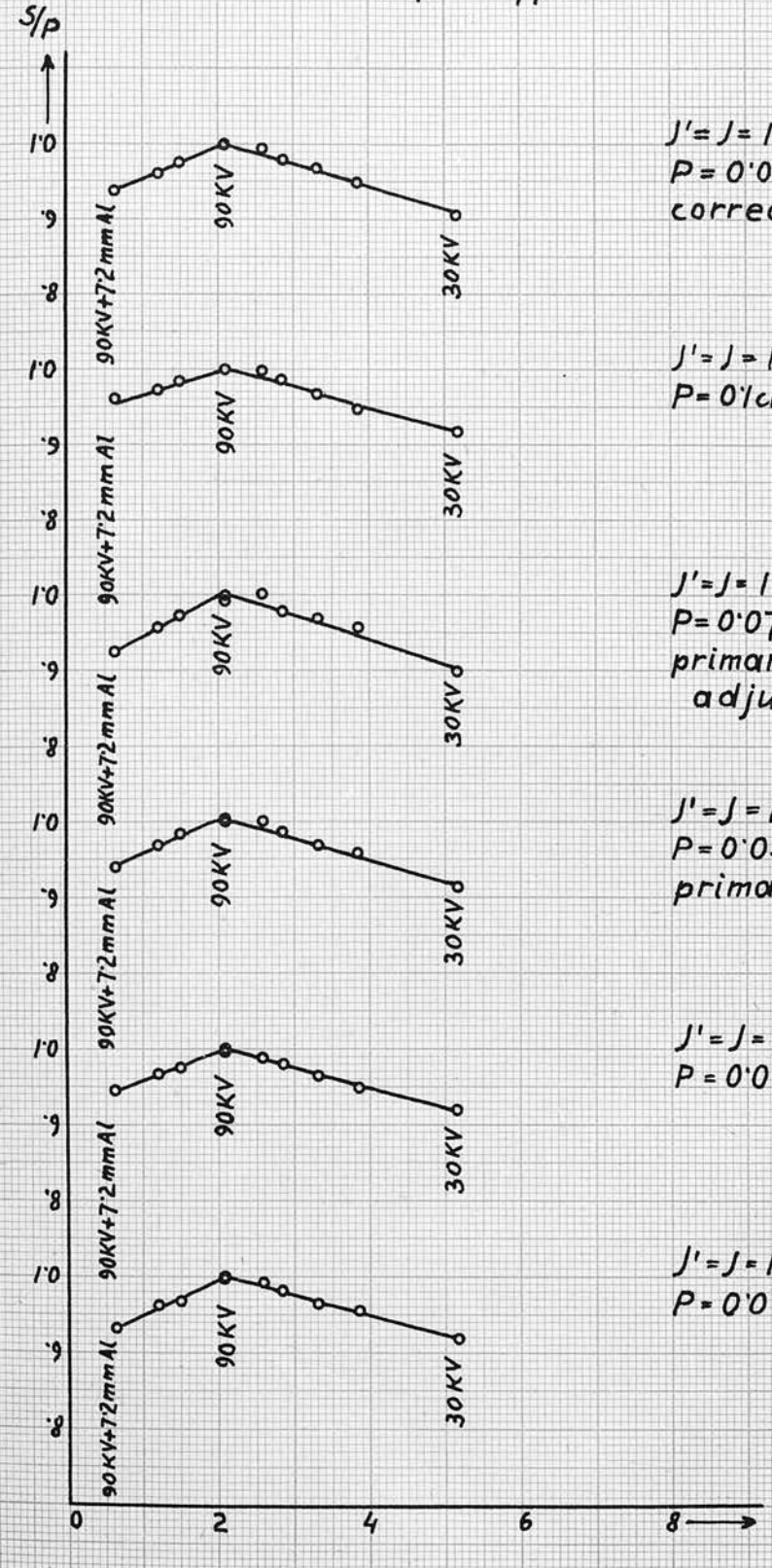

$J' = J = 1·6$ cm, $S_1 = S_2 = 3·0$ cm
$P = 0·08$ cm, 2·0 MA
correction for leaks not exact.

$J' = J = 1·6$ cm, $S_1 = S_2 = 3·0$ cm
$P = 0·1$ cm, 1·0 MA.

$J' = J = 1·6$ cm, $S_1 = S_2 = 3·0$ cm
$P = 0·07$ cm, 2·6 MA
primary aperture not adjusted properly.

$J' = J = 1·6$ cm, $S_1 = S_2 = 3·0$ cm
$P = 0·05$ cm, 2·6 MA
primary aperture adjusted.

$J' = J = 1·6$ cm, $S_1 = S_2 = 3·0$ cm
$P = 0·08$ cm, 1·8 MA.

$J' = J = 1·6$ cm, $S_1 = S_2 = 1·6$ cm
$P = 0·07$ cm, 2·6 MA.

Fig. 14.

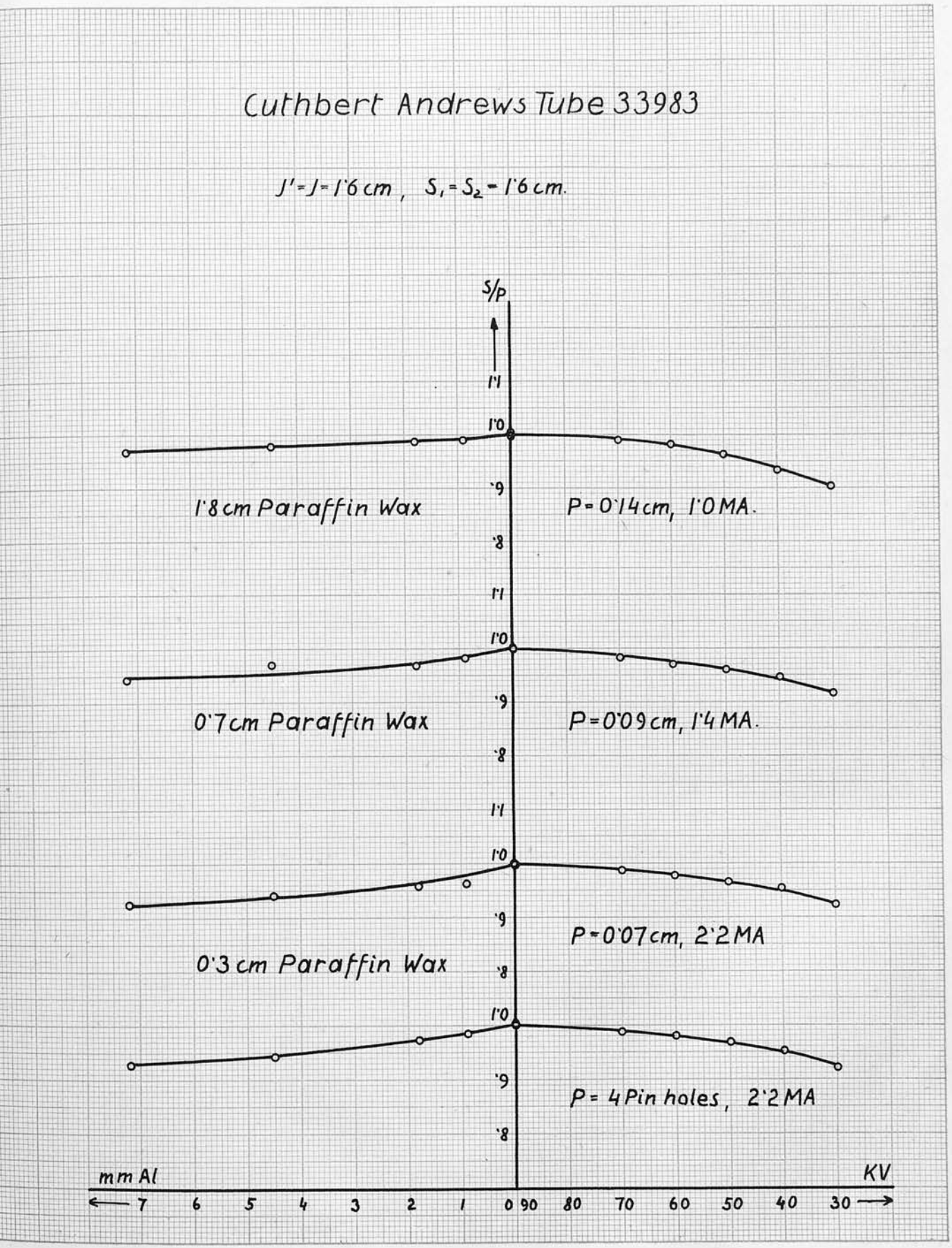
Cuthbert Andrews Tube 33983
J'=J=1·6 cm, S1=S2=1·6 cm.
S/P
1·1
1·0
·9
·8
1·8 cm Paraffin Wax
P=0·14 cm, 1·0 MA.
0·7 cm Paraffin Wax
P=0·09 cm, 1·4 MA.
0·3 cm Paraffin Wax
P=0·07 cm, 2·2 MA
P=4 Pin holes, 2·2 MA
mm Al
7 6 5 4 3 2 1 0
90 80 70 60 50 40 30
KV

Fig. 15.

with the above-mentioned aperture is of exactly the same type as all other scattering curves obtained with other apertures. In fact, the difference between this result and a scattering curve obtained under similar experimental conditions (i.e. same tube, scatterer, etc.) but using a single hole primary aperture 0·07 cms. in diameter, is not greater than 0·5% (for S/P against KV). From this it must be concluded that as far as the writer's experiments are concerned, the scattering curve is entirely independent of the primary aperture.

A question has arisen as to why in some experiments, using thick scatterers, (mainly performed on apparatus C and D) the ratio S/P remains constant even when the radiation is filtered by an appreciable amount of aluminium, while in other experiments (performed on apparatus A and B), S/P decreases even when the radiation is intercepted by a very thin sheet of aluminium. It has been mentioned before (Page 6), that experiments to investigate this difference (which was thought to be of the greatest importance) were carried out by Miss Wilson[1] but without success. She suggests that the difference in the results may be due to some difference in the rooms, but as this is highly improbable and the cause of this effect is more likely to be found in the apparatus itself than anywhere else, a systematic study of the influence of the dimensions of the apertures has been carried out. The experiments were carried out with Coolidge tube

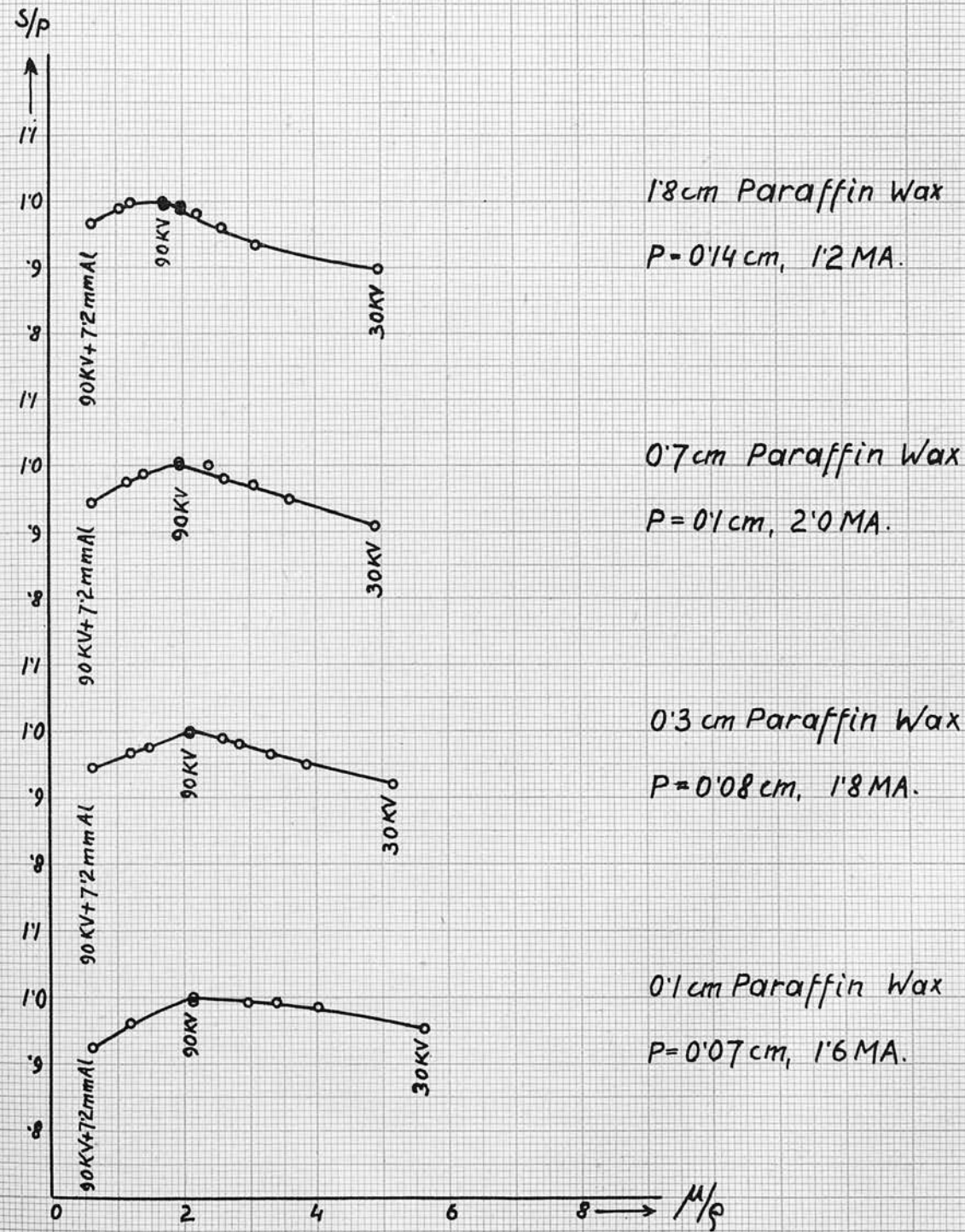
Philips Metalix Tube 1325
J' = J = 1·6 cm, S1 = S2 = 3·0 cm.
S/P
1·1
1·0
·9
·8
90 KV + 7·2 mm Al
90 KV
30 KV
1·8 cm Paraffin Wax
P = 0·14 cm, 1·2 MA.
0·7 cm Paraffin Wax
P = 0·1 cm, 2·0 MA.
0·3 cm Paraffin Wax
P = 0·08 cm, 1·8 MA.
0·1 cm Paraffin Wax
P = 0·07 cm, 1·6 MA.
0
2
4
6
8
μ/ρ

Fig. 16.

tube used was Coolidge tube No. 31395 and the aperture J was 2·5 cms. in diameter. The tube was placed so that the distance between anticathode and the aperture J' was 13·5 cms, 15·5 cms, 25 cms and 40 cms. respectively. The results in Fig. 17 show that the slope depends on the distance between anticathode and aperture.

A further test was now applied. A small aperture (0·4 cms) was fixed on to the tube itself, thereby eliminating almost all the radiation emitted by the glass wall of the tube. The results (see Fig. 18) show that the rapid fall of the ratio S/P with increased intercepting aluminium has now disappeared. The slope, however, may still be sensitive to the size of the aperture J (2·5 cms. and 1·6 cms.).

These experiments were unfortunately not carried far enough to establish definite rules defining the conditions and the way in which they affect the slope of the graph. It has, however, been established that considerable differences in the experimental results may be due to the relative sizes of the apertures before the scatterer limiting the radiation emitted by the X-ray tube. It also appears that an increase of J (as compared with J') reduces the slope of the graph until S/P remains constant and independent of the thickness of the filtering aluminium. These results are not in agreement with results reported by Miss Wilson.(1)

The same results as those obtained for thick

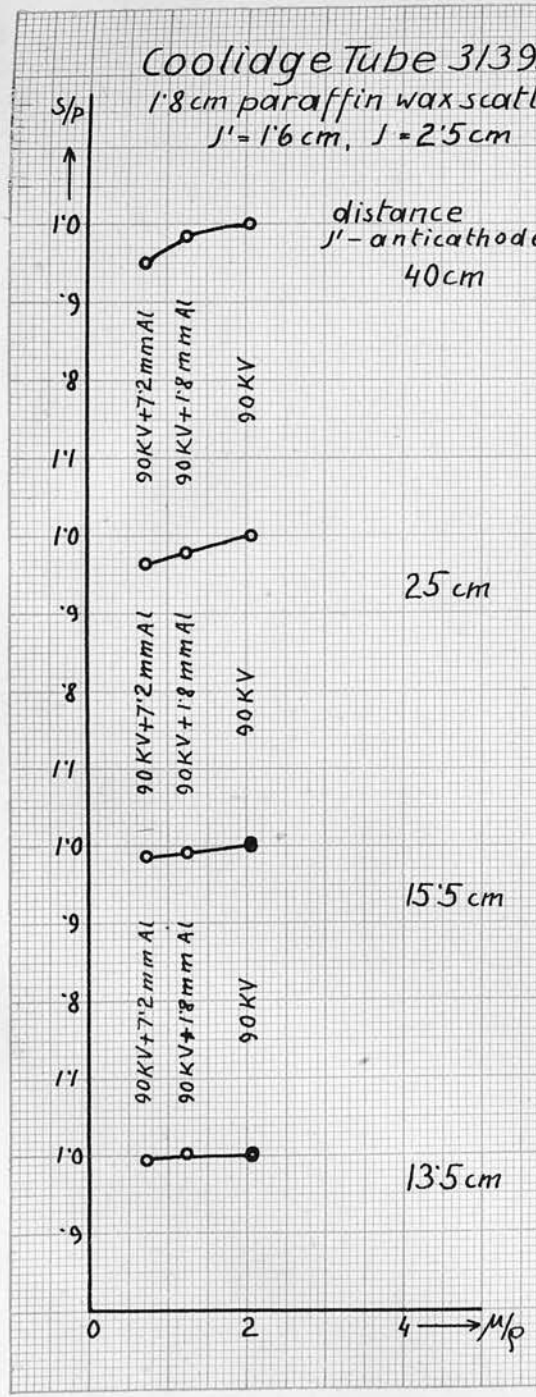
Coolidge Tube 31395
1·8 cm paraffin wax scatterer
J' = 1·6 cm, J = 2·5 cm
S/P
distance
J'-anticathode:
40 cm
25 cm
15·5 cm
13·5 cm
90KV+7·2 mm Al
90KV+1·8 mm Al
90 KV
1·0
·9
·8
1·1
0
2
4
μ/ρ

Fig. 17.

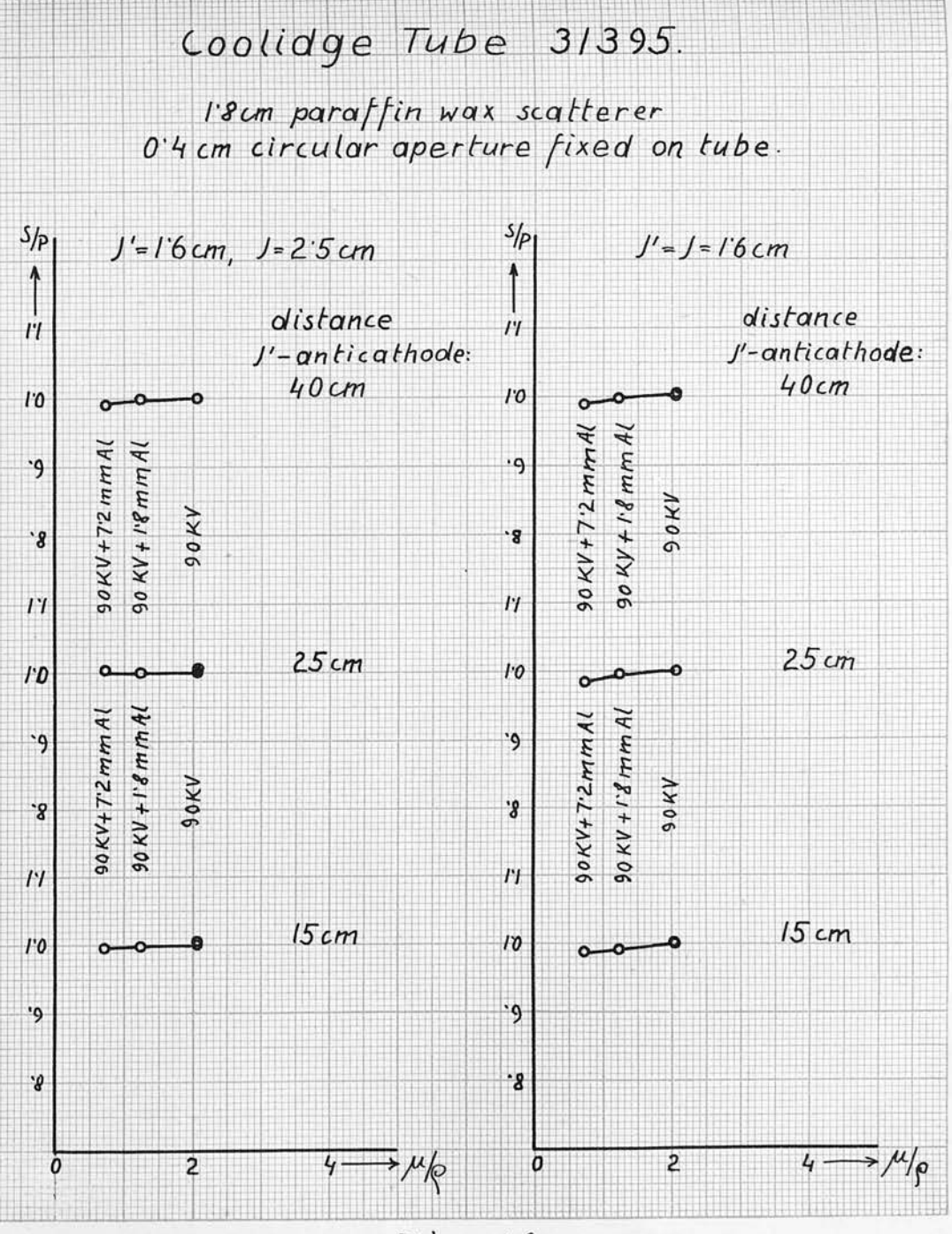
Coolidge Tube 31395.
1·8 cm paraffin wax scatterer
0·4 cm circular aperture fixed on tube.
J' = 1·6 cm, J = 2·5 cm
J' = J = 1·6 cm
S/P
distance
J'-anticathode:
40 cm
25 cm
15 cm
90KV+7·2 mm Al
90 KV+1·8 mm Al
90 KV
1·1
1·0
·9
·8
0
2
4
μ/ρ

Fig. 18.

scatterers apply for thin scatterers as well, but with a difference that the slope of the graph is initially bigger for thin scatterers than for thick ones. It is possible by choosing small apertures for thick scatterers (and greater distance between anti-cathode and apertures), and large apertures for thin scatterers (and smaller distance between anticathode and apertures) to obtain identical results.

Fig. 19 shows the whole of the scattering curve (S/P plotted against $\overline{\mu/\rho}$) for two different tubes at various distances from the apertures. Although the difference in the results is not very marked for the Philips tube, it can be seen nevertheless, that even the slope of that part of the scattering curve, which results from the variation of voltage only, depends on the distance between tube and aperture. From all these experiments it can be concluded that it is of the greatest importance to keep the apertures J' and J and the distance between tube and apertures constant if the scattering curve is to be studied as a function of the material or thickness of the scatterer.

iii. Effect of X-ray Tube.

The same kind of results as those of Fig. 12 have also been obtained with other tubes. Fig. 20 shows the scattering curve for 1·8 cms. and 0·3 cms. paraffin wax scatterers using Coolidge Tube No.31395 whose radiation is just a little softer than that

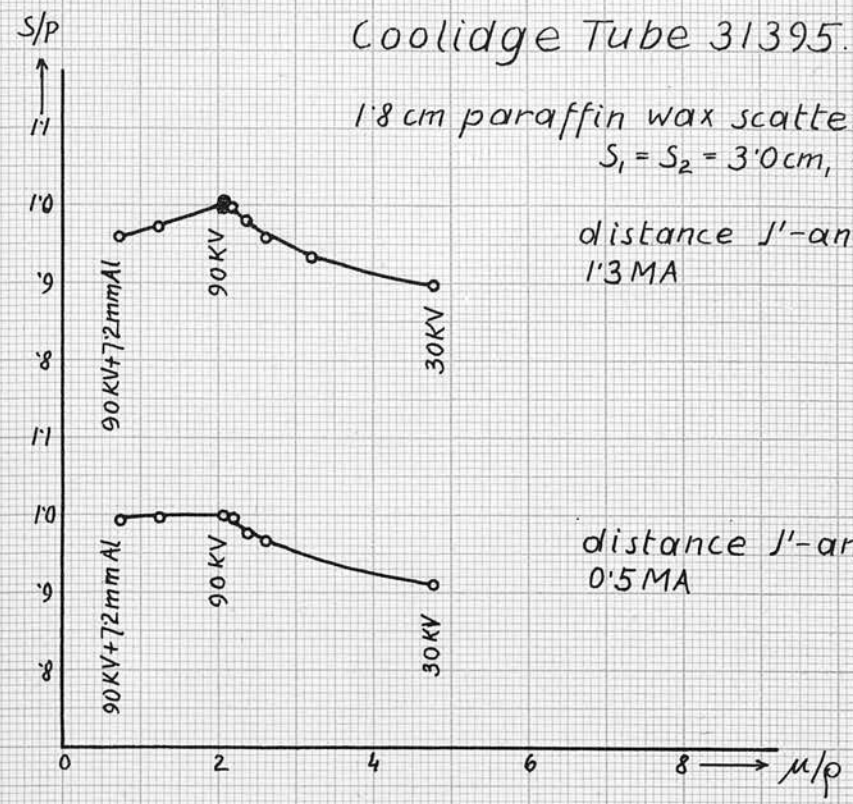
S/P
Coolidge Tube 31395.
1·8 cm paraffin wax scatterer, J'=1·6 cm, J=2·5 cm
S1 = S2 = 3·0 cm, P=0·17 cm
distance J'-anticathode 25·0 cm
1·3 MA
distance J'-anticathode 13·5 cm
0·5 MA
90 KV+7·2 mm Al
90 KV
30 KV
1·1
1·0
·9
·8
0
2
4
6
8
μ/ρ

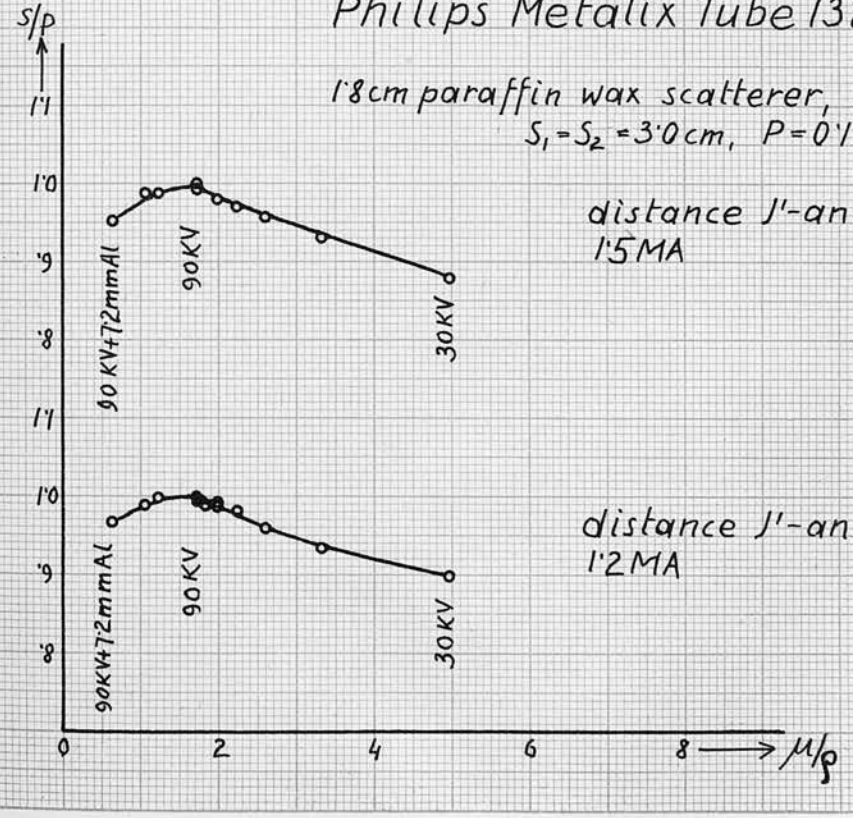
S/P
Philips Metalix Tube 1325
1·8 cm paraffin wax scatterer, J'=J=1·6 cm
S1 = S2 = 3·0 cm, P=0·14 cm
distance J'-anticathode 40 cm
1·5 MA
distance J'-anticathode 25 cm
1·2 MA
90 KV+7·2 mm Al
90 KV
30 KV
1·1
1·0
·9
·8
0
2
4
6
8
μ/ρ

Fig. 19.

Coolidge Tube 31395

$S_1 = S_2 = 3{\cdot}0\,cm$

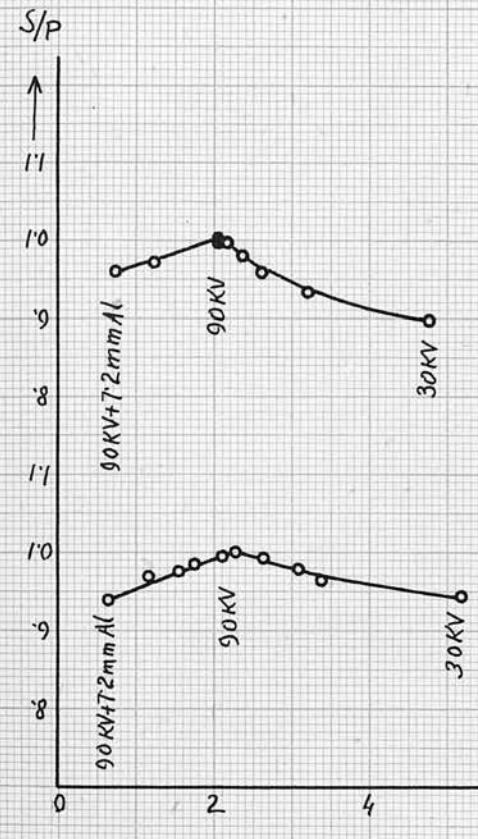

1·8 cm Paraffin Wax

J'=1·6 cm, J=2·5 cm, P=0·17 cm, 1·3 MA

0·3 cm Paraffin Wax

J'=J=1·6 cm, P=0·08 cm, 1·6 MA
(0·8 cm circular aperture fixed on tube)

Fig. 20.

emitted by the Philips Tube. The results are very similar to those obtained with the Philips tube.

Fig. 15 shows the results obtained with Cuthbert Andrews Tube No. 33983. These are of special interest as this tube when used on apparatus D (by another worker) gave results similar to those of Fig. 2 and with this fact in mind, the writer has chosen this tube to test what kind of result will be obtained with it on apparatus A, i.e. to test whether in general the results of the scattering experiments do depend on the X-ray tube. As has been mentioned before, this is not the case. The results are always the same, independent of the tube and similar to those of Figs. 12 and 13.

The only difference between the results obtained from different tubes is a variation in the slope of the graphs, which is, however, not very pronounced. This variation in slope is probably due to the different spectral distribution of the radiations emitted by the tubes.

iv. Experiments with intercepted radiation.

Since the intensity-wave length distribution of the radiations, emitted by different tubes with the same anticathode material (tungsten), is to a very great extent affected by the varying amount of filtration of the radiations in the glass walls of the tubes, it may be of interest to mention a series of experiments performed with Philips tube No. 1325, where the radiation was filtered by aluminium before it

reached the scatterer. Fig. 21 shows the results obtained from these experiments. The scatterer was paraffin wax 0·3 cms. thick. The experiments were carried out for the radiation unintercepted and intercepted (at AA of Fig. 1) by 0·09 cms. and 0·18 cms. of aluminium respectively. A further increase of the thickness of the intercepting aluminium was not practicable owing to the rapid decrease of intensity at lower voltages. Although the difference between the results is not very marked (it may perhaps be regarded to be within the experimental error), it can be seen nevertheless, that there is a tendency to increase the slope of the graphs for increasing filtration of the radiation. It appears from these experiments that a softer heterogeneous radiation would decrease the slope of the scattering curve. This on the whole is consistent with the results obtained by other workers using tubes with a Lindemann window were S/P constant over an extensive range of voltage.

(b) Scattering from filter paper, carbon and aluminium.

Similar results as those for paraffin wax scatterers have been obtained for scatterers made of filter paper, carbon and aluminium. Philips Metalix Tube No. 1325 was used for these experiments and the apertures in all cases were $J' = J = 1{\cdot}6$ cms. and $S_1 = S_2 = 3{\cdot}0$ cms. in diameter. Primary aperture and

Philips Metalix Tube 1325
(horizontal)

0·3 cm paraffin wax scatterer, 2·6 MA

$J' = J = 1{\cdot}6$ cm, $S_1 = S_2 = 1{\cdot}6$ cm, $P = 0{\cdot}07$ cm.

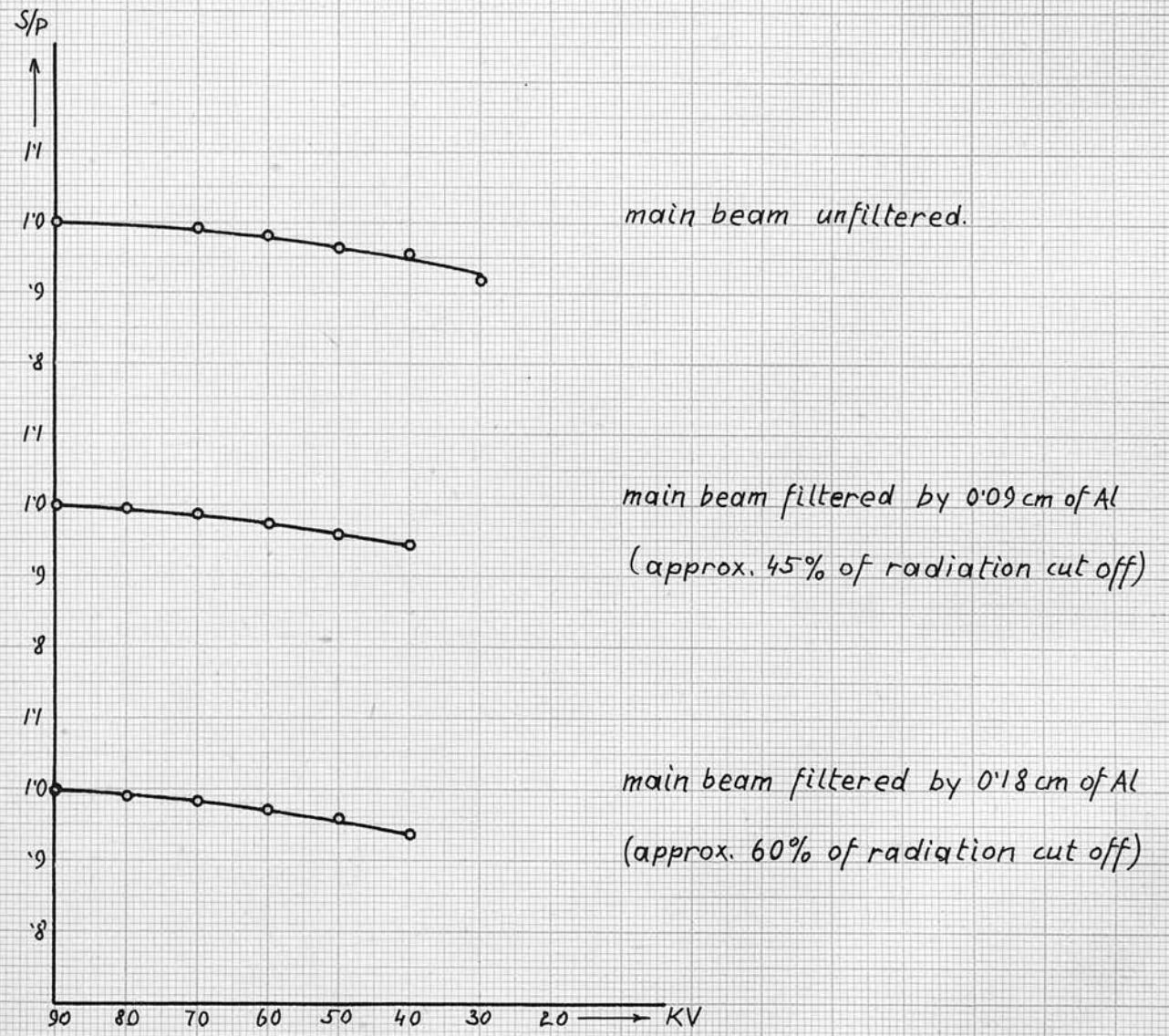

Fig. 21.

tube current have been adjusted in each case, so as to give a reasonable ratio S/P within reasonable time limits. The sensitivity of the secondary electroscope was kept unaltered except in one case, when, scattering from five sheets of filter paper, it had to be increased considerably. In each case S/P was plotted against KV and thickness of filtering aluminium respectively.

Fig. 22 shows the results obtained for filter paper scatterers made of 60 sheets, 20 sheets and 5 sheets of filter paper. Owing to the very high sensitivity of the secondary electroscope involving big corrections for leaks, the result for the scattering from 5 sheets of filter paper should not be taken as very reliable. The results for carbon scatterers are shown in Fig. 23 for 1·27 cms., 0·63 cms and 0·23 cms. of carbon. Fig. 24 gives the scattering curve for aluminium scatterers 0·32 cms., 0·21 cms. and 0.09 cms. thick. In some cases the measurements could only be carried out between 90 KV and 40 KV or 50 KV respectively and not for lower voltages on the tube. This is due to the tremendous amount of absorption taking place within the scatterer.

Comparing the results obtained from paraffin wax, filter paper, carbon and aluminium scatterers (Figs.13, 22, 23 and 24) it is possible to draw certain conclusions. The scattering curve, which is obtained by the variation of the voltage only, shows in all cases

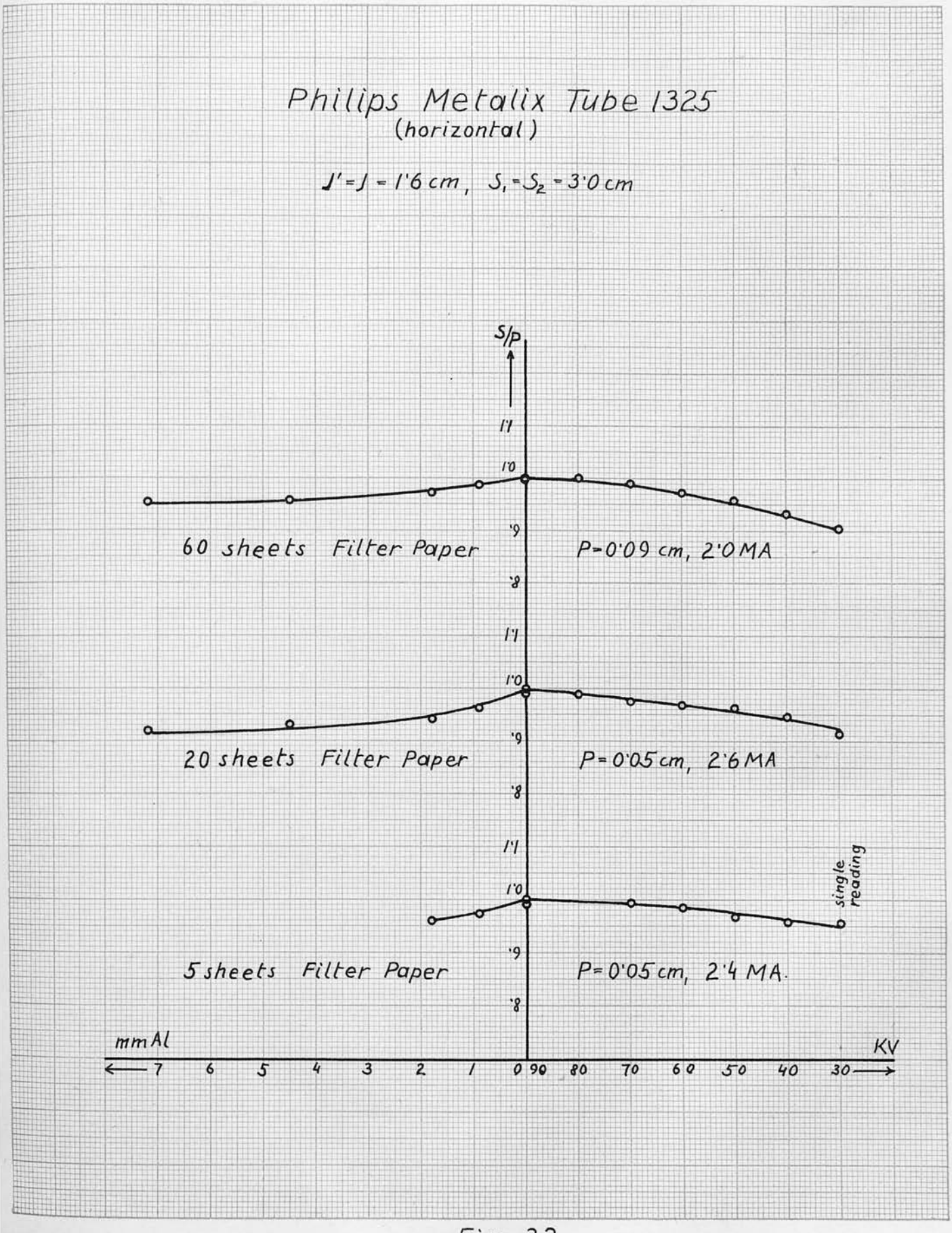
Philips Metalix Tube 1325
(horizontal)
J' = J = 1·6 cm, S1 = S2 = 3·0 cm
S/P
1·1
1·0
·9
·8
60 sheets Filter Paper
P = 0·09 cm, 2·0 MA
20 sheets Filter Paper
P = 0·05 cm, 2·6 MA
5 sheets Filter Paper
P = 0·05 cm, 2·4 MA.
single reading
mm Al
7 6 5 4 3 2 1 0
90 80 70 60 50 40 30
KV

Fig. 22.

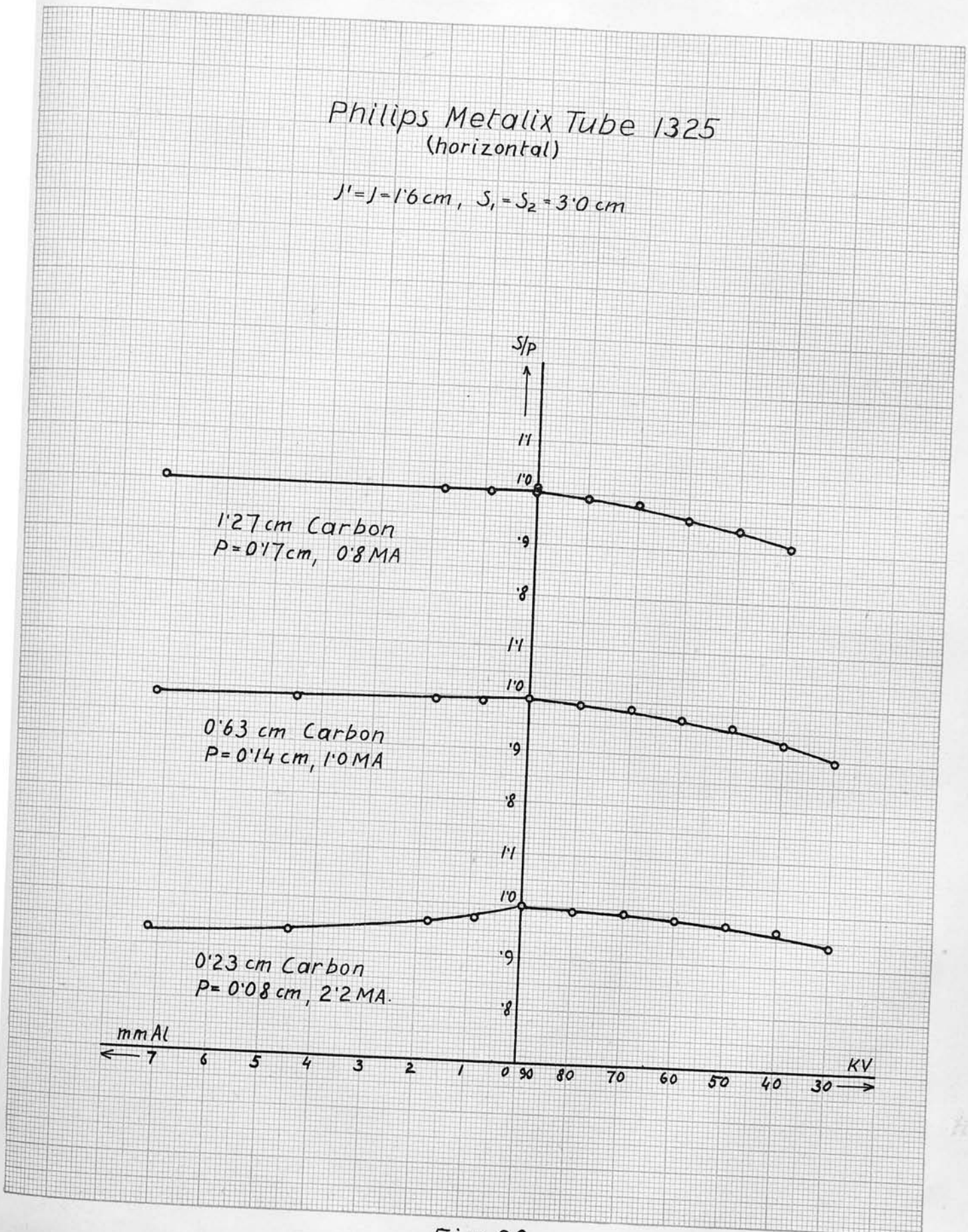
Philips Metalix Tube 1325
(horizontal)
J'=J=1·6 cm, S1=S2=3·0 cm
S/P
1·1
1·0
·9
·8
1·27 cm Carbon
P=0·17 cm, 0·8 MA
1·1
1·0
·9
·8
0·63 cm Carbon
P=0·14 cm, 1·0 MA
1·1
1·0
·9
·8
0·23 cm Carbon
P=0·08 cm, 2·2 MA.
mm Al
7 6 5 4 3 2 1 0
90 80 70 60 50 40 30
KV

Fig. 23.

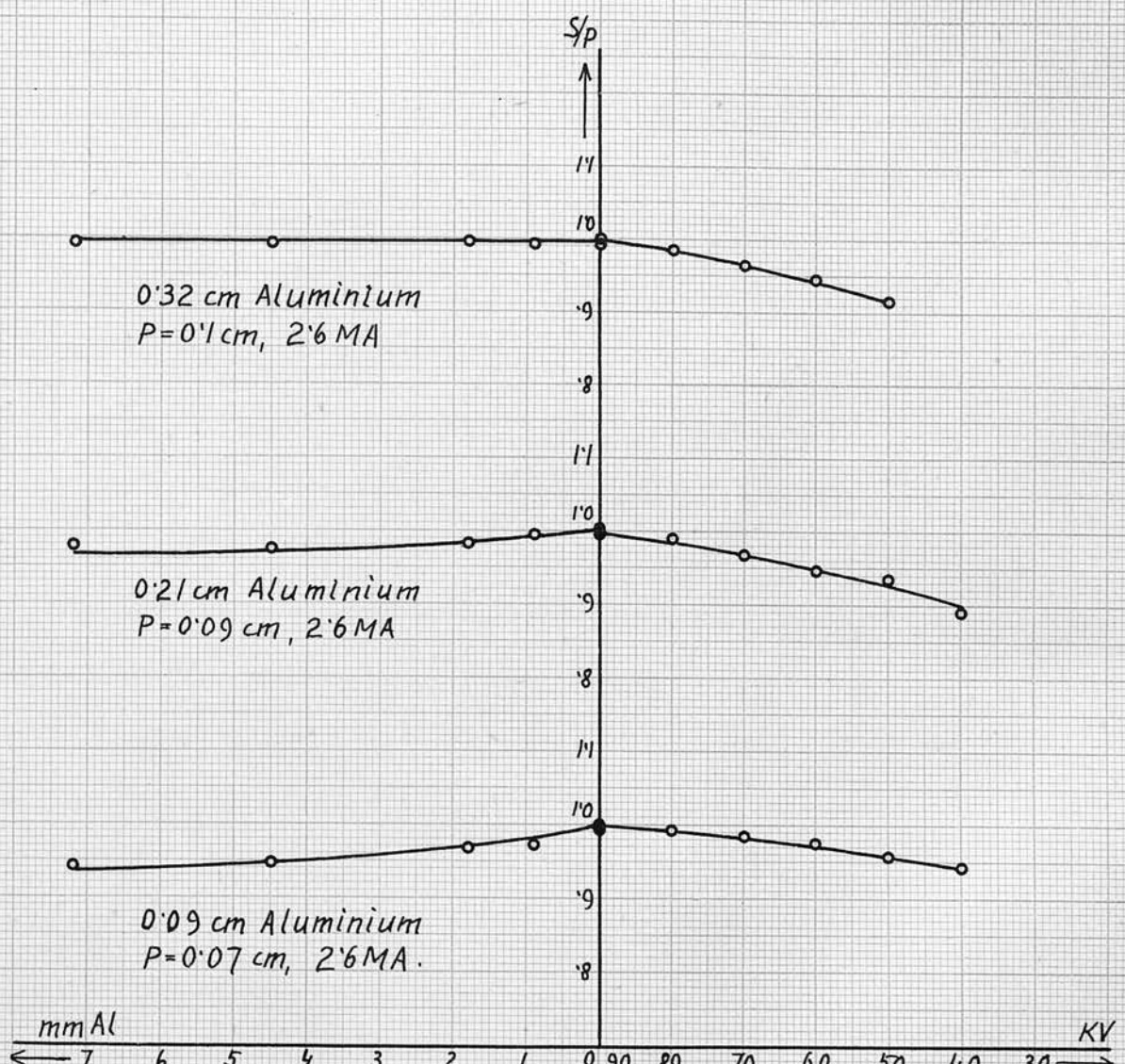
Philips Metalix Tube 1325.
(horizontal)
J' = J = 1·6 cm, S1 = S2 = 3·0 cm
S/p
1·1
1·0
·9
·8
0·32 cm Aluminium
P = 0·1 cm, 2·6 MA
1·1
1·0
·9
·8
0·21 cm Aluminium
P = 0·09 cm, 2·6 MA
1·1
1·0
·9
·8
0·09 cm Aluminium
P = 0·07 cm, 2·6 MA.
mm Al
7 6 5 4 3 2 1 0
90 80 70 60 50 40 30
KV

Fig. 24.

a definite dependence on the thickness of the scatterer. The slope of the graph decreases for decreasing thickness of scatterer. Apart from that, there is a definite connection between the material of the scatterer and the slope of the graph for equal thicknesses of scatterer. Aluminium (0·21 cms.) shows a much greater slope than carbon (0·23 cms.) or filter paper (20 sheets). This point will be dealt with in more detail later on. In no case, however, does the graph show the least sign of a horizontal line or discontinuity in slope. The scattering curve obtained by filtration of the main radiation (at constant voltage) shows that the slope also depends on the thickness of the scatterer, there being an increase in slope for decreasing thickness of the scatterer. It can also be seen that as the density of the scatterer increases (filter paper ⟶ paraffin wax ⟶ carbon ⟶ aluminium), a much thinner scatterer is required to make the graph horizontal. It has never been possible to obtain a graph showing an increase of S/P with increasing thickness of filtering aluminium.

The fact that all graphs are of the same type and quite independent of the scatterer is in sharp contrast with the results obtained by Reekie[7] for his experiments carried out with aluminium scatterers. He investigated only the variation of S/P with different voltages on the tube. His graphs show first an increase of S/P which gradually changes over to a

decrease of S/P with decreasing voltage. The maximum value of S/P depends on the thickness of the scatterer, moving towards lower voltages for decreasing thickness of scatterer. His experiments with filter paper scatterers are similar to those obtained with paraffin wax scatterers, showing a horizontal part and a discontinuity similar to those of Fig. 2.

(c) Polarization correction experiments.

According to classical and wave-mechanical theories of the production of X-rays, the radiation emitted from an X-ray tube is expected to be partially polarized. This partial polarization was first discovered by Barkla[10] and has since been confirmed on many occasions. The plane of polarization is perpendicular to the plane formed by the cathode-ray beam and the primary beam. Owing to this polarization, the intensity of the radiation scattered at 90° to the primary will be a minimum if the scattered beam and cathode-ray stream are parallel, and a maximum if they are perpendicular to each other. Measurements have shown that the polarization of the primary beam depends on the voltage applied to the tube; the polarization becomes somewhat more complete with decreasing voltage.

All the writer's experiments described so far have been performed with the X-ray tube in a horizontal position, i.e. the scattered beam was parallel to the cathode-ray beam and in this case the intensity

of the scattered radiation is a minimum. Owing to the increase in polarization with decreasing voltage, the intensity of the scattered radiation will be affected differently at different voltages. As all results arrived at by theory (Page 32 ff.), were based on the assumption of an unpolarized primary radiation, a correction for polarization will have to be applied to the results if a comparison with theory is to be made. The theory of this experimental polarization correction has been worked out in detail by Miss Ross(40). She has shown, that if the radiation scattered at 90° is observed in a direction making an angle of 45° with the plane of polarization, the ionization measured by the secondary chamber is the same as if the primary radiation were unpolarized. A second, less accurate method is to observe the 90° scattering in a direction perpendicular to the plane of polarization and in a direction lying in the plane of polarization and to take the mean value of both observations. Both methods have been used in the present work. In order to study the 90° scattered radiation in various directions regarding the plane of polarization, the X-ray tube has been turned so that the cathode-ray beam is inclined at various angles to the horizontal, i.e. with the direction of the scattered radiation. The method of turning the tube and with it the plane of polarization, is preferred to the alternate way of keeping the tube fixed and

rotating the secondary aperture system and secondary ionization chamber in a plane perpendicular to the primary beam. Unfortunately the experiments for a particular scatterer with the tube in various positions (horizontal, vertical and at 45^{o}), could not be carried out at the same time (i.e. the same day), which would have avoided the small errors introduced by day to day changes in the apparatus. Such small changes in the experimental conditions, did not, however, seem to have any significant influence on the results. These experiments, although carried out at widely different times, were performed under identical experimental conditions as far as they could be controlled.

The following graphs show the scattering curves for the different positions of the tube. Figs. 25, 26, 27 and 28 give the curves for various thicknesses of scatterers made of paraffin wax, filter paper, carbon, and aluminium respectively for the tube in a vertical position. Figs. 29, 30, 31 and 32 give the corresponding results for the tube making an angle of 45^{o} to the horizontal. The curves exhibited in Figs. 29, 30, 31 and 32 which represent the scattering curves for unpolarized primary radiation are, within experimental error, the mean value of the corresponding curves shown in Figs. 12, 22, 23 and 24 for the tube in a horizontal position and Figs. 29, 30, 31 and 32 for the tube in a vertical position. The corresponding results to Fig. 21 are shown in Figs. 33 and 34.

Philips Metalix Tube 1325.
(vertical)

$J' = J = 1'6$ cm, $S_1 = S_2 = 1'6$ cm

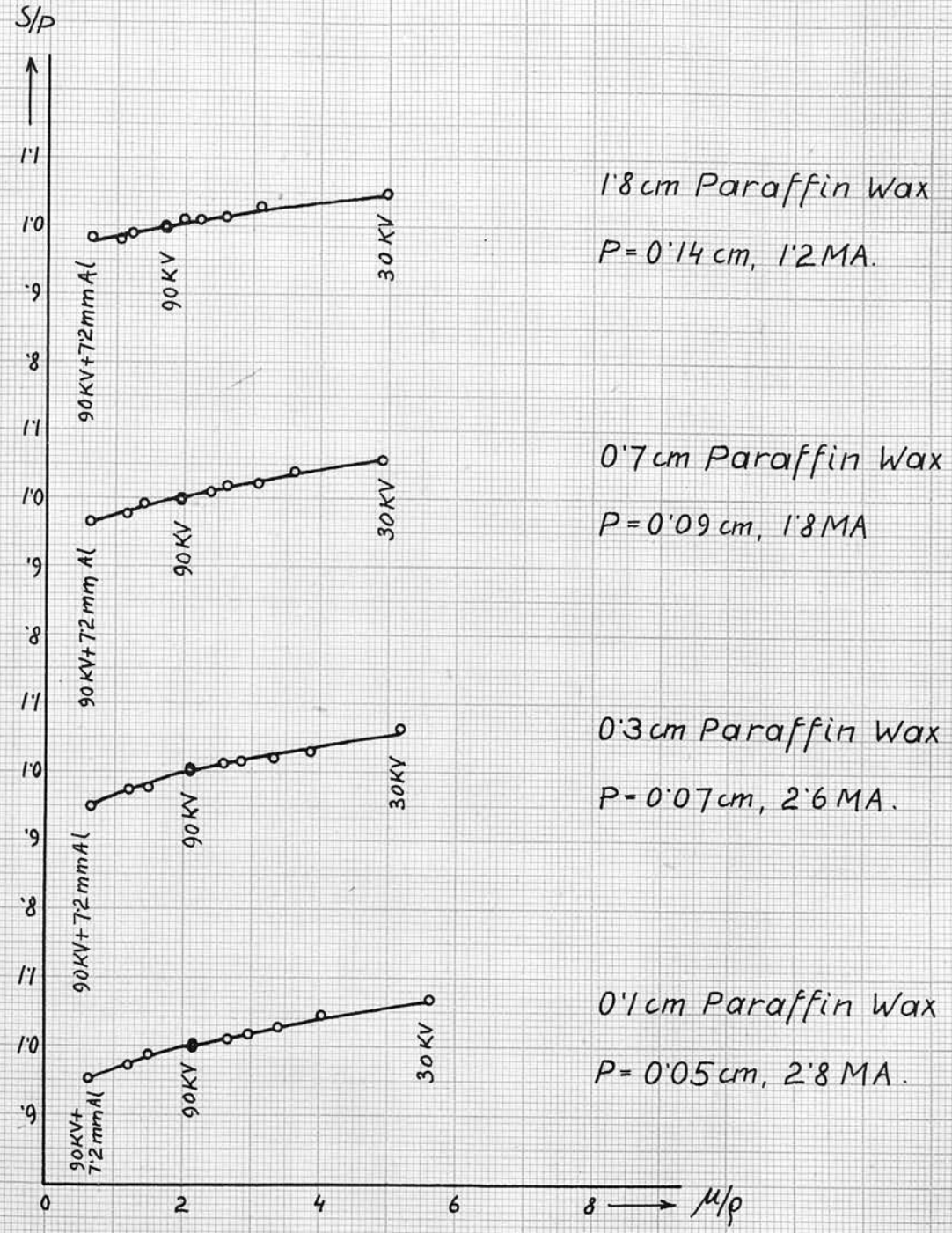

Fig. 25.

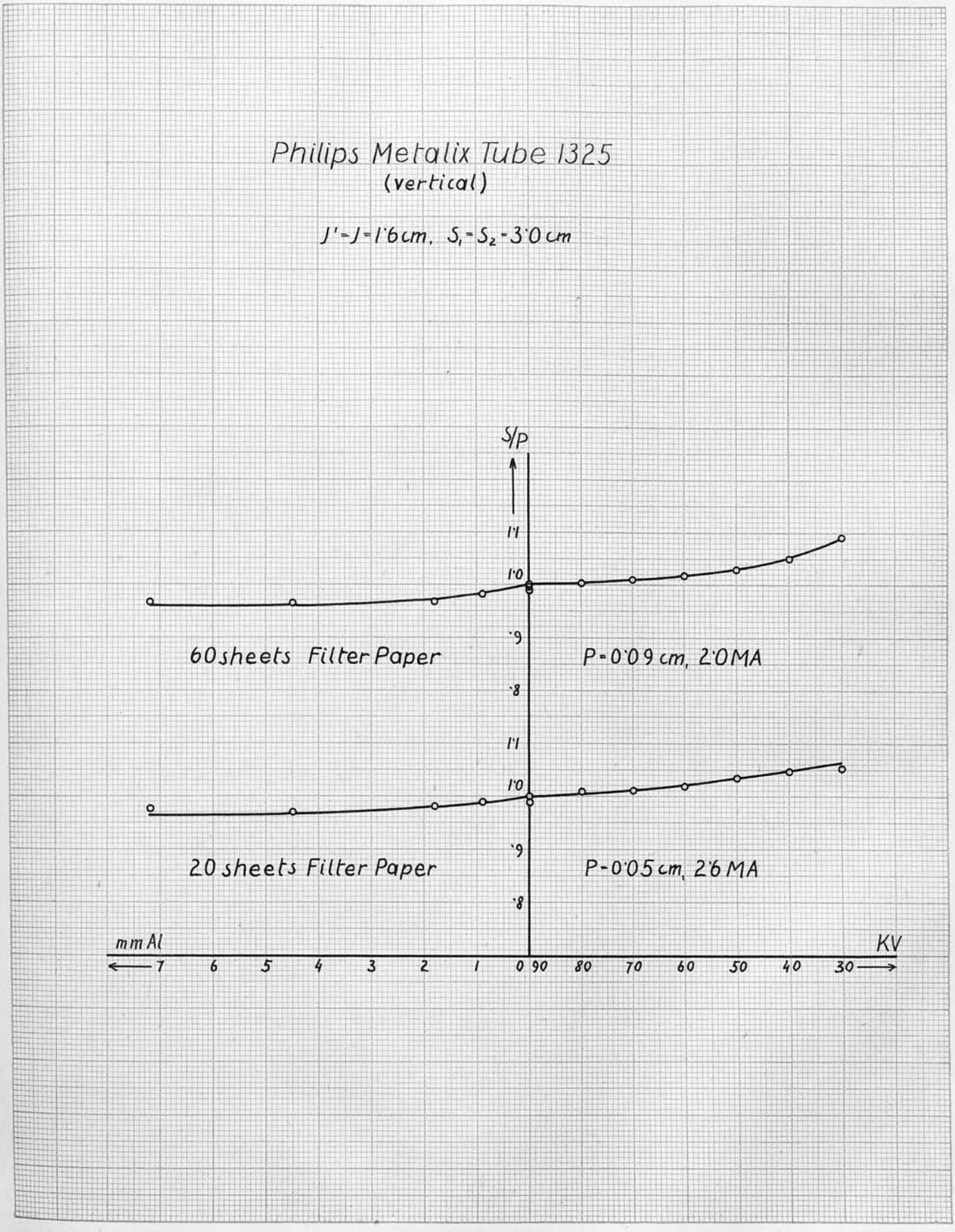
Philips Metalix Tube 1325
(vertical)
J'-J=1·6cm. S1-S2=3·0cm
S/P
1·1
1·0
·9
·8
60 sheets Filter Paper
P=0·09 cm, 2·0MA
1·1
1·0
·9
·8
20 sheets Filter Paper
P=0·05 cm, 2·6 MA
mm Al
7 6 5 4 3 2 1 0
90 80 70 60 50 40 30
KV

Fig. 26.

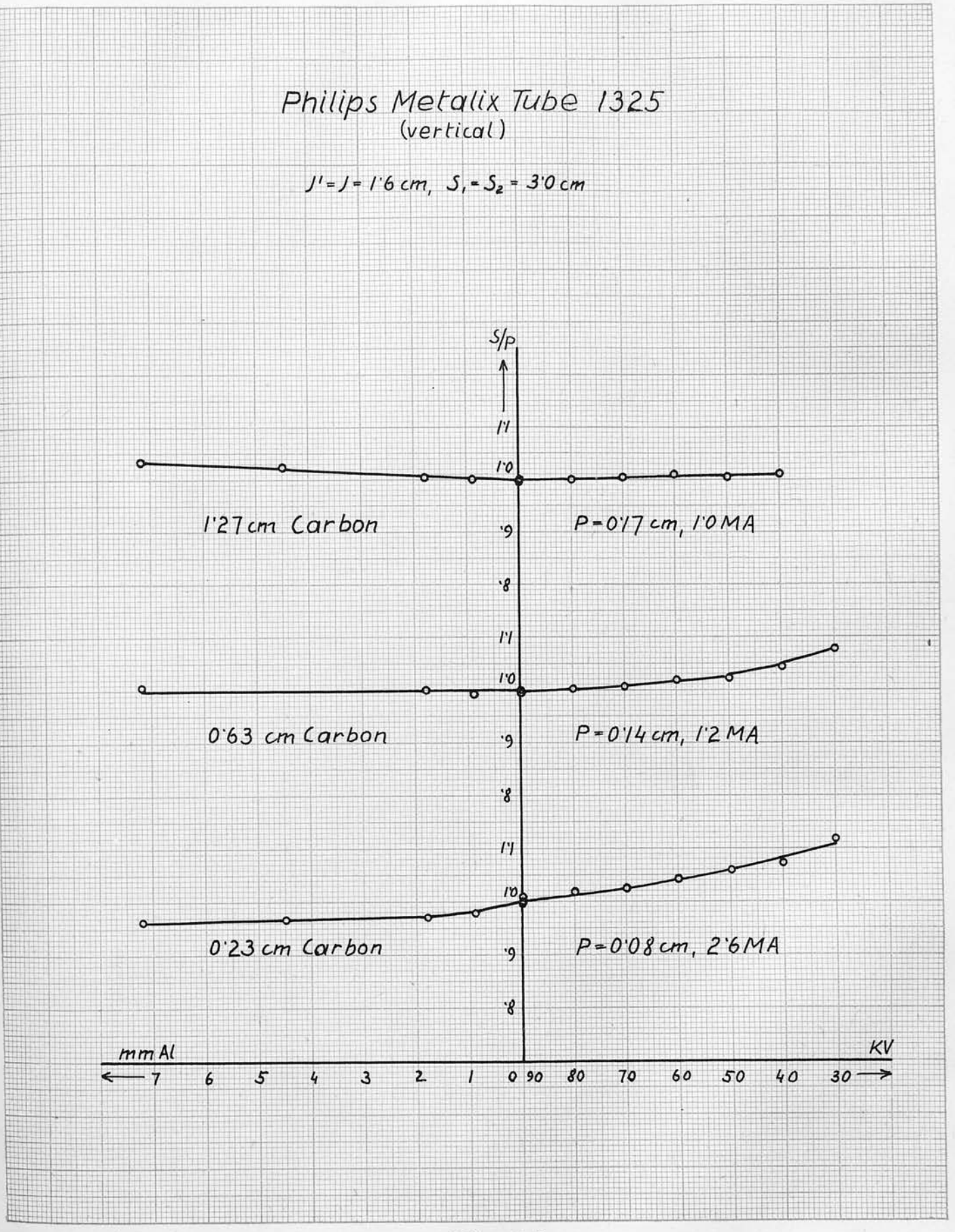
Philips Metalix Tube 1325
(vertical)
J' = J = 1·6 cm, S1 = S2 = 3·0 cm
S/P
1·1
1·0
·9
·8
1·27 cm Carbon
P = 0·17 cm, 1·0 MA
0·63 cm Carbon
P = 0·14 cm, 1·2 MA
0·23 cm Carbon
P = 0·08 cm, 2·6 MA
mm Al
KV
7 6 5 4 3 2 1 0 90 80 70 60 50 40 30

Fig. 27.

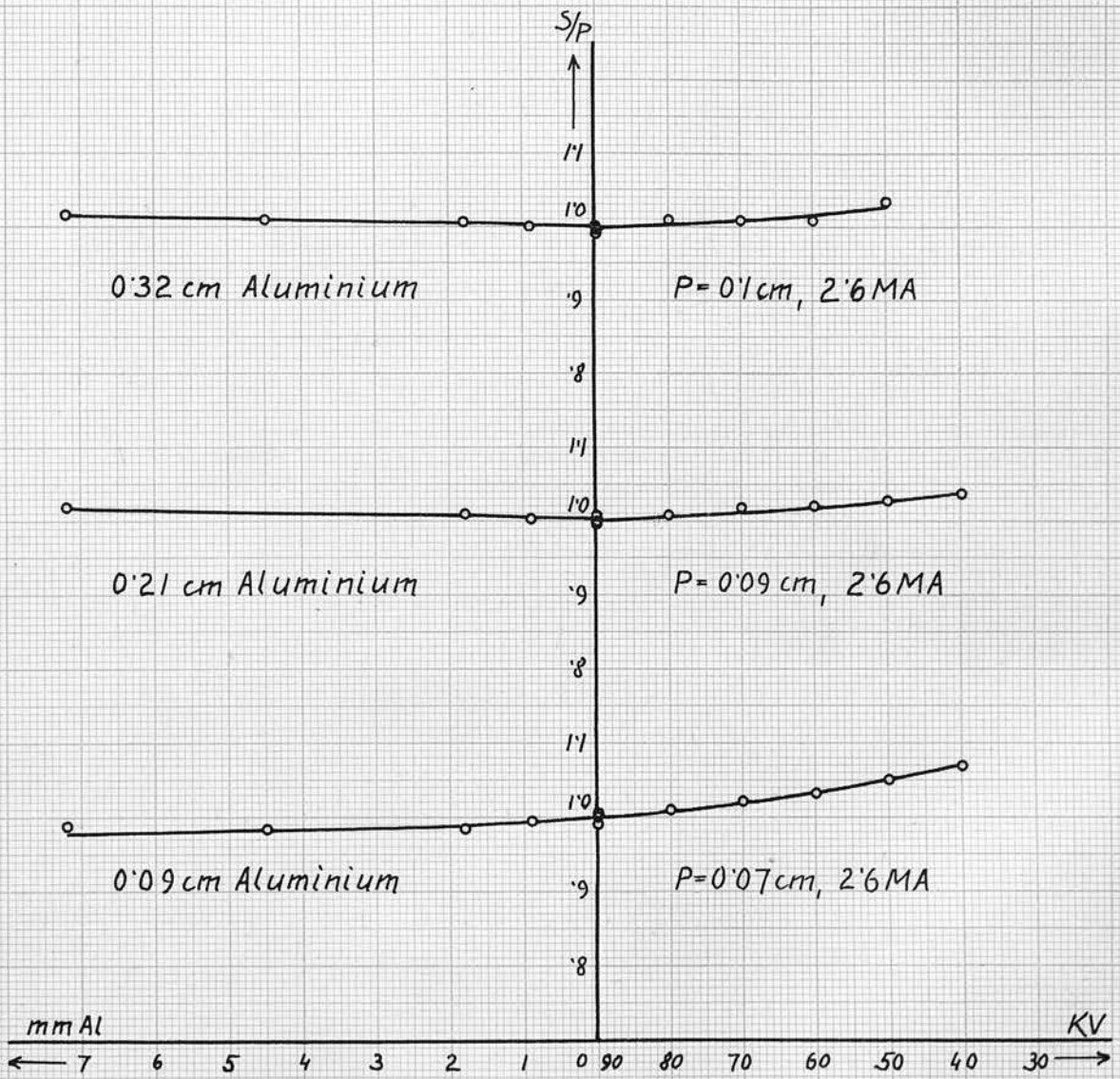
Philips Metalix Tube 1325
(vertical)
J'=J=1'6 cm, S1=S2=3'0 cm
S/P
1·1
1·0
·9
·8
0·32 cm Aluminium
P=0·1 cm, 2·6 MA
0·21 cm Aluminium
P=0·09 cm, 2·6 MA
0·09 cm Aluminium
P=0·07 cm, 2·6 MA
mm Al
KV
7 6 5 4 3 2 1 0 90 80 70 60 50 40 30

Fig. 28.

Philips Metalix Tube 1325.
(45°)

$J' = J = 1'6$ cm, $S_1 = S_2 = 1'6$ cm.

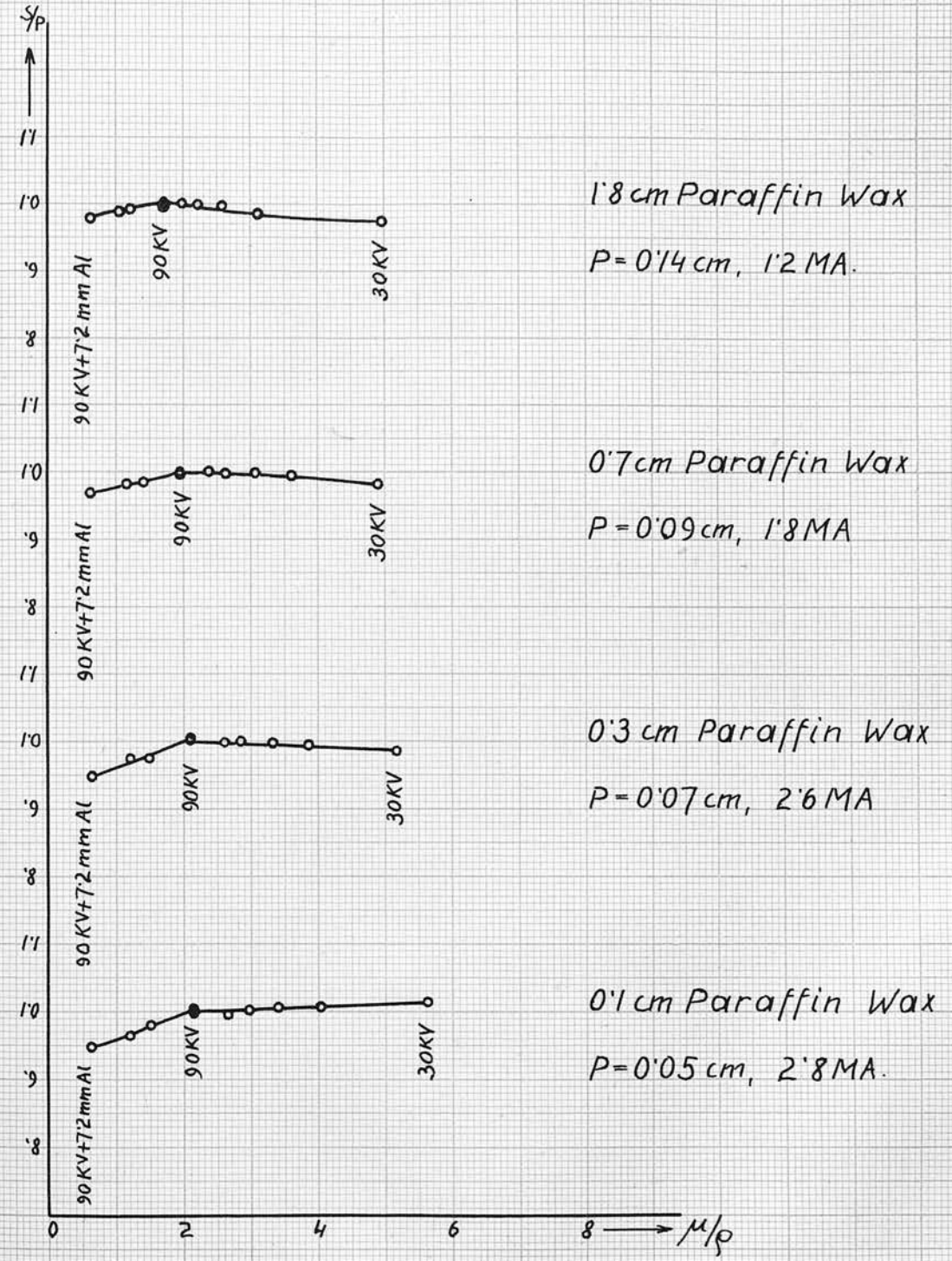

1·8 cm Paraffin Wax

P = 0·14 cm, 1·2 MA.

0·7 cm Paraffin Wax

P = 0·09 cm, 1·8 MA

0·3 cm Paraffin Wax

P = 0·07 cm, 2·6 MA

0·1 cm Paraffin Wax

P = 0·05 cm, 2·8 MA.

Fig. 29.

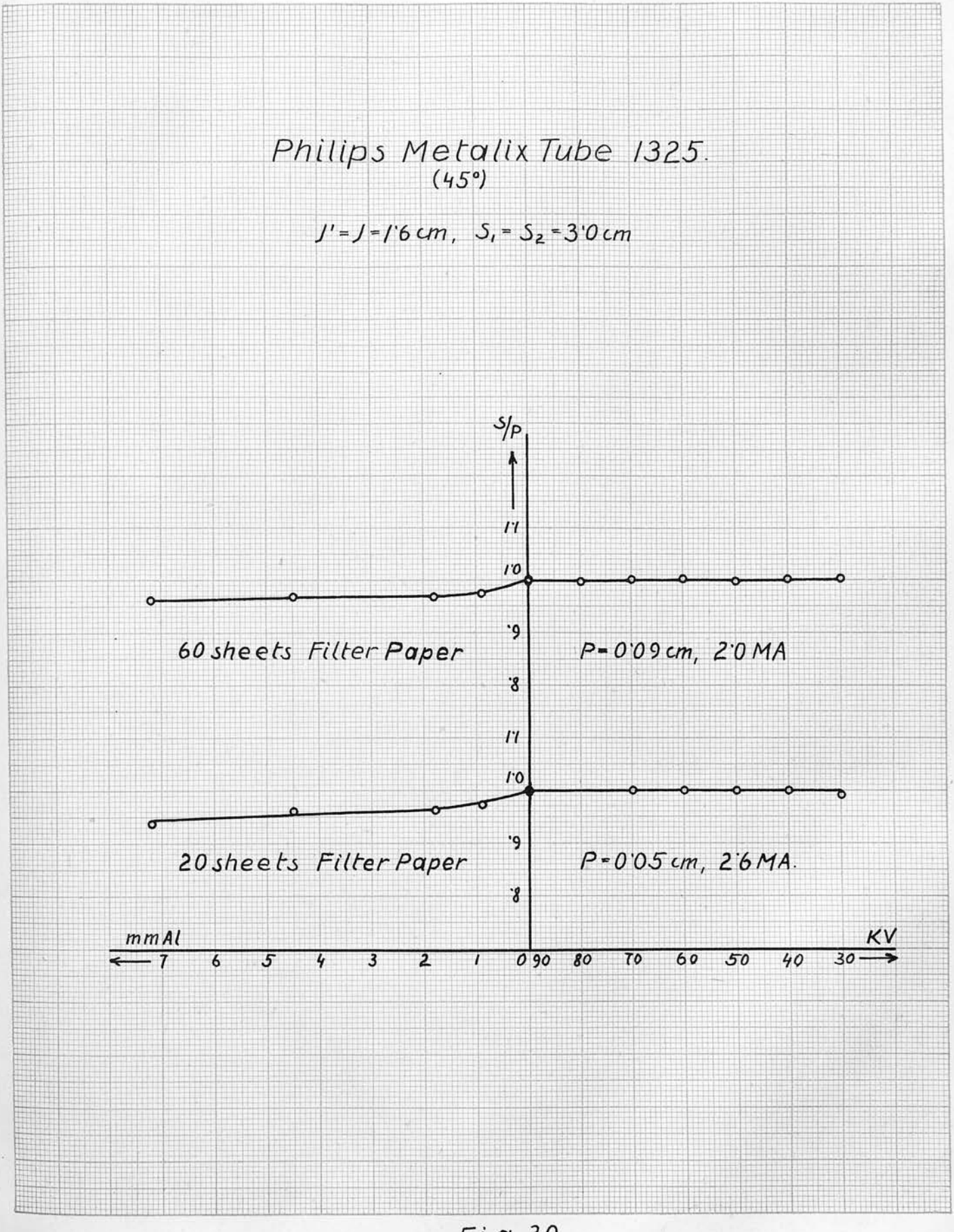
Philips Metalix Tube 1325.
(45°)
J' = J = 1'6 cm, S1 = S2 = 3'0 cm
S/P
1·1
1·0
·9
·8
60 sheets Filter Paper
P = 0'09 cm, 2·0 MA
1·1
1·0
·9
·8
20 sheets Filter Paper
P = 0'05 cm, 2·6 MA.
mmAl
7 6 5 4 3 2 1 0
90 80 70 60 50 40 30
KV

Fig. 30.

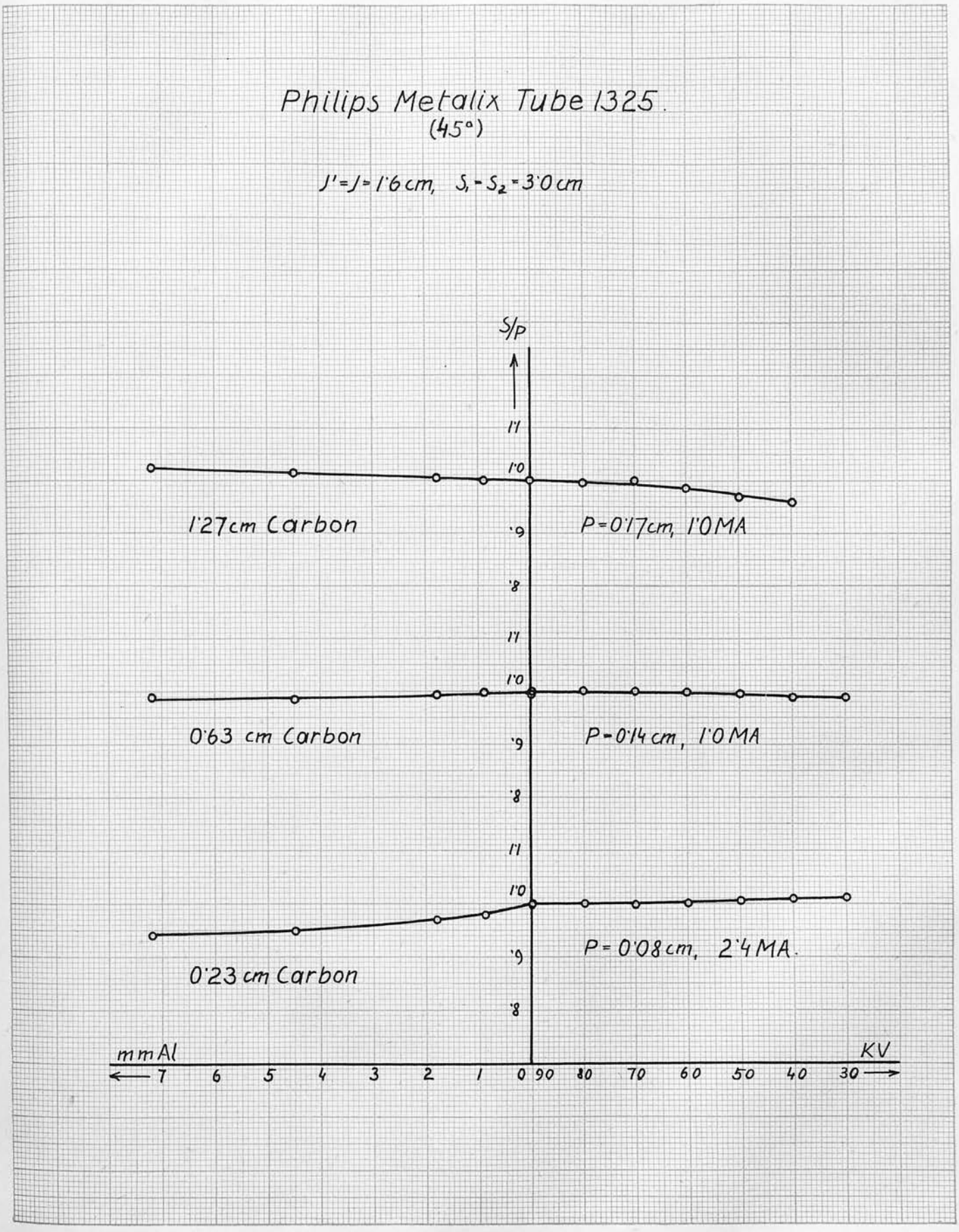
Philips Metalix Tube 1325.
(45°)
J'=J=1·6 cm, S1-S2=3·0 cm
S/P
1·1
1·0
·9
·8
1·27 cm Carbon
P=0·17 cm, 1·0 MA
0·63 cm Carbon
P=0·14 cm, 1·0 MA
0·23 cm Carbon
P=0·08 cm, 2·4 MA.
mmAl
7 6 5 4 3 2 1 0
KV
90 80 70 60 50 40 30

Fig. 31.

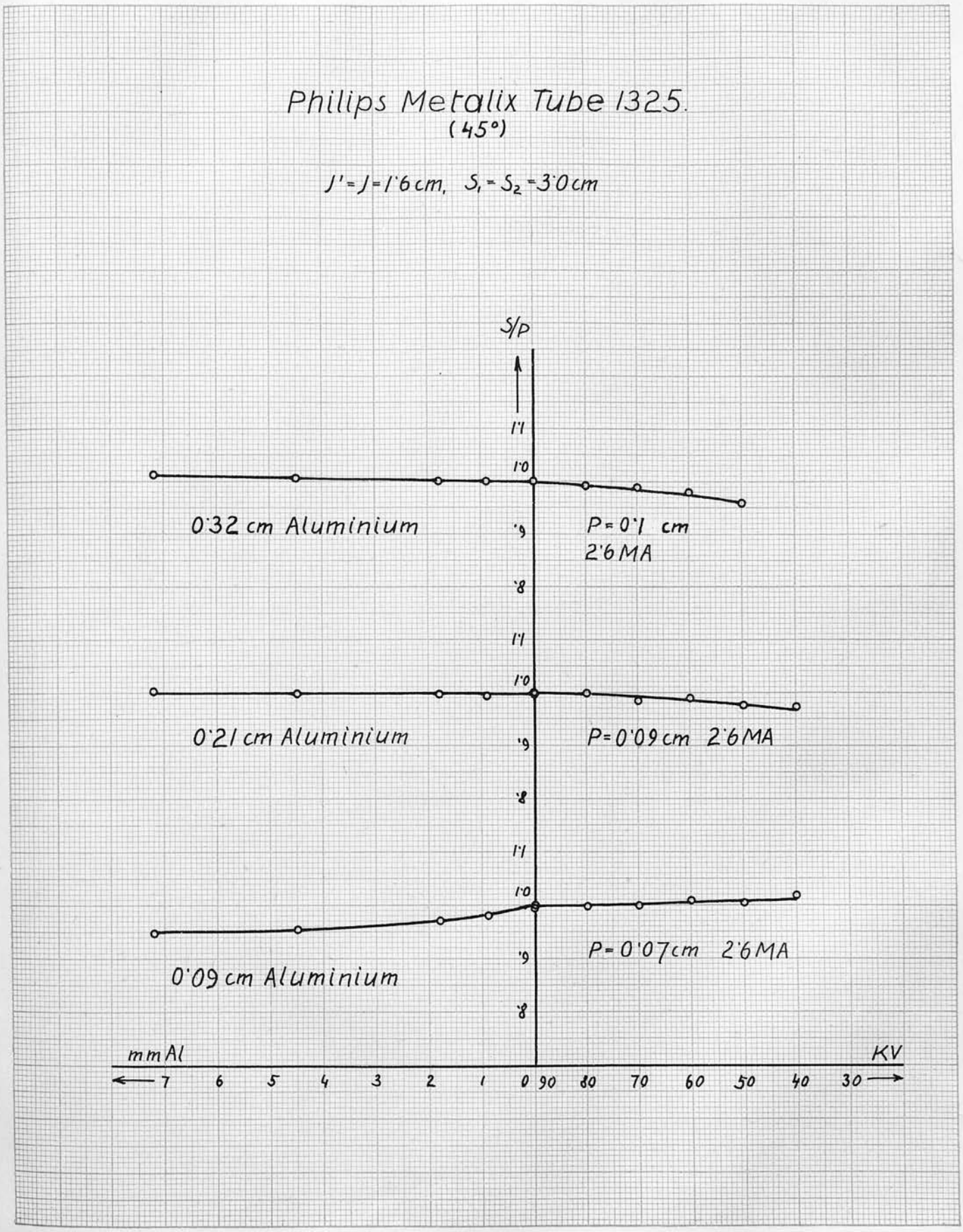
Philips Metalix Tube 1325.
(45°)
J' = J = 1·6 cm, S1 = S2 = 3·0 cm
S/P
1·1
1·0
·9
·8
0·32 cm Aluminium
P = 0·1 cm
2·6 MA
0·21 cm Aluminium
P = 0·09 cm 2·6 MA
0·09 cm Aluminium
P = 0·07 cm 2·6 MA
mm Al
KV
7 6 5 4 3 2 1 0
90 80 70 60 50 40 30

Fig. 32.

Philips Metalix Tube 1325.
(vertical)

0·3 cm Paraffin wax scatterer, 2·6MA

$J' = J = 1{\cdot}6$ cm, $S_1 = S_2 = 1{\cdot}6$ cm, $P = 0{\cdot}07$ cm.

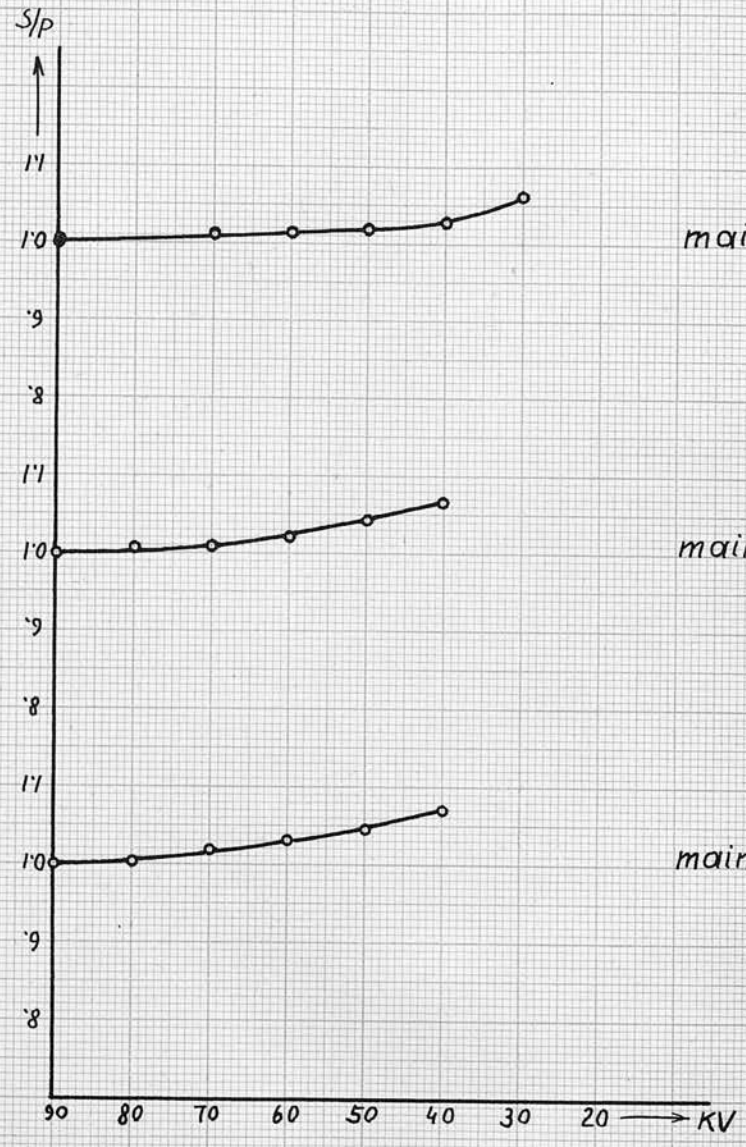

Fig. 33.

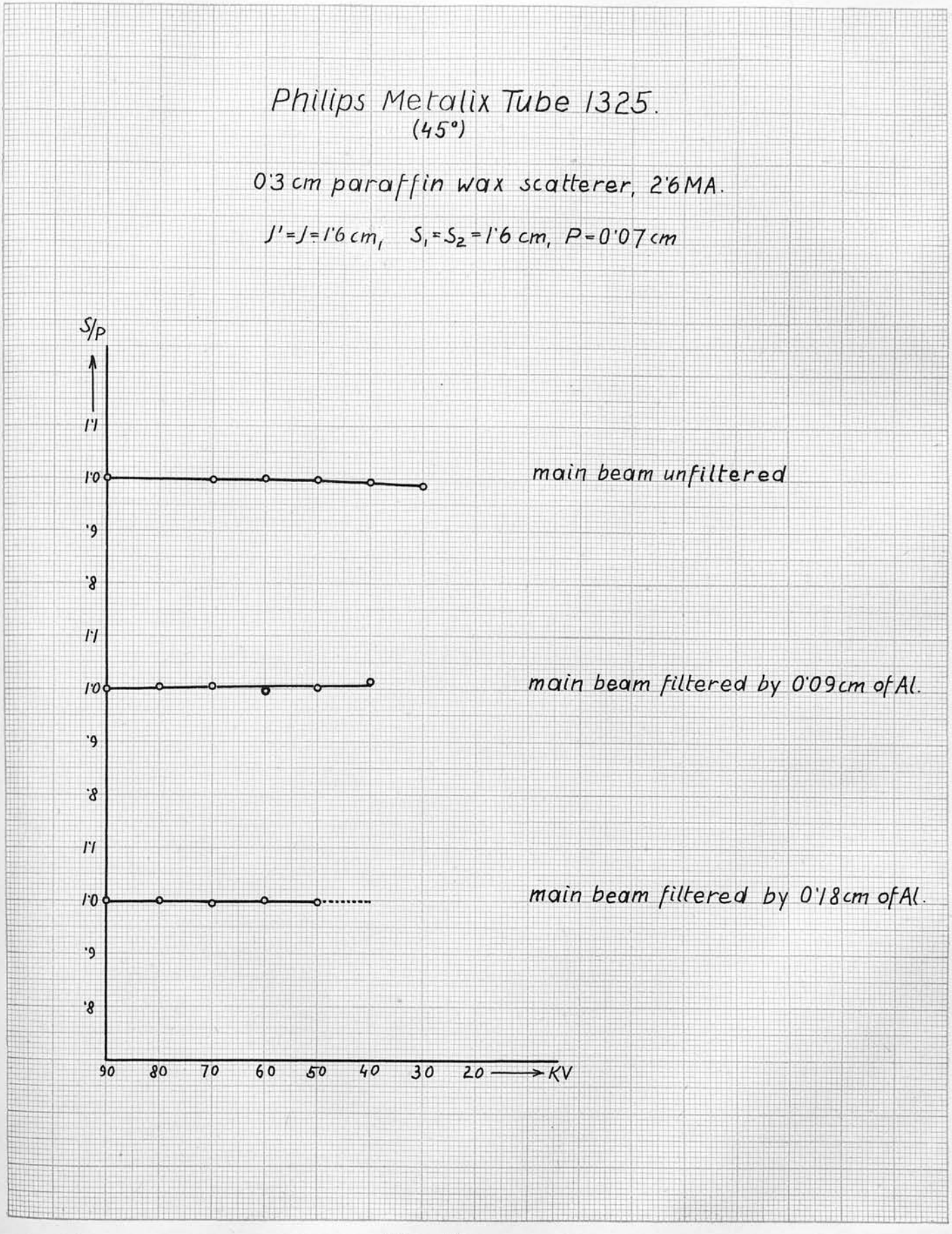
Philips Metalix Tube 1325.
(45°)
0·3 cm paraffin wax scatterer, 2·6 MA.
J' = J = 1·6 cm, S1 = S2 = 1·6 cm, P = 0·07 cm
S/P
1·1
1·0
·9
·8
main beam unfiltered
main beam filtered by 0·09 cm of Al.
main beam filtered by 0·18 cm of Al.
90 80 70 60 50 40 30 20 KV

Fig. 34.

Here again the curves on Fig. 34 represent the mean value of the corresponding curves shown in Figs. 21 and 33.

The polarization correction that has to be applied to the curve S/P against KV for a particular kind of scatterer varies, as can be seen from the graphs, with varying thickness of the scatterer. This, of course, is to be expected since a relatively greater amount of unpolarized softer radiation is scattered by thin scatterers than by thick ones, (thick scatterers absorb a greater fraction of the unpolarized soft radiation), thus making the primary radiation appear to be less polarized when scattered by thin scatterers. For the part of the scattering curve which is obtained by intercepting the radiation with aluminium, the correction for polarization is very small, and at most 2%.

The scattering curves obtained with the tube making an angle of 45° and 90° with the horizontal, again show the dependence of the slopes of the graphs on the thickness of the scatterer. In all cases (for S/P against KV) the slope becomes smaller (including negative slopes) as the thickness of the scatterer is diminished. A similar relationship holds also for the graphs S/P against the thickness of filtering aluminium. In no case does a discontinuity appear in the slope of the graphs, as has frequently been obtained by workers in this laboratory for experiments carried out with the tube in these positions.

It has been stated before that when the plane of polarization is vertical and the scatterer sufficiently thick, the graph S/P against thickness of filtering aluminium becomes horizontal. This statement, however, does not hold when the plane of polarization is parallel or inclined at an angle of 45^{o} to the horizontal. As can be seen from the scattering curves for carbon and aluminium (Figs. 27, 28, 31 and 32), S/P increases for increasing thickness of aluminium filter.

DISCUSSION OF THE SCATTERING EXPERIMENT.

A comparison with theory of the results of the scattering experiment described in the previous section, can only be made if account is taken of the fact that the theory is only valid for unpolarized radiation and for an ideal scattering process, i.e. for an infinitely thin scatterer where no absorption of the radiation takes place. Whereas it is relatively simple to correct for the polarization experimentally, it is impossible to use scatterers thin enough to neglect absorption taking place within them.*) It is, however, possible to extrapolate the results obtained for various thicknesses of scatterers down to a scatterer of zero thickness. This extrapolation can only be carried out by a graphical method, but owing to the fact that the variation in number of the scatterers used is very small (2 to 4) the error introduced by this method will necessarily be rather large. This applies especially to the case of filter paper scatterers. The results of this extrapolation are shown in Fig. 35. Despite the uncertainty involved in this process, these graphs, obtained from the 45° scattering curves, are considered to be the most reliable results which could be obtained by the

---

*) Apart from that, there is a certain amount of filtering by the windows of the ionization chambers, which has been neglected here.

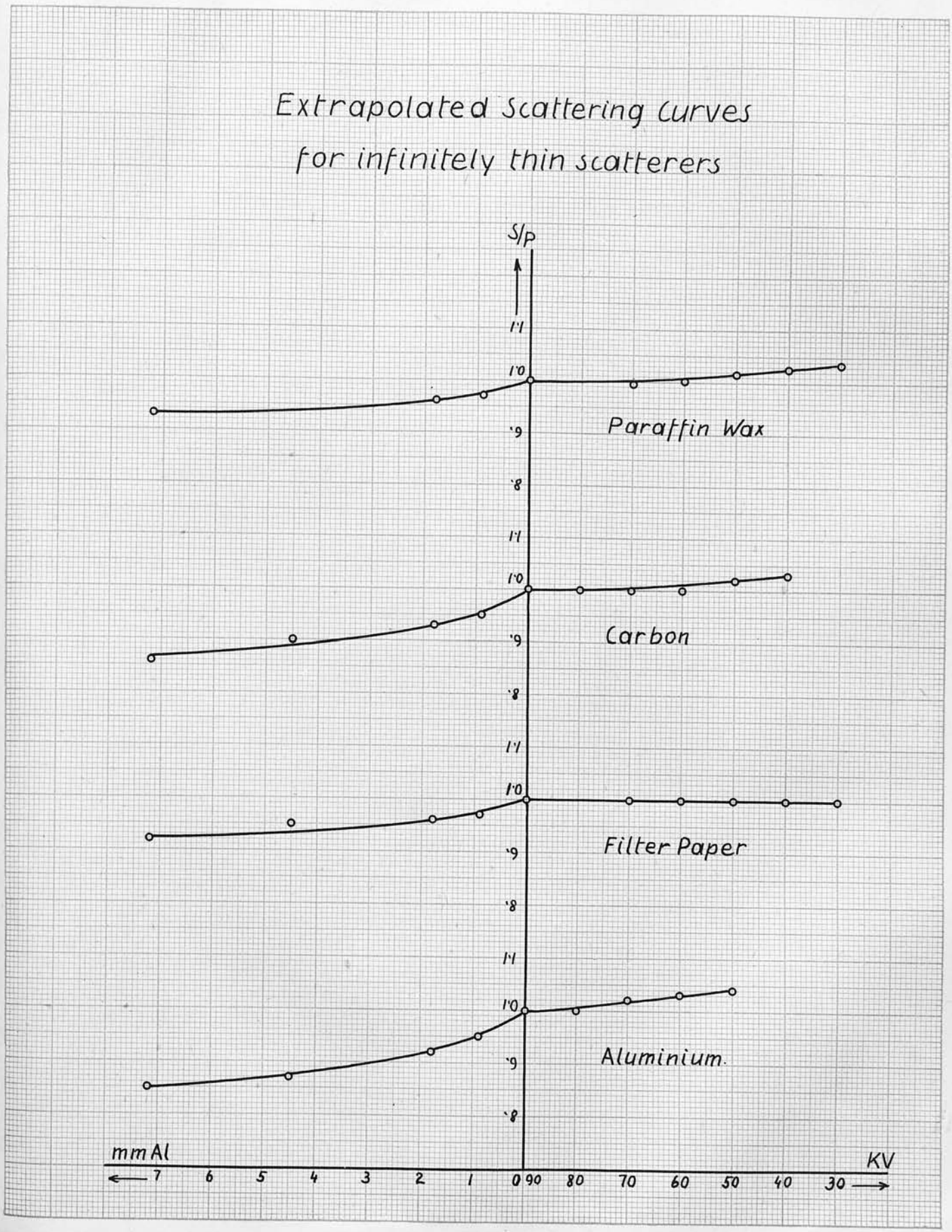
Extrapolated Scattering Curves
for infinitely thin scatterers
S/P
1·1
1·0
·9
·8
Paraffin Wax
Carbon
Filter Paper
Aluminium.
mm Al
7
6
5
4
3
2
1
0
90
80
70
60
50
40
30
KV

Fig. 35.

experimental method employed in this work. These, therefore, are the results to be compared with theory. Considering the fact that the radiation is heterogeneous, with a spectrum which could not be determined, the comparison of theory and experiment can only be of a qualitative nature. In this limited sense, the results of the comparison between the theory illustrated in Fig. 4 and the experimental results of Fig. 35 is considered to be satisfactory. The experimental scattering curve for paraffin wax, for an infinitely thin scatterer, shows a slight increase of the scattered intensity as the voltage is lowered, that is, as the mean wave length is increased. The curve for carbon shows a bigger increase and that for aluminium a still bigger increase. The curve for filter paper does not show this increase of the scattered intensity with lowered voltage. This is considered to be not very significant because the accuracy of the work with filter paper is on the whole less than with other scatterers and the extrapolation in this case is a doubtful procedure, since it has been carried out on two points only, for each voltage setting. For carbon and aluminium there were three points for each extrapolation and for paraffin wax four.

For the scattering curve which is obtained by progressive filtering of the main primary radiation before scattering takes place, a theoretical inter-

pretation of the results on a mathematical basis was found to be impossible owing to the complexity of the problem. As the thickness of the filtering aluminium increases, a relatively greater amount of the softer radiation is absorbed, which would result in a decrease of the scattered intensity, provided an infinitely thin scatterer is being used. This is confirmed by the experiments described in the previous chapter.

As regards the comparison of scattering curves for different scattering substances, in the portions of the graphs obtained by progressive filtering (Fig. 35), the results show that interception of the beam by a given thickness of aluminium gives a drop of S/P which increases with increasing mean atomic number of the scattering material. This result is in close agreement with accepted theory of X-ray scattering. The drop with filter paper is somewhat less than that of carbon and this may be regarded as an indication that the filter paper results are less accurate than those of the other scatterers. The reasons why this should be regarded as true have already been given.

This work differs from that of previous experimenters in that the experimental results are remarkably constant despite great variations in experimental conditions. This is perhaps the most important feature of this work. Up till now the results of the scattering experiments have often been stated to depend on the primary beam aperture subsequent to the scatterer.

Relatively large primary apertures (bigger than approximately 0·07 cms. in diameter) gave results similar to those in Fig. 2, while small primary apertures (pinhole apertures; diameter less than 0·05 cms.) gave a constant ratio S/P no matter what the value of $\overline{\mu/\rho}$. Such dependence of the result on the primary aperture could not be observed by the writer.

Evidence has, however, been obtained that the apertures previous to the scatterer and the divergence of the main beam must be kept as constant as possible.

When care was taken to keep the experimental conditions fully under control the sudden change of slope, whose position depends on the thickness of the scatterer (as shown in Fig. 2) was not obtained.

PART 2. THE FILTERING EXPERIMENT.

Variation of voltage on tube.
Paraffin wax scatterers of varying thickness.
Variation of scattering material.

Like the scattering experiment, the results obtained from the filtering experiment are all of one type. Typical results are shown in Figs. 36 and 37. These were obtained with Philips Metalix Tube No. 1325 and 0·3 cms. paraffin wax scatterer. Primary and secondary beams were intercepted simultaneously with aluminium up to 0·09 cms. thick, each curve corresponding to a particular voltage between 50 Kv and 90 KV, or to 90 KV with the radiation filtered by a certain amount of aluminium placed before the scatterer. The graphs are all reduced to S/P = 1·00 for the unintercepted radiation. In all these graphs the ratio S/P decreases with increasing thickness of aluminium. The graphs seem to follow an exponential function although in many cases the slope is too small to permit deductions regarding its shape to be made. But in no case is there the least sign of a discontinuity (J-discontinuity) as observed occasionally by many workers in this laboratory, or a region of constant S/P connected with a sudden change in slope as reported by Reekie[7] and Miss Wilson.[1] A region of constant S/P could hardly be expected here since the corresponding scattering experiment shows no such constancy and

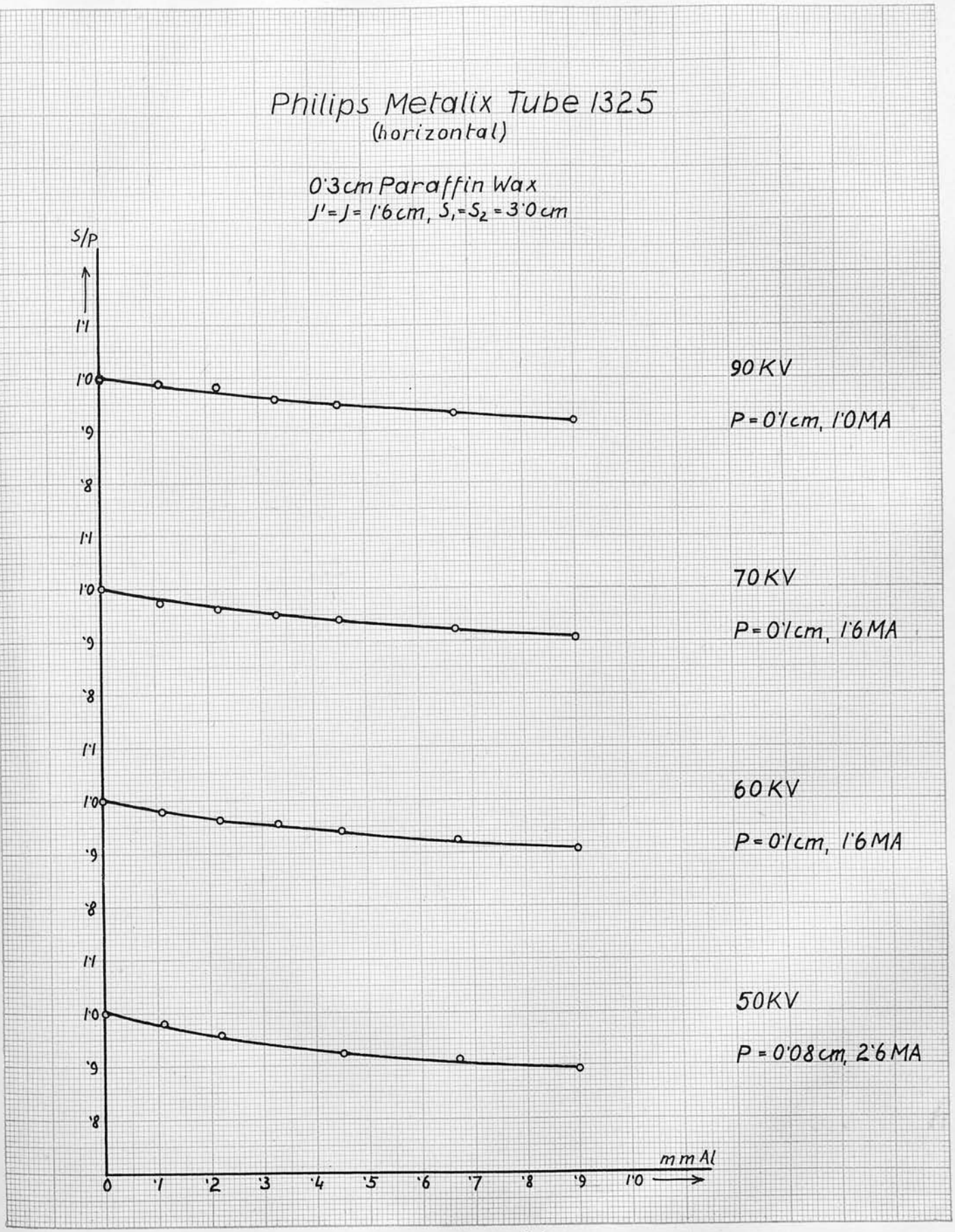
Philips Metalix Tube 1325
(horizontal)
0·3 cm Paraffin Wax
J'=J= 1·6 cm, S1=S2 = 3·0 cm
S/P
1·1
1·0
·9
·8
90 KV
P = 0·1 cm, 1·0 MA
70 KV
P = 0·1 cm, 1·6 MA
60 KV
P = 0·1 cm, 1·6 MA
50 KV
P = 0·08 cm, 2·6 MA
0
·1
·2
·3
·4
·5
·6
·7
·8
·9
1·0
mm Al

Fig. 36.

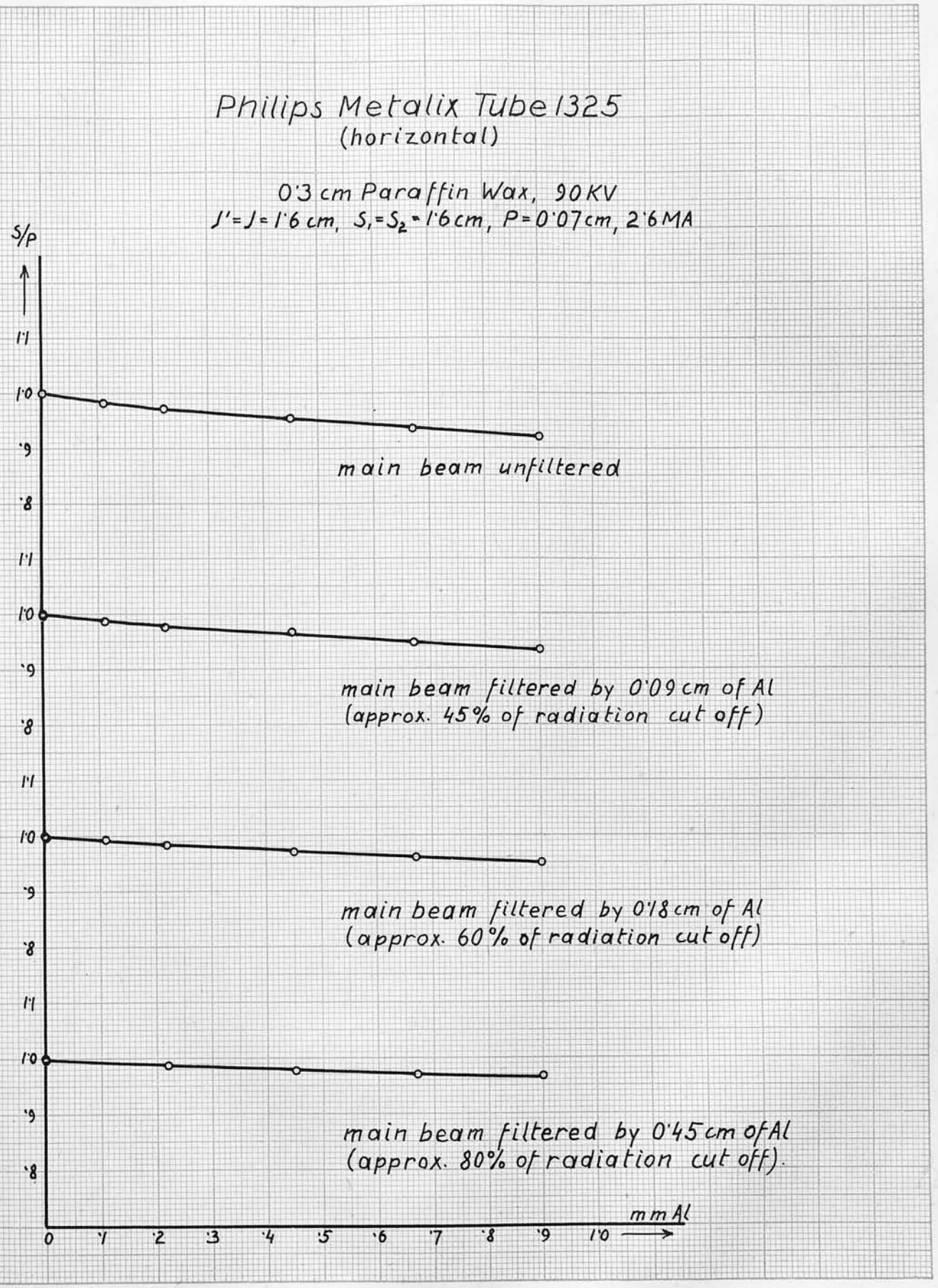
Philips Metalix Tube 1325
(horizontal)
0·3 cm Paraffin Wax, 90 KV
J'=J=1·6 cm, S1=S2=1·6 cm, P=0·07 cm, 2·6 MA
S/P
1·1
1·0
·9
·8
main beam unfiltered
main beam filtered by 0·09 cm of Al
(approx. 45% of radiation cut off)
main beam filtered by 0·18 cm of Al
(approx. 60% of radiation cut off)
main beam filtered by 0·45 cm of Al
(approx. 80% of radiation cut off).
mm Al
0
·1
·2
·3
·4
·5
·6
·7
·8
·9
1·0

Fig. 37.

according to Reekie, the constant ratio S/P in the results of the filtering experiment only appear if the voltage exciting the X-ray tube lies within the region of constant S/P for the corresponding scattering experiment. The only variations in the results under varying experimental conditions are variations in the slopes of the graphs. It is evident from Figs. 36 and 37, that as the radiation is made more penetrating, i.e. by increasing voltage and increasing amount of filtration of the main radiation, the slope of the graph becomes less. In the case where the main primary radiation is filtered by 0·45 cms. of aluminium, as much as 80% of the radiation is cut off, (as measured by its ionizing power) but the slope is still appreciable.

Figs. 38, 39, 40 and 41 show the results of the filtering experiments performed with scatterers of various thicknesses made of paraffin wax, filter paper, carbon and aluminium. The tube used for these experiments and all other filtering experiments to be mentioned was Philips Metalix Tube No. 1325 and the voltage applied in every case was 90 KV. It can be seen that the results are very similar to each other, the only difference being a very small variation in the slope of the graphs. Although in some cases for a particular kind of scatterer, the amount by which the ratio S/P for the greatest thickness of intercepting aluminium (i.e. 0·09 cms.) differs from unity

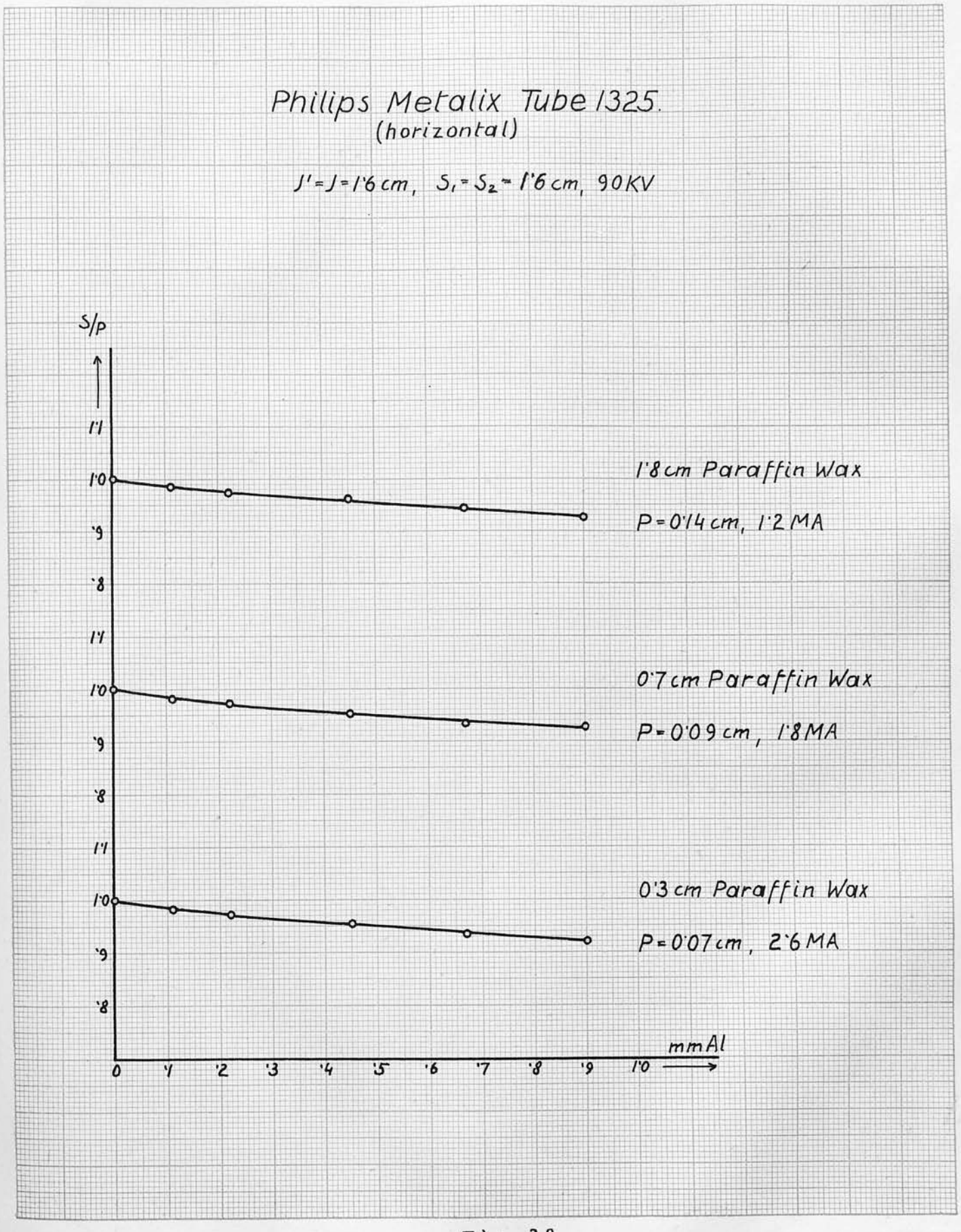
Philips Metalix Tube 1325.
(horizontal)
J' = J = 1·6 cm, S1 = S2 = 1·6 cm, 90 KV
S/P
1·1
1·0
·9
·8
1·8 cm Paraffin Wax
P = 0·14 cm, 1·2 MA
0·7 cm Paraffin Wax
P = 0·09 cm, 1·8 MA
0·3 cm Paraffin Wax
P = 0·07 cm, 2·6 MA
mm Al
0 ·1 ·2 ·3 ·4 ·5 ·6 ·7 ·8 ·9 1·0

Fig. 38.

Philips Metalix Tube 1325
(horizontal)

$J' = J = 1'6$ cm, $S_1 = S_2 = 3'0$ cm, 90KV

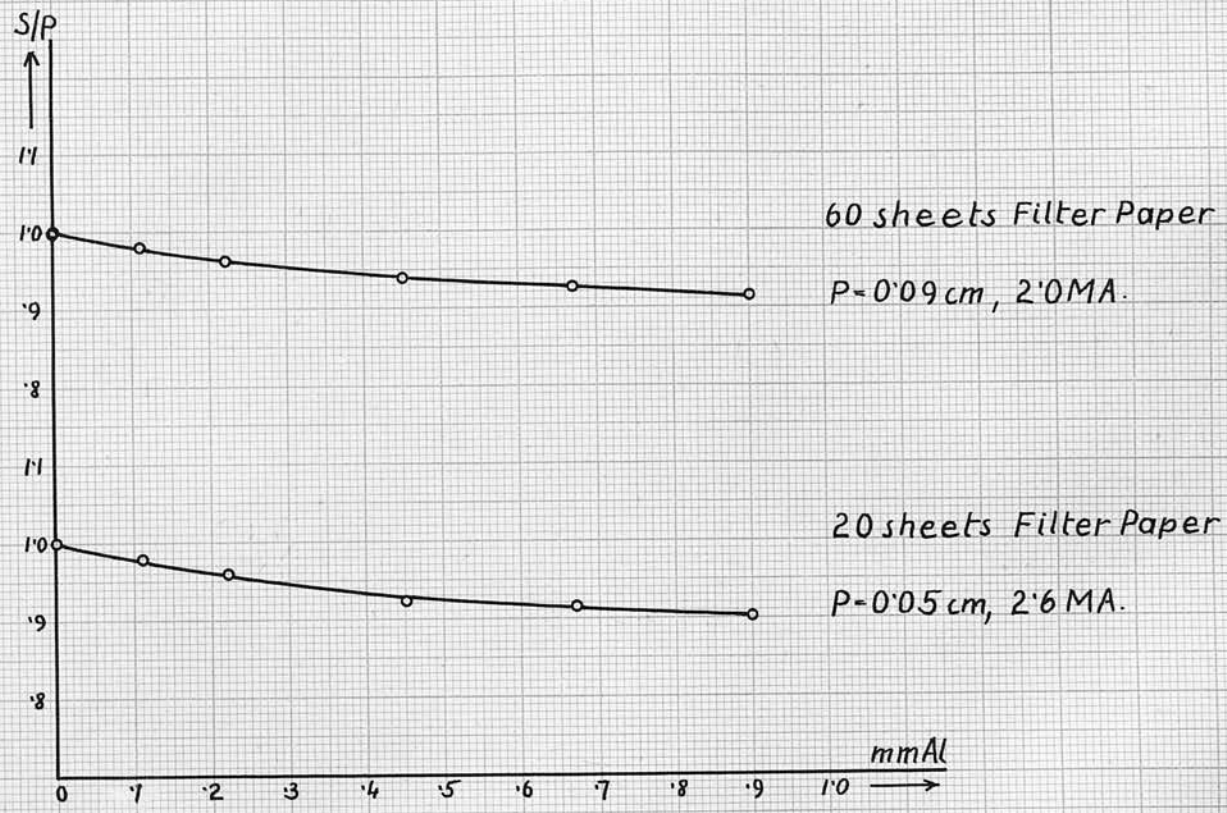

Fig. 39.

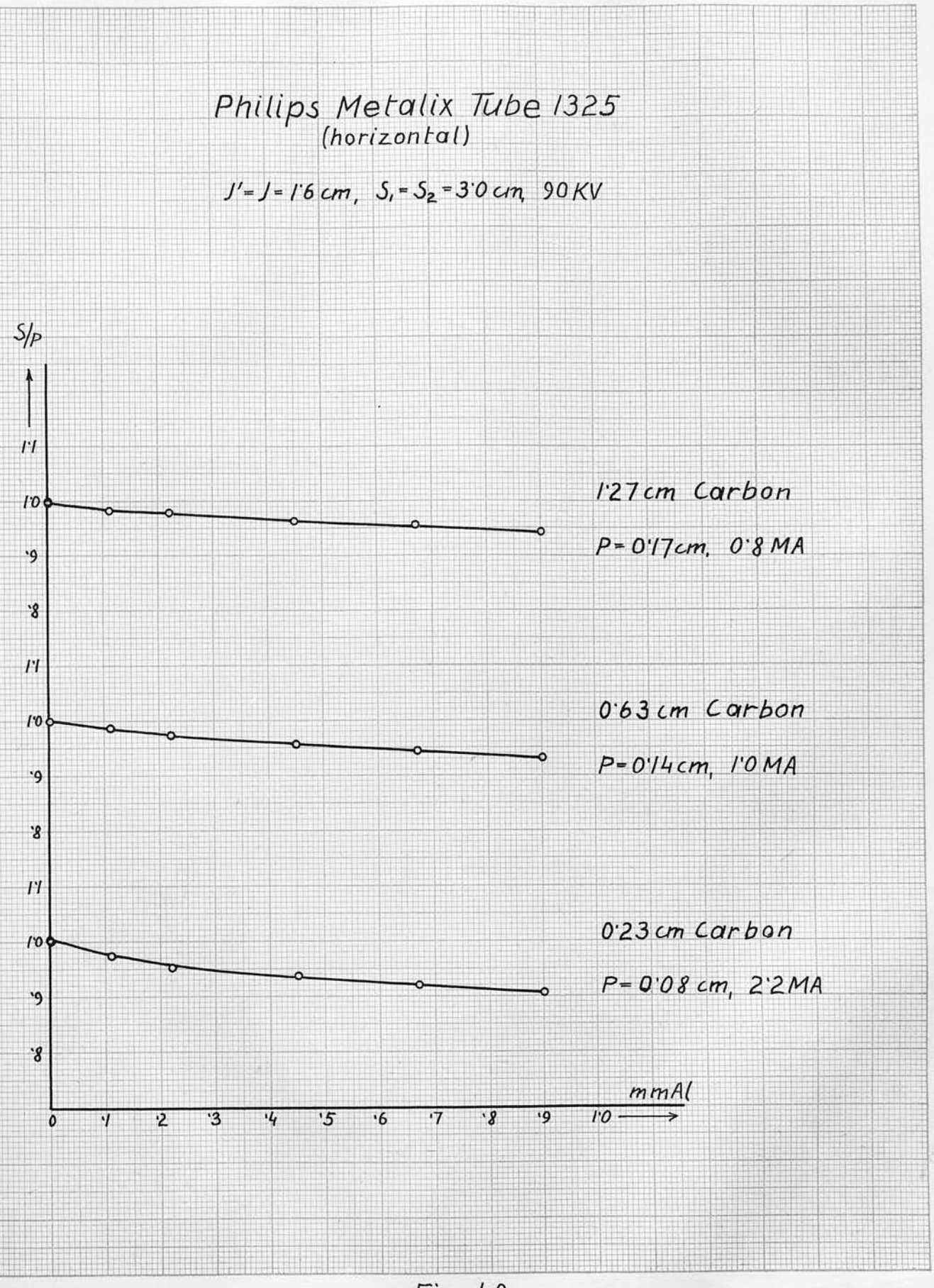
Philips Metalix Tube 1325
(horizontal)
J'=J=1·6 cm, S1=S2=3·0 cm, 90 KV
S/P
1·1
1·0
·9
·8
1·27 cm Carbon
P=0·17 cm, 0·8 MA
0·63 cm Carbon
P=0·14 cm, 1·0 MA
0·23 cm Carbon
P=0·08 cm, 2·2 MA
mmAl
0
·1
·2
·3
·4
·5
·6
·7
·8
·9
1·0

Fig. 40.

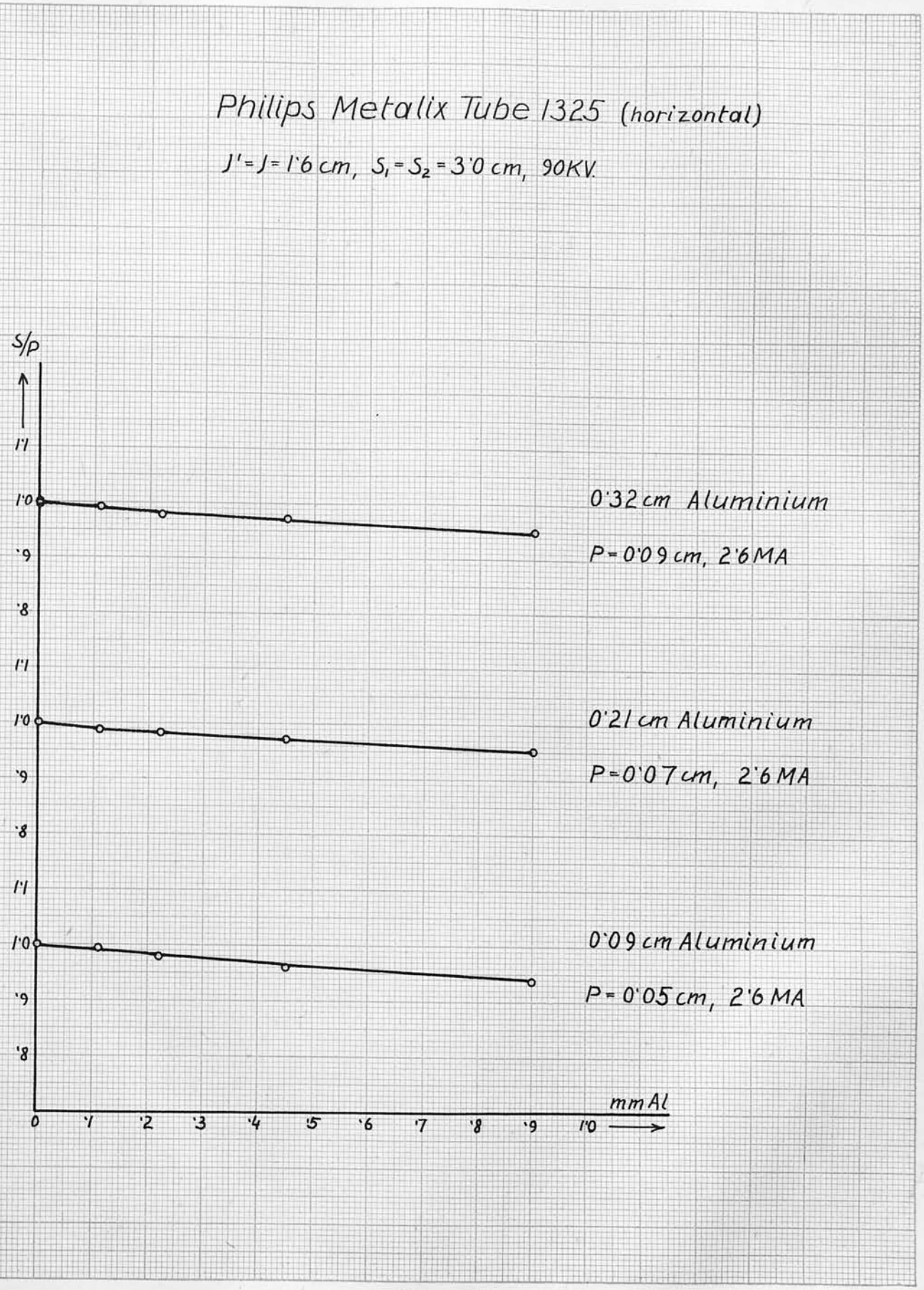
Philips Metalix Tube 1325 (horizontal)
J' = J = 1·6 cm, S1 = S2 = 3·0 cm, 90KV.
S/P
1·1
1·0
·9
·8
0·32 cm Aluminium
P = 0·09 cm, 2·6MA
0·21 cm Aluminium
P = 0·07 cm, 2·6 MA
0·09 cm Aluminium
P = 0·05 cm, 2·6 MA
mm Al
0
·1
·2
·3
·4
·5
·6
·7
·8
·9
1·0

Fig. 41.

(S/P = 1·00 for unintercepted radiation) does not vary very much with varying thickness of scatterer, it can easily be seen that

$$S/P_{\text{unintercepted}} - S/P_{\text{intercepted}}$$

increases for decreasing thickness of scatterer. To establish a definite rule from these results as to how $S/P_{\text{unint.}} - S/P_{\text{int.}}$ depends on the material of the scatterer is impossible since the variations are of the order of the experimental error.

Correction for Polarization.

In her thesis, Miss Ross(40) pointed out that in order to compare theory and experiment, the filtering experiment should be carried out in such a manner as to correct for the polarization of the primary radiation. These experiments have therefore been done by the writer with the tube in the same positions as in the scattering experiment, i.e. with the cathode-ray beam inclined at an angle of 90° and 45° respectively to the horizontal. The results of these experiments are shown in Figs. 42 to 46 and Figs. 47 to 52. As in the graphs obtained with the tube in a horizontal position, the results do not show any trace of discontinuity or region of constant S/P. The correction for polarization is very small and in all cases within experimental error, although it appears that $S/P_{\text{unint.}} - S/P_{\text{int.}}$ becomes smaller if the cathode-ray beam is inclined at an angle of 90° to the horizontal, and that the

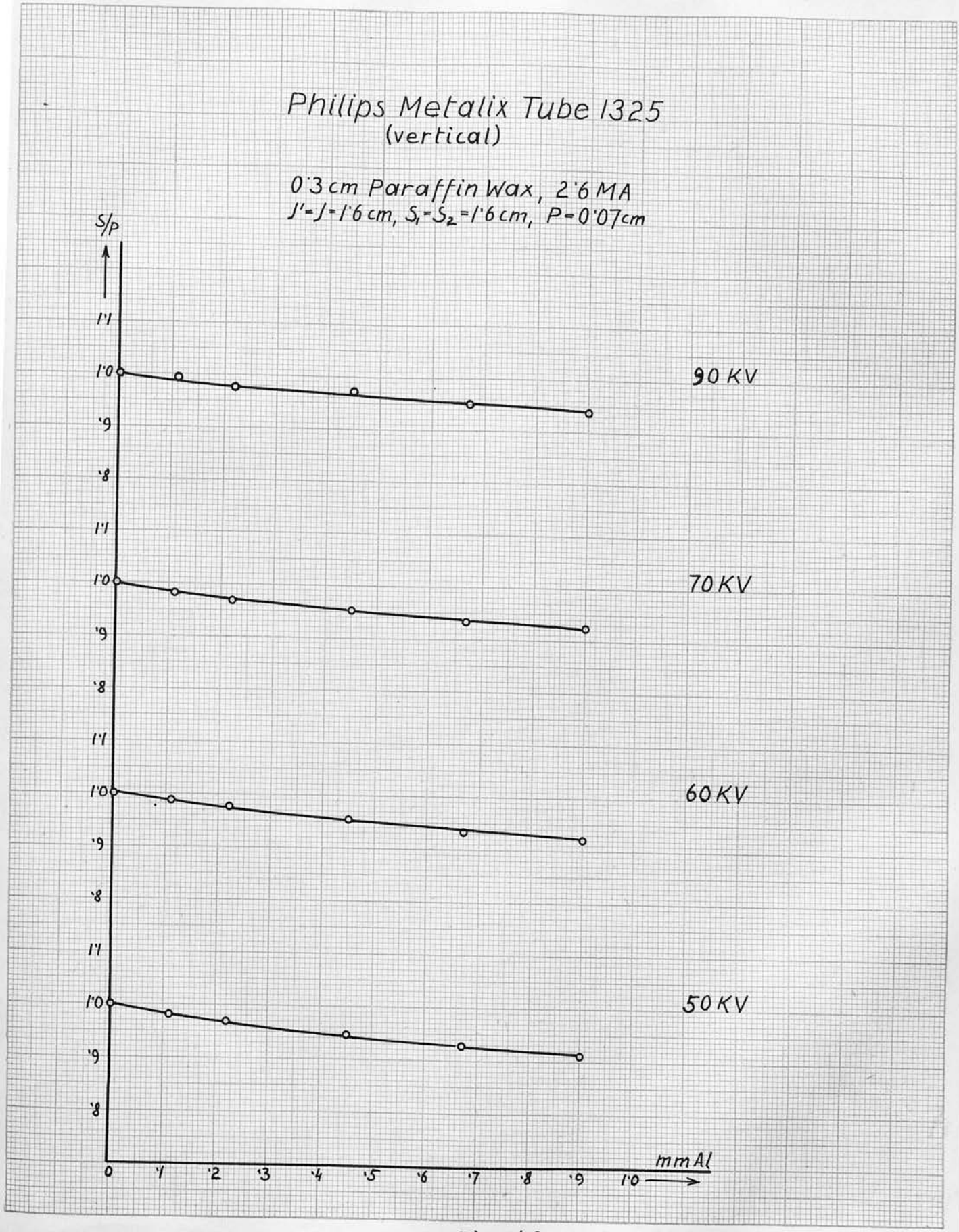
Philips Metalix Tube 1325
(vertical)
0·3 cm Paraffin Wax, 2·6 MA
J'=J=1·6 cm, S1=S2=1·6 cm, P=0·07cm
S/P
1·1
1·0
·9
·8
90 KV
70 KV
60 KV
50 KV
0
·1
·2
·3
·4
·5
·6
·7
·8
·9
1·0
mmAl

Fig. 42.

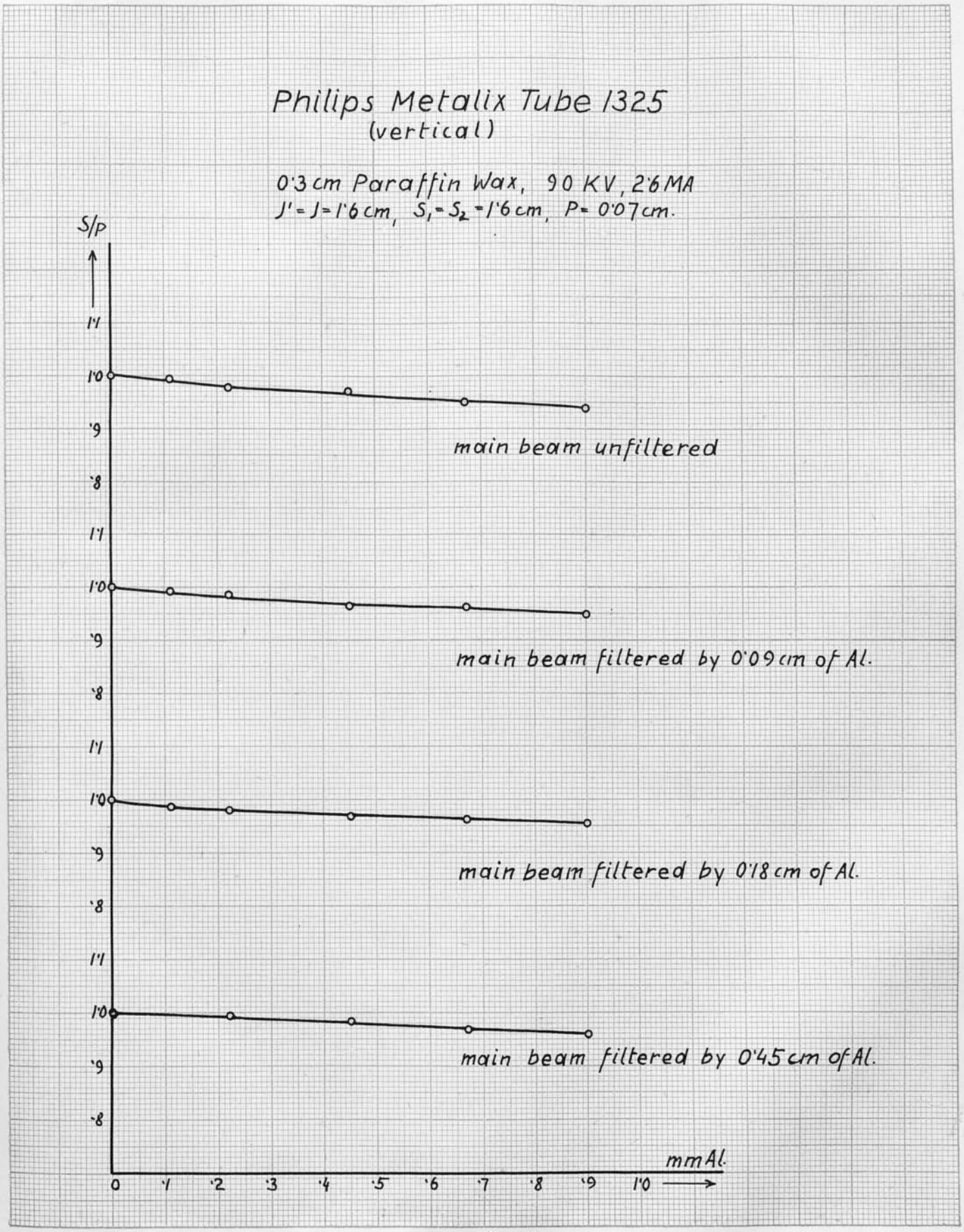
Philips Metalix Tube 1325
(vertical)
0·3 cm Paraffin Wax, 90 KV, 2·6 MA
J' = J = 1·6 cm, S1 = S2 = 1·6 cm, P = 0·07 cm.
S/P
1·1
1·0
·9
·8
main beam unfiltered
main beam filtered by 0·09 cm of Al.
main beam filtered by 0·18 cm of Al.
main beam filtered by 0·45 cm of Al.
mm Al.
0
·1
·2
·3
·4
·5
·6
·7
·8
·9
1·0

Fig. 43.

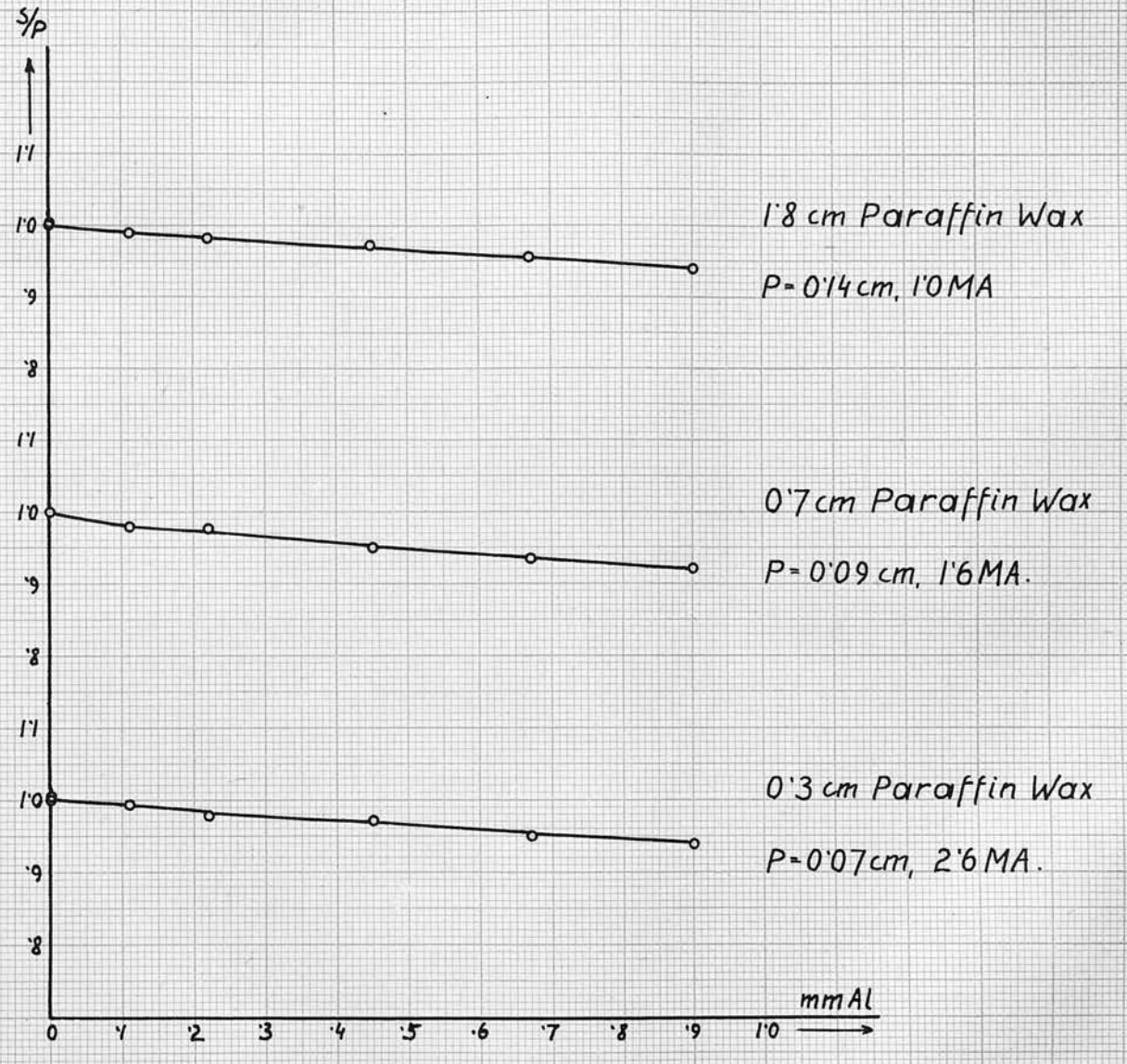
Philips Metalix Tube 1325
(vertical)
J'-J = 1'6 cm, S1 = S2 = 1'6 cm, 90 KV
S/P
1·1
1·0
·9
·8
1·1
1·0
·9
·8
1·1
1·0
·9
·8
1'8 cm Paraffin Wax
P = 0'14 cm, 1'0 MA
0'7 cm Paraffin Wax
P = 0'09 cm, 1'6 MA.
0'3 cm Paraffin Wax
P = 0'07 cm, 2'6 MA.
mm Al
0
·1
·2
·3
·4
·5
·6
·7
·8
·9
1·0

Fig. 44.

Philips Metalix Tube 1325
(vertical)

$J' = J = 1.6$ cm, $S_1 = S_2 = 3.0$ cm, 90 KV

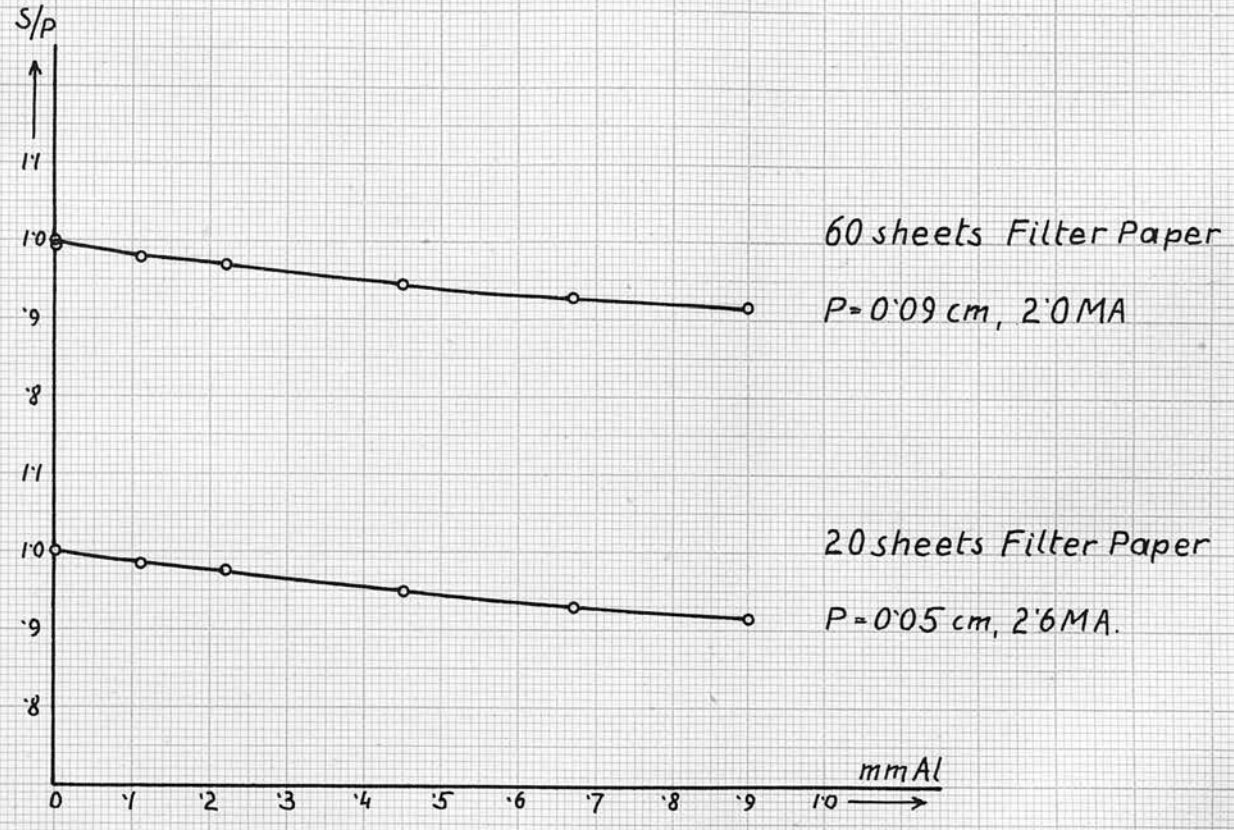

Fig. 45.

Philips Metalix Tube 1325.
(vertical)

$J' = J = 1{\cdot}6$ cm, $S_1 = S_2 = 3{\cdot}0$ cm, 90 KV.

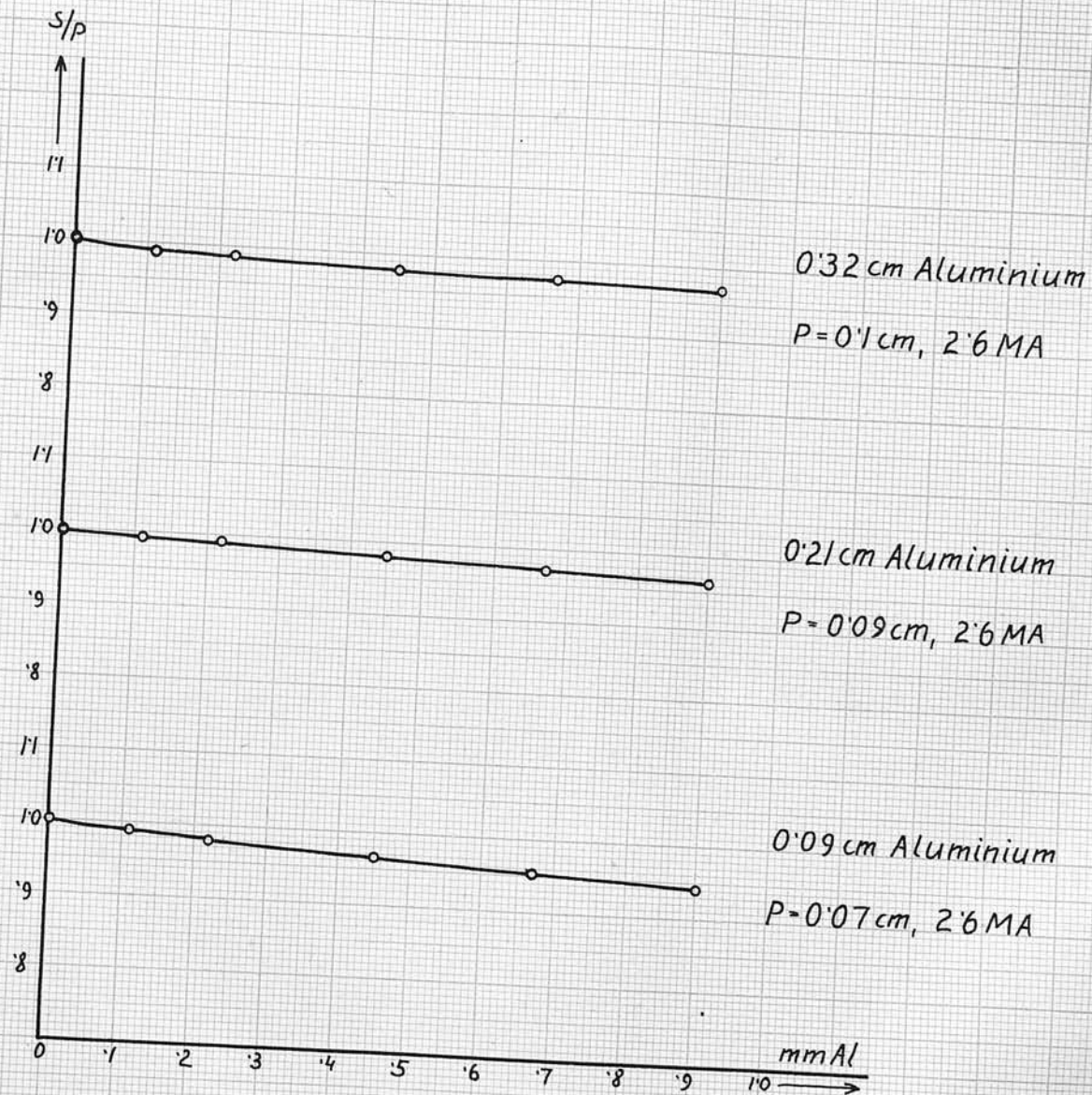

Fig. 46.

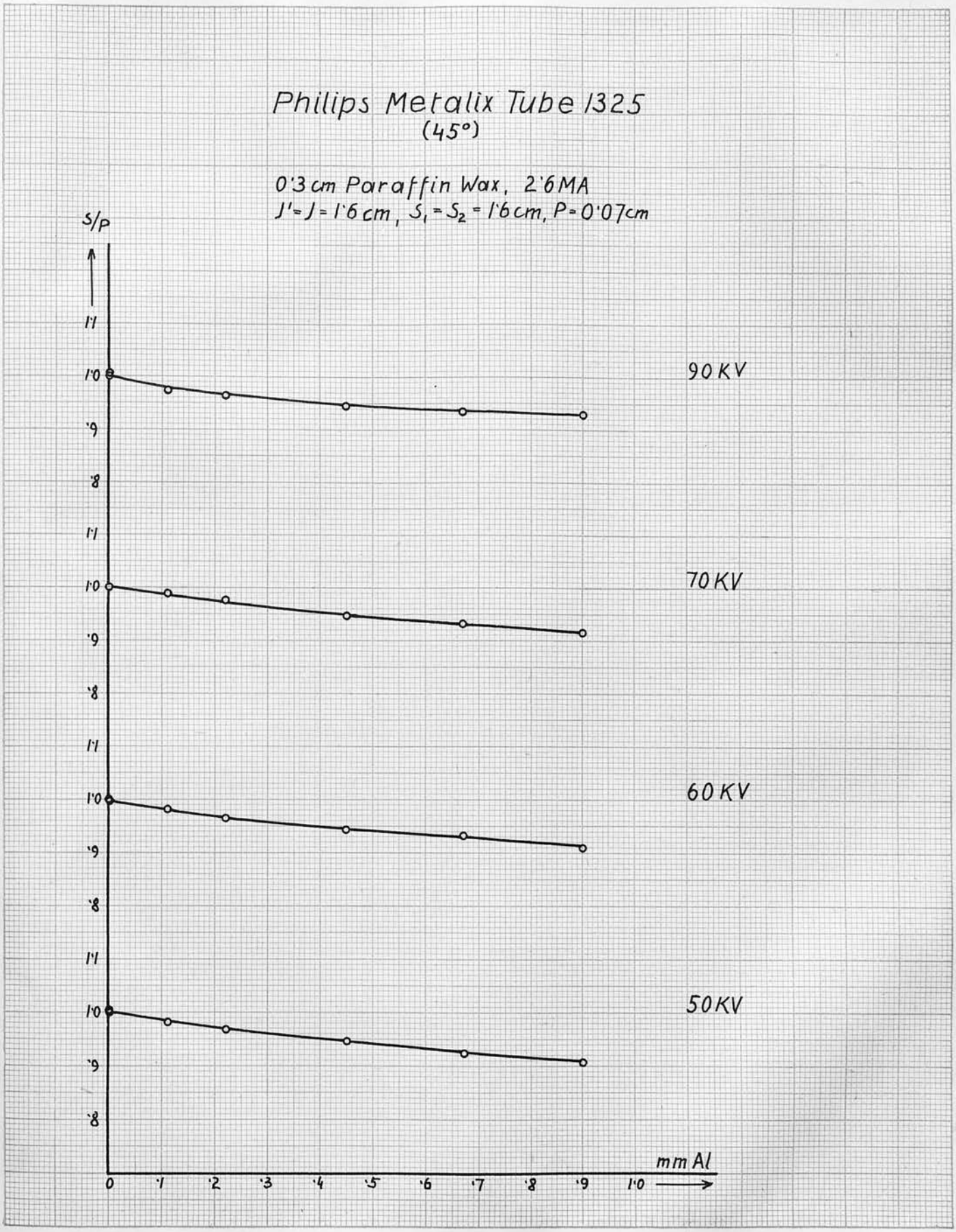
Philips Metalix Tube 1325
(45°)
0·3 cm Paraffin Wax, 2·6 MA
J' = J = 1·6 cm, S1 = S2 = 1·6 cm, P = 0·07 cm
S/P
1·1
1·0
·9
·8
90 KV
70 KV
60 KV
50 KV
mm Al
0
·1
·2
·3
·4
·5
·6
·7
·8
·9
1·0

Fig. 47.

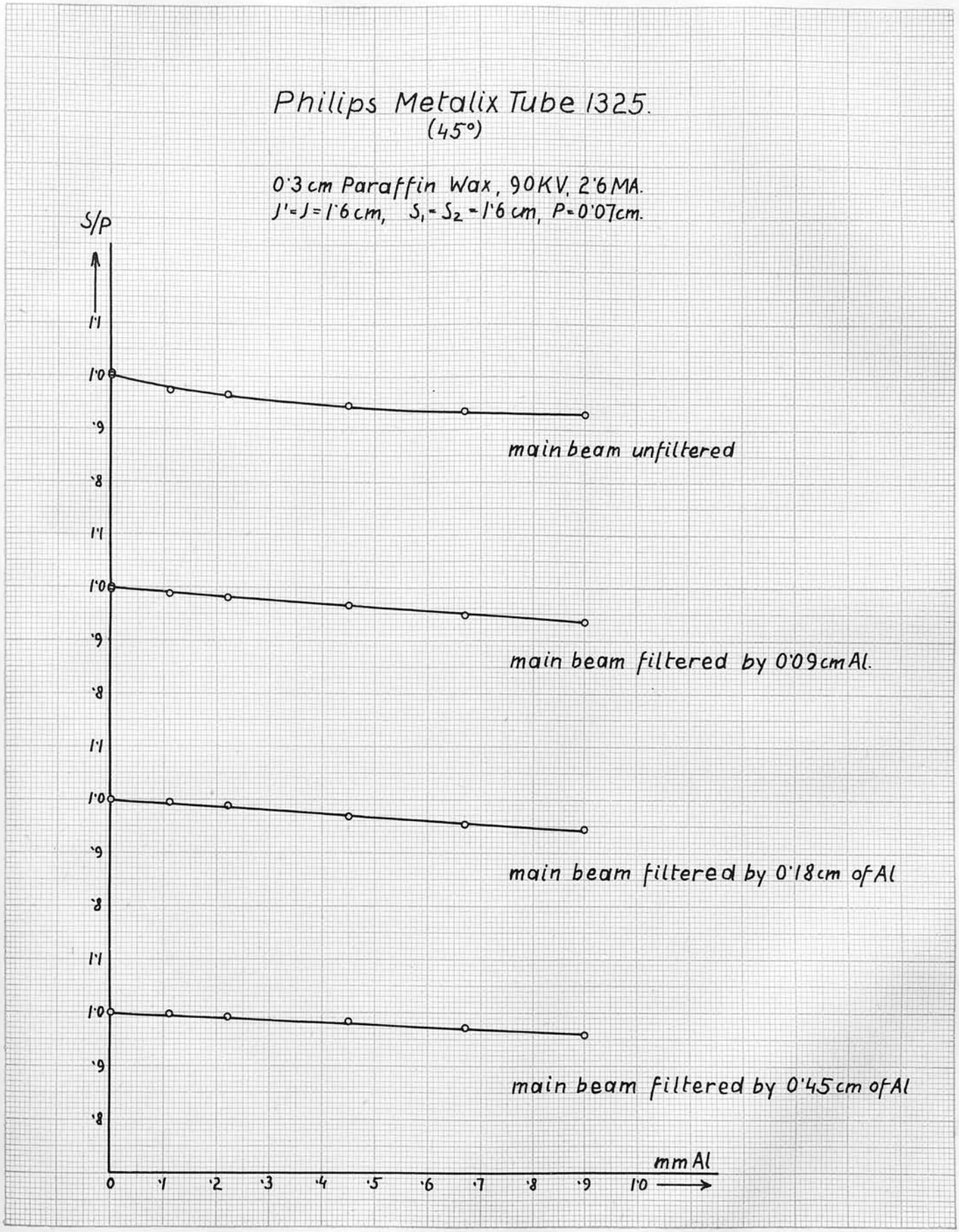
Philips Metalix Tube 1325.
(45°)
0·3 cm Paraffin Wax, 90 KV, 2·6 MA.
J' = J = 1·6 cm, S1 - S2 = 1·6 cm, P = 0·07 cm.
S/P
1·1
1·0
·9
·8
main beam unfiltered
main beam filtered by 0·09 cm Al.
main beam filtered by 0·18 cm of Al
main beam filtered by 0·45 cm of Al
mm Al
0
·1
·2
·3
·4
·5
·6
·7
·8
·9
1·0

Fig. 48.

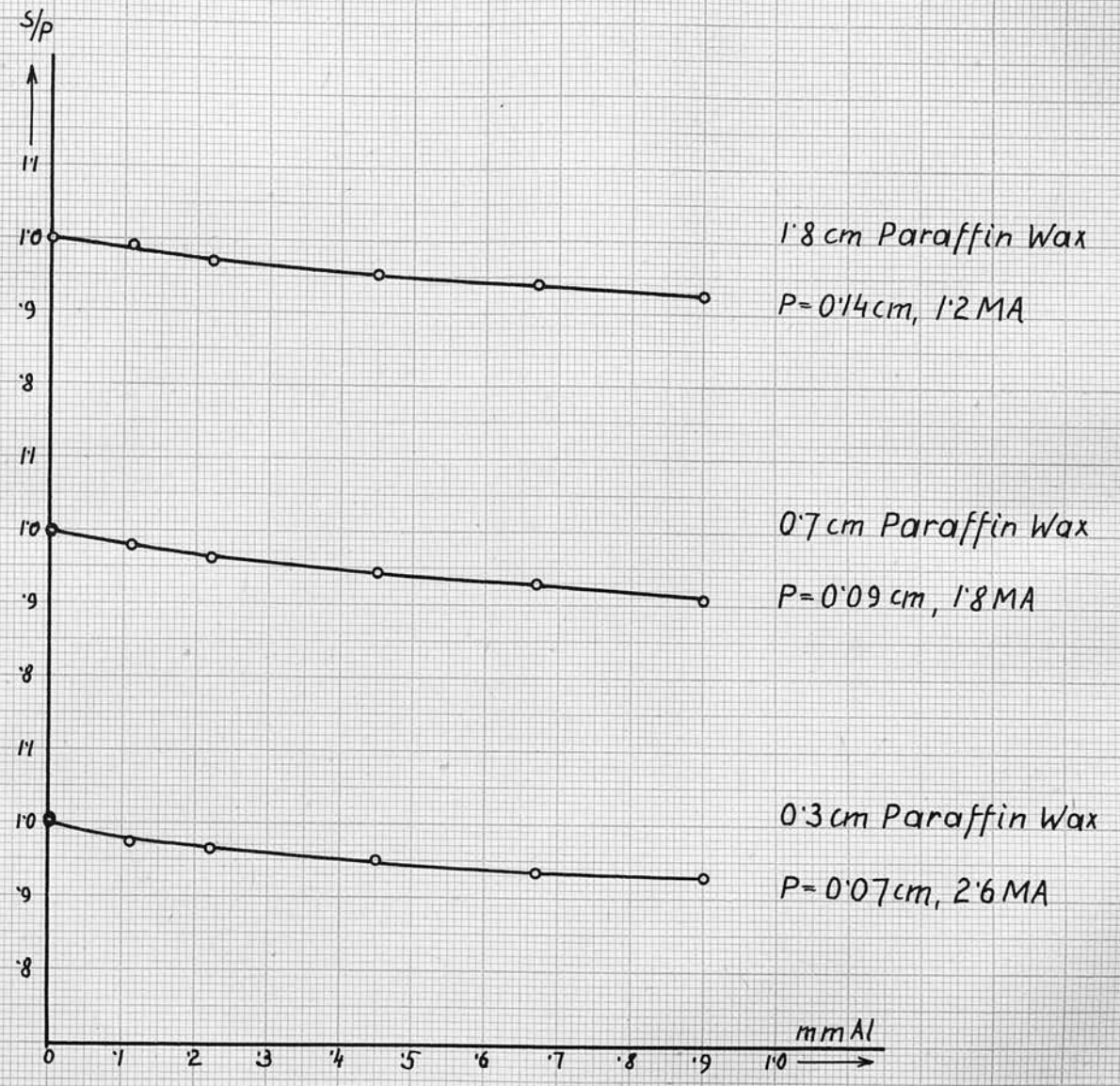
Philips Metalix Tube 1325
(45°)
J'=J=1·6 cm, S1=S2=1·6 cm, 90 KV
S/P
1·1
1·0
·9
·8
1·8 cm Paraffin Wax
P=0·14 cm, 1·2 MA
0·7 cm Paraffin Wax
P=0·09 cm, 1·8 MA
0·3 cm Paraffin Wax
P=0·07 cm, 2·6 MA
mm Al
0
·1
·2
·3
·4
·5
·6
·7
·8
·9
1·0

Fig. 49.

Philips Metalix Tube 1325.
(45°)

$J' = J = 1{\cdot}6$ cm, $S_1 = S_2 = 3{\cdot}0$ cm, 90 KV

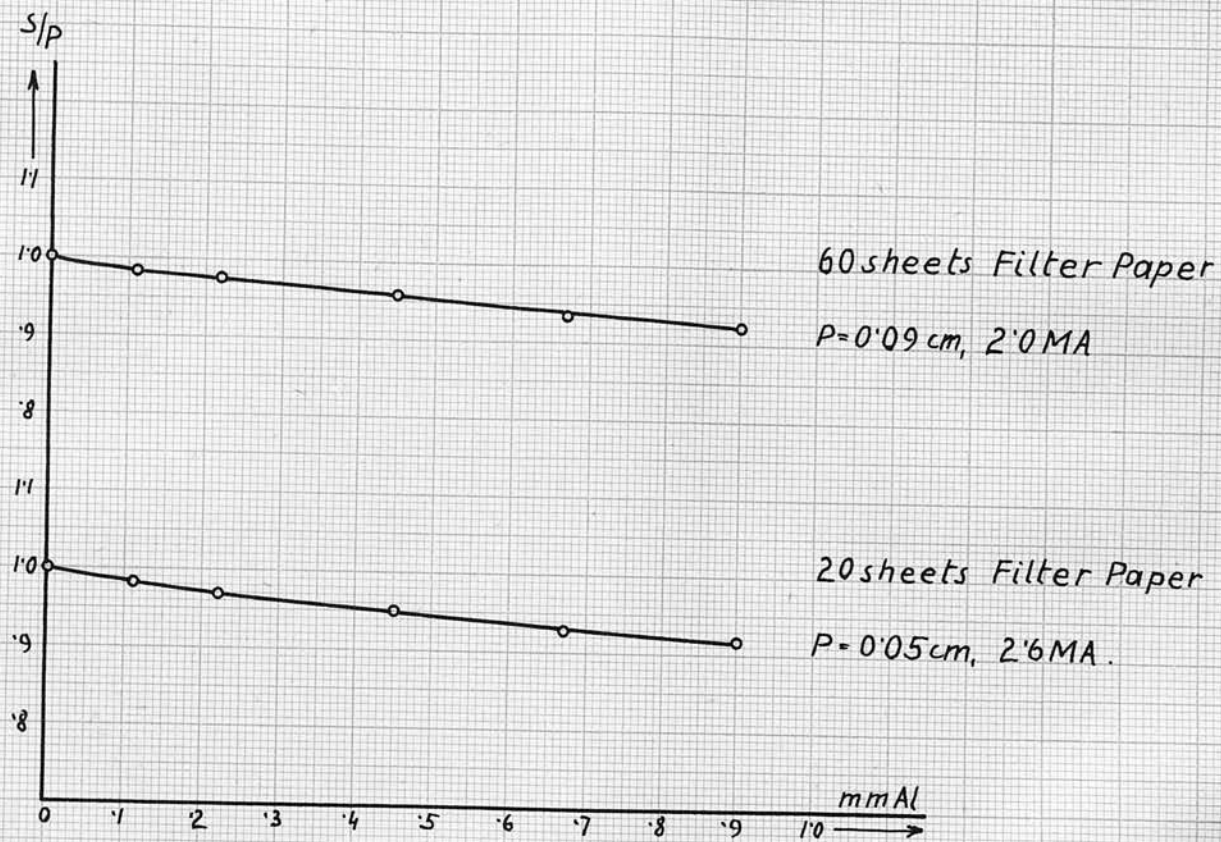

Fig. 50.

Philips Metalix Tube 1325.
(45°)

$J' = J = 1{\cdot}6$ cm, $S_1 = S_2 = 3{\cdot}0$ cm, 90 KV.

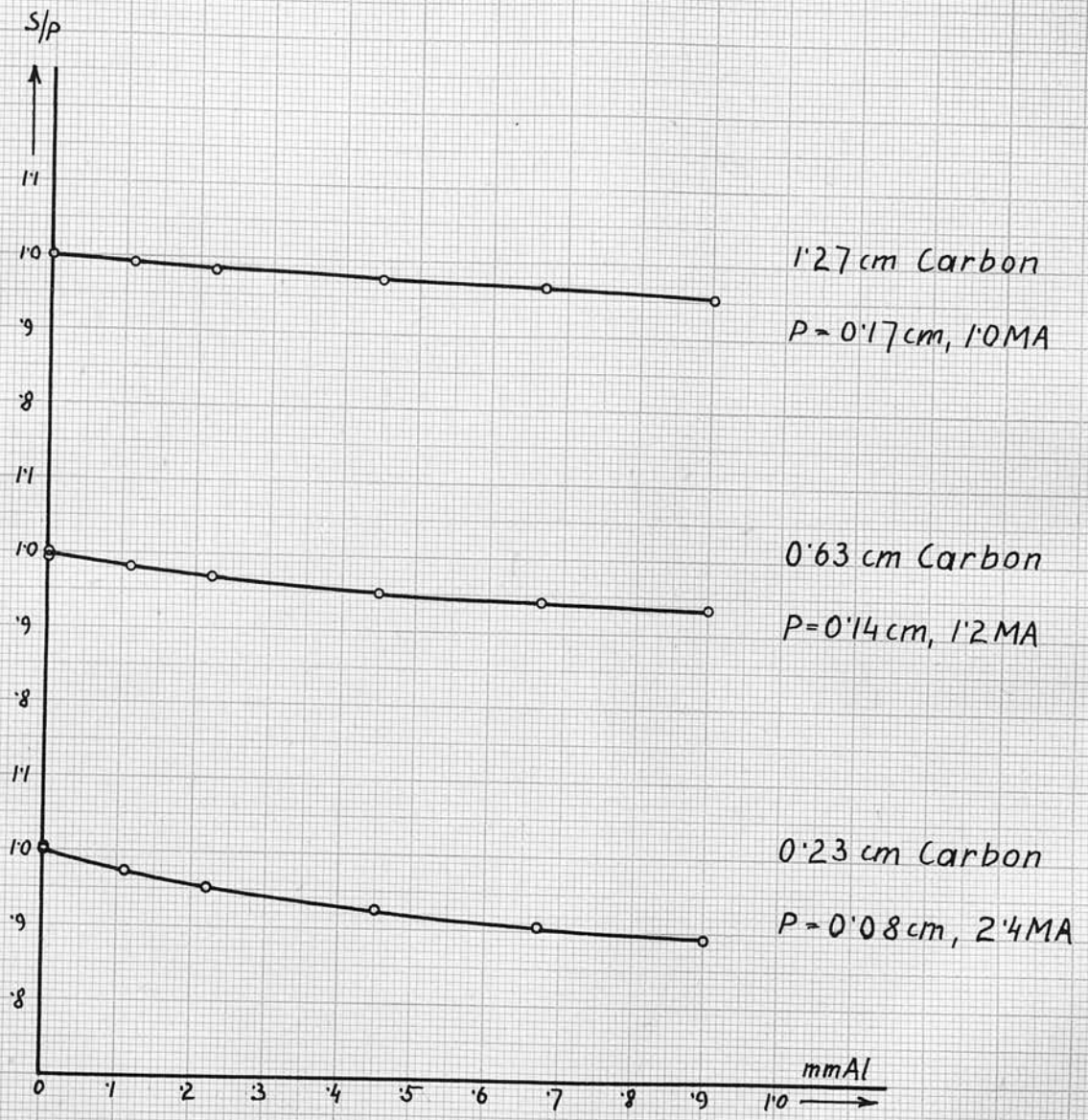

Fig. 51.

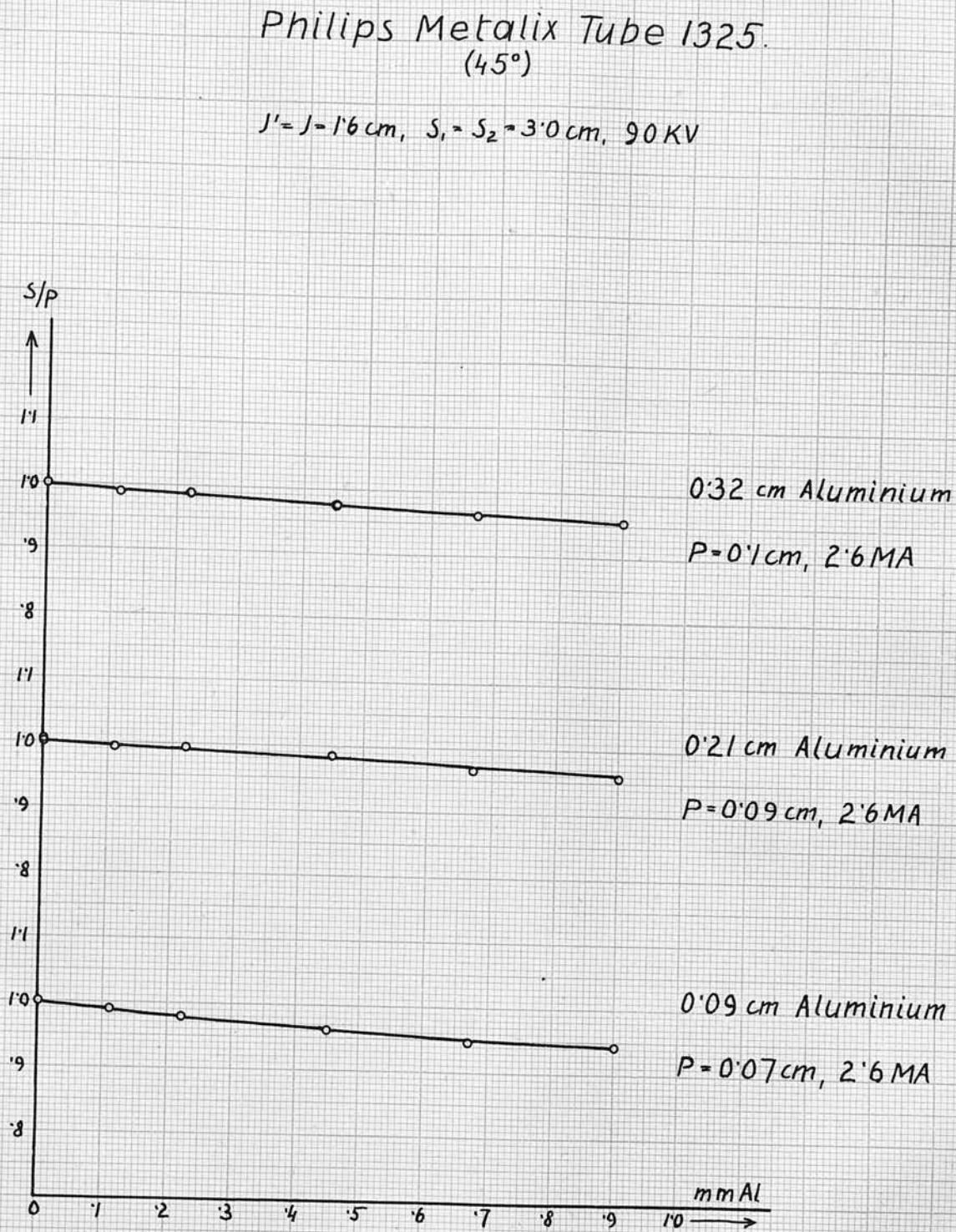
Philips Metalix Tube 1325.
(45°)
J'=J=1·6 cm, S1=S2=3·0 cm, 90 KV
S/P
1·1
1·0
·9
·8
0·32 cm Aluminium
P=0·1 cm, 2·6 MA
0·21 cm Aluminium
P=0·09 cm, 2·6 MA
0·09 cm Aluminium
P=0·07 cm, 2·6 MA
0
·1
·2
·3
·4
·5
·6
·7
·8
·9
1·0
mm Al

Fig. 52.

graphs obtained with the tube in position making an angle of 45° to the horizontal are the mean value of the results obtained with the tube in a horizontal and vertical position. In this respect, the filtering experiment behaves like the scattering experiment.

DISCUSSION OF THE FILTERING EXPERIMENT.

The results of the filtering experiment as they were obtained by the writer are simple and all alike, except for small variations in the slope of the graphs. Since the theory of X-ray absorption (page 36 ff.) does not take account of the polarization of the primary radiation, the filtering experiment was carried out under conditions which would eliminate all effects due to such a polarization. A comparison of the results shown in Figs.47 to 52 with the theoretically obtained filtering curves of Fig. 5 show a satisfactory agreement. The graph of Fig. 5 was obtained under the assumption of the existence of the Compton effect and of the validity of the principle of superposition for heterogeneous beams. Nothing in the experimental evidence obtained by the writer would lead us to deny the validity of these assumptions.

To establish a definite ruling as to how the filtering curves depend on the thickness of the scatterer and on the material of the scatterer is rather difficult owing to the smallness of such effects, although there is not much doubt that such dependences exist. For the same reason, it is impossible to investigate the filtering curves for infinitely thin scatterers, which is necessary if absorption of the radiation within the scatterer is to be taken into account. From experimental results,

it appears that $S/P_{unint.} - S/P_{int.}$ increases for decreasing thickness of scatterer.

The polarization correction which is very small indeed (Miss Ross [40] expected it to be of the order of 10%, similar to the scattering experiment) appears to flatten the graphs a little. This flattening of the graphs is in agreement with theory, and can be explained in terms of the effective hardness of the primary and secondary beams. With the X-ray tube in the horizontal position the secondary beam is on the average slightly softer than the primary. This is because, with the tube in this position, the shortest wave lengths of the primary beam are, owing to its polarization, scattered to a much less degree in the observed direction of the secondary beam than with the tube in any other position. With the tube in a vertical position, i.e. with the plane of polarization horizontal, the secondary beam becomes effectively harder than the primary since, in this case, the polarization results in an excess proportion of the harder components of the primary beam being scattered in the particular direction of the secondary beam. It is due to this additional hardness of the secondary beam that the graph of the filtering experiment for the tube in a vertical position, shows a somewhat smaller slope than that for the tube in a horizontal position. It is only with the tube inclined at 45° to the horizontal, that, if the Compton effect could be

neglected, the two beams would show equal hardness. Only in this case can a comparison between theory and experimental results be made, but, as is evident from the graphs, the error due to polarization caused by working with the tube in a horizontal position is not very large.

In no filtering experiment has there been an indication of a discontinuity as frequently observed by other workers. This is consistent with the assumption that the softening of the scattered radiation is due to the Compton effect. In the absence of exact knowledge of the spectrum of the heterogeneous beam, a proper comparison between theory and experiment is not possible. The graphs of the filtering experiment, conducted so as to be free from polarization errors, are however of such a shape as might reasonably be expected to be produced, if the Compton effect were the only factor causing the secondary beam to differ from the primary.

SUMMARY.

The variability of experimental results frequently obtained by different workers in this laboratory from experiments conducted under apparently well controlled conditions, caused investigations to be carried out under Professor Barkla's direction to try to determine what influence was producing the variations. The idea was expressed that the results could not be explained by current theories and that a hitherto unknown physical process was at work. Ideas regarding the nature of this unknown quantity changed with time as new results were obtained, but all efforts to reach a satisfactory position were unsuccessful. When it became impossible to explain the J-discontinuities in terms of a characteristic radiation, the hypothesis was put forward that heterogeneous radiation behaves differently from the sum of its homogeneous components, especially as regards the scattering process. According to this theory, a beam of heterogeneous radiation has properties depending on some average quality of the beam, which Professor Barkla suggested to be something equivalent to a 'temperature of the radiation'. Since a close connection between scattering and filtering experiments could be established, it was only natural to assume that the governing factor would be the same in both experiments.

Such was the situation when this work was begun.

The main object of the researches carried out in this laboratory in the past few years was to throw some light on that quantity the 'temperature of the radiation', a problem that could be attacked from several sides. The problems with which the writer was faced were therefore to investigate

(1) the reason why apparatus A and B in one room gave different results for the scattering experiment (S/P against thickness of filtering aluminium at constant KV) than apparatus C and D in another room.

(2) the nature of the sudden change in the slope of the graphs which is so characteristic of most results of the scattering experiment (S/P against KV.)

(3) the unknown controlling factor which causes the J-discontinuity to appear and disappear without any apparent reason and which changes the result of the scattering experiment from one type into another one.

In addition to this, another problem arose in connection with the scattering experiment, namely the fact that in some experiments a pinhole primary aperture had been found to give a result which is entirely different from the result obtained with relatively larger primary apertures. This problem did not seem to have any connection with the problems mentioned before, as it could be strictly controlled just by inserting one or other of the primary apertures.

An investigation was conducted by the writer into the influence of the apertures on the result of the scattering experiment. It was found that the result (i.e. the slope of the graph) depends only on the sizes of the incident apertures J' and J and not, within the limits of normal working, on the apertures subsequent to the scatterer limiting the primary and secondary beams. These experiments were not continued, once it had been established that the difference in the results could not be ascribed to an unknown fundamental physical quantity.

In the scattering experiment, the investigations of the sudden change in slope of the graph did not lead to positive results, for, with the exception of a few early experiments, these abrupt changes could not be reproduced despite extensive changes in experimental conditions: changes which according to other workers would have changed the results completely. Although the writer was not successful in solving this particular problem, an important fact emerged from the work. Provided the experimental conditions were varied within the normal working limits, the results were all similar and certainly not contrary to theory. This statement covers variations in the scatterer material and thickness, in apertures subsequent to the scatterer, in the X-ray tube current and covers also the use of 3 different X-ray tubes.

As regards the filtering experiment, it was impossible to observe any trace of a J-discontinuity.

As in the scattering experiments, the results were remarkably uniform. In the filtering experiments observations have, for the first time, been made free from errors due to polarization of the primary beam.

The experimental work which has been reported in this thesis has given results which, within the limits of accuracy of observation, are not in conflict with accepted theory. No evidence has been obtained of a J-discontinuity and none of any discontinuous process in the scattering experiment.

BIBLIOGRAPHY.

(1) Miss M.A. Wilson. Ph.D. Thesis 1939.

(2) C.G. Barkla and C.A. Sadler, Phil. Mag. 15, 550, 1908.

(3) C.G. Barkla and Margaret P. White.
Phil. Mag. 34, 270, 1917.

(4) C.G. Barkla and Miss M.P. White loc. cit.
C.G. Barkla, Phil. Mag. 49, 1033, 1925.

(5) W. Duane and Shimizu, Phys.Rev. 13, 288, 1919.
Phys.Rev. 14, 389, 1919.

F.K. Richtmyer, Phys. Rev. 17, 433, 1921
19, 418, 1922.

(6) C.G. Barkla and Miss G.I. Mackenzie.
Phil. Mag. 1, 542, 1926.
2, 1116, 1926.

C.G. Barkla and S.R. Khastgir,
Phil. Mag. 4, 735, 1927
and other papers.

(7) J. Reekie, Ph.D. Thesis 1937.

Miss M.A. Wilson, loc. cit.

(8) E. Wiechert, Wied. Ann. 59, 283, 1896.

G. Stokes, Proc. Cambr. Phil. Soc. 9, 125, 1898.

J.J. Thomson, Phil. Mag. 45, 172, 1898.

A. Sommerfeld, Phys. Zs. 10, 969, 1909.
11, 99, 1910.

Compton and Allison, X-rays in Theory and Experiment 1934, p. 56 ff. and appendix 1,2.

Wien-Harms, Handbuch der Experimentalphysik, 1930, Vol. 24/1 (F. Kirchner, Allgemeine Physik der Röntgenstrahlen, 1930, p.151 ff.)

(9) J.J. Thomson, Conduction of Electricity through Gases.

Compton and Allison, X-rays in Theory and Experiment 1934, p.116 ff.

F. Kirchner, Allgemeine Physik der Röntgenstrahlen, 1930, p.504 ff.

(10) C.G. Barkla, Proc. Roy. Soc. 77, 247, 1906.

(11) P. Debye, Ann. d. Phys. 46, 809, 1915.

J.J. Thomson, See Compton and Allison loc. cit. Page 134.

(12) C.V. Raman, Ind. J. of Phys. 3, 357, 1928.

A.H. Compton, Phys. Rev. 35, 925, 1930.

(13) Y.H. Woo, Phys. Rev. 41, 21, 1932.

G.E.M. Jauncey, Phys. Rev. 37, 1193, 1931.

(14) R.W. James and G.W. Brindley
Phil. Mag. 12, 81, 1931.

(15) C.S. Barrett, Proc. Nat. Acad. 14, 20, 1928.
Phys. Rev. 32, 22, 1928.

E.O. Wollan, Proc. Nat. Acad. 17, 475, 1931.
Phys. Rev. 37, 862 and 38, 15, 1931.

(16) I. Maizlish, Jour. Frankl. Inst. 197, 667, 1924.

A.H. Compton, Jour. Washington Acad. Sci., 8, 1, 1918.
Phys. Rev. 14, 20, 1919.

(17) A.H. Compton, Bulletin Nat. Res. Council, No. 20, p.16, 1922.
Phys. Rev. 21, 715 and 22, 409, 1923.

(18) A.H. Compton, Bulletin Nat. Res. Council, No. 20, p.19, 1922.
Phys. Rev. 21, 207 and 483, 1923.

P. Debye, Phys. Zeits. 24, 161, 1923.

(19) Compton and Allison, loc. cit. p.207 ff.

(20) P.A. Ross, Science 57, 614, 1923.

(21) A.H. Compton, Phil. Mag. 41, 760, 1921.

(22) E. Schrödinger, Ann. d. Phys. 82, 257, 1927.

(23) G. Breit, Phys. Rev. 27, 362, 1926.

P.A.M. Dirac, Proc. Roy. Soc. 111, 405, 1926.

W. Gordon, Zeits. f. Phys. 40, 117, 1926.

E. Schrödinger, Ann. d. Phys. 82, 257, 1927.

(24) O. Klein and Y. Nishina,
Zeits. f. Phys. 52, 853, 1929.

(25) P.A.M. Dirac, Proc. Roy. Soc. 114, 710, 1927.
117, 610, 1928.
126, 360, 1930.

(26) Klein and Nishina,
Zeits. f. Phys. 52, 867, 1929.

Y. Nishina, Zeits. f. Phys. 52, 869, 1929.

(27) J. Read and C.C. Lauritsen,
Phys. Rev. 45, 433, 1934.

(28) C.Y. Chao, Phys. Rev. 36, 1519, 1930.

(29) G. Wentzel, Zeits. f. Phys. 43, 1, 1927.

A. Sommerfeld, Wave mechanics, 1929.

(30) P.A.M. Dirac, Proc. Roy. Soc. 111, 405, 1926.

(31) E. Rodgers, Phys. Rev. 50, 875, 1936.

(32) G. Wentzel, Zeits. f. Phys. 43, 781, 1927.

(33) I. Waller, Phil. Mag. 4, 1228, 1927.
Zeits. f. Phys. 51, 213, 1928.

I. Waller and D.R. Hartree,
Proc. Roy. Soc. 124, 119, 1929.

(34) D.R. Hartree, Proc. Cambr. Phil. Soc.
24, 89 and 111, 1928.

(35) E.O. Wollan, Proc. Nat. Acad, 17, 475, 1931.
Phys. Rev. 37, 862 and 38, 15,1931.

(36) E.O. Wollan, Phys. Rev. 35, 1019, 1930.
Proc. Nat. Acad. 17, 475, 1931.

(37) G.G. Harvey, P.S. Williams and G.E.M. Jauncey,
Phys. Rev. 46, 365, 1934.

(38) A.H. Compton, Phil. Mag. 41, 749, 1921.

C.Y. Chao, loc. cit (28).

(39) F. Dessauer and R. Herz, Zeits. f. Phys.,
27, 56, 1924.

W. Friedrich and G. Goldhaber, Zeits. f. Phys.
44, 700, 1927.

S. Chylinsky, Phys. Rev. 42, 153, 1932.

(40) Miss Marion A.S. Ross, Ph.D. Thesis, 1943.

(41) S.K. Allison and V.J. Andrews,
Phys. Rev. 38, 441, 1931.

(42) W.H. Bragg and S.E. Pierce, Phil. Mag.
28, 626, 1914.

E.A. Owen, Proc. Roy. Soc. London,
A86, 426, 1912.

W.H. Bragg, Phil. Mag. 29, 407, 1915.

A.W. Hull and M. Rice, Phys. Rev. 8, 326, 1916.

Also F. Kirchner, Allgemeine Physik der
Röntgenstrahlen loc. cit.

ACKNOWLEDGEMENTS.

In conclusion, I wish to express my sincere thanks to Professor C.G. Barkla for his encouraging supervision of this work, and to members of the staff of this laboratory for assistance and advice on many occasions.

Physical Laboratory,
Edinburgh University.
August 1944.